Università degli Studi di Padova

Dipartimento di Scienze Chirurgiche, Oncologiche e Gastroenterologiche

---

CORSO DI DOTTORATO IN ONCOLOGIA CLINICA
E SPERIMENTALE E IMMUNOLOGIA
XXX CICLO

NOTCH1 inhibition regulates evolutionary conserved miRNAs in T-cell Acute Lymphoblastic Leukemia (T-ALL)

Direttore della Scuola : Ch.mo Prof. PAOLA ZANOVELLO

Supervisore : Dott. ERICH PIOVAN

Co-Supervisore : Dott. VALERIA TOSELLO

Dottorando : VALENTINA SACCOMANI

INDEX

Summary

T-cell acute lymphoblastic leukemia (T-ALL) is an aggressive hematologic tumor, resulting from the transformation of T-cell progenitors. Activating mutations in the NOTCH1 ligand-activated transcription factor oncogene are found in over 60% of T-ALL cases. Recently, several microRNAs have been shown to cooperate with NOTCH1 in the pathogenesis of T-ALL. However, little is currently known on the microRNAs that are regulated following NOTCH1 inhibition. Thus, in view of future therapies that may combine NOTCH1 inhibition with microRNA based therapy we pursued to study the microRNAs regulated following NOTCH1 inhibition and their functional role in T-ALL pathogenesis. We first generated a mouse model of NOTCH1-induced leukemia, that carries a NOTCH1 mutation recurrently found in human T-ALL patients (L1601P-ΔPEST), and inhibited NOTCH1 signaling *in vivo* by treating diseased animals with a potent gamma secretase inhibitor (DBZ). These NOTCH1-induced T-ALL samples were subjected to miRNA profiling using a mouse array (8X60K release 19.0; Agilent) and, in parallel, gene expression analysis using SurePrint G3 Mouse Gene Expression v2 array (Agilent). The MYC and NOTCH signatures resulted strongly down-regulated following NOTCH1 inhibition by Gene Set Enriched Analysis (GSEA) demonstrating the efficacy of our experimental model. Among the NOTCH1 down-regulated miRNAs, we found the miR-17-92 cluster, previously reported to be highly expressed in T-ALL samples. Their regulation was also confirmed in another mouse model of NOTCH1-induced T-ALL and in human T-leukemia cells. Notably, we identified miR-34a-5p, miR-22a-3p and miR-199a-5p to be significantly up-regulated following NOTCH1-inhibition suggesting a putative role as tumor suppressors in NOTCH1-driven leukemia. Even if we can hypothesize that these miRNAS could play an important role in murine T-cell leukemia, they resulted not expressed in human T-ALL cells. Differently, miR-22a-3p resulted significantly up-regulated following NOTCH1 inhibition both in mouse and human T-ALL cells. Moreover, the overexpression of miR-22a-3p inhibited *in vitro* colony formation in T-ALL cell lines carrying constitutive NOTCH1 activation and significantly impaired tumor growth *in vivo*

when overexpressed in human T-ALL cells, suggesting a tumor suppressor role for miR-22 in T-ALL downstream of NOTCH1. Meta-analysis from the human T-ALL dataset already published showed, amongst the significantly up-regulated gene sets, targets of the microRNAs belonging to the miR-17/92 cluster. These results are in accordance with our murine microRNA differential expression analysis, in which we found components of miR-17/92 cluster to be strongly down-regulated.

Moreover, using the same human dataset, we ran GSEA against the C3 sub collection of mir targets in the MSigDB v6.0, including additional gene sets with putative targets of miR-22. Amongst the downregulated gene sets, we identified 23 down-regulated genes that were consistently contributing to the negative enrichment of all the three selected gene sets of miR-22 targets. Amongst these genes, we found the Peroxisome Proliferator-Activated Receptor Gamma, Coactivator 1 Beta (PGC-1β), that is involved in mitochondrial metabolism. Notably, GSEA analysis, identified transcription factors significantly regulated upon treatment with DBZ in human T-ALL cells, finding that the PPARG_01 gene set, containing targets of the PPARG transcription factor, was significantly down-regulated in this context. PGC-1β resulted significantly down-regulated following NOTCH1 inhibition *in vivo* in human PDTALL xenografts and in one of three miR-22 overexpressing T-ALL cell lines at transcription level. On the other hand, the amount of PGC-1b protein was found to be very high and insensitive to NOTCH1 inhibition or miR-22 overexpression.

In conclusion, we found that miR-22-3p was down-regulated in T-ALL cells and its expression level could be restored following NOTCH1 inhibition. miR-22-3p over-expression affected *in vivo* tumor growth, possibly altering homing to supportive niches and so favouring disease progression, supporting its tumor suppressor role in NOTCH1-mutated T-ALL cells. Meta-analysis of NOTCH1 regulated genes in human T-ALL cell lines indicated PGC-1β as a putative miR-22 target gene, whose expression appeared significantly regulated only at the transcriptional level, while protein level was found unaltered.

Thus, we are still investigating on the role of NOTCH1/has-miR-22/PPARG axis because understanding the mechanism of action of miR-22-3p in T-ALL cells could be contribute to the successful treatment for T-ALL, opening possibilities of

future therapeutic interventions that may combine NOTCH1 inhibition with microRNA based therapy.

1 Introduction

1.1 T-cell Acute Lymphoblastic Leukemia

T-cell acute lymphoblastic leukemia (T-ALL) is an aggressive hematologic tumor that accounts for 10%–15% of pediatric and 20-25% of adult ALL cases [1,2], it is about twice as prevalent in males as in females [3]. T-ALL clinical presentation consist of elevated white cell counts in patient blood and haematopoietic failure, associated with anemia, neutropenia and thrombocytopenia. In addition, it can include hyperleukocytosis with extramedullary involvement of lymph nodes and central nervous system and the presence of a mediastinal mass, arising from the thymus.

T-ALL results from the malignant transformation of T cell progenitors that cause diffuse infiltration of the bone marrow by immature T cell lymphoblasts [4]. T-cell transformation is characterized by accumulation of genomic mutations, which alter several oncogenes and tumor suppressor genes leading to disruption of the normal pathways involved in T-cell development leading to uncontrolled cell proliferation and cell cycle progression, differentiation arrest and abnormal cellular metabolism.

1.1.1 Molecular pathogenesis

T-ALL transformation shows a prominent role of NOTCH1, a key T cell fate specification and thymocyte development factor, that is activated by oncogenic gain-of-function mutations in over 60% of cases [5]. NOTCH1 activating mutations result in a ligand-independent release of the intracellular domain of NOTCH1 (ICN), which subsequently translocates to the nucleus where it acts as a transcription factor. Alternatively, NOTCH1 mutations in the proline, glutamic acid, serine, threonine-rich (PEST) domain or inactivating mutations in the E3-ubiquitin ligase gene F-box and WD repeat domain containing 7 (FBXW7) preserve ICN from ubiquitin-mediated degradation by the proteasome [6]. In

addition, in more than 70% of all T-ALL cases deletion of the cyclin dependent kinase inhibitor 2A (CDKN2A) locus in chromosome band 9p21 affecting the p16/INK4A and p14/ARF suppressor genes which regulate cell cycle progression and p53 mediated apoptosis, respectively are present [7]. NOTCH1 activating mutations are often found together with CDKN2A alterations or chromosomal translocations, resulting in aberrant expression of different transcription factors involved in T-cell development. These transcription factors include basic helix-loop-helix (bHLH) family members such as T cell acute lymphocytic leukaemia 1 (*TAL1), TAL2[8]*, lymphoblastic leukaemia associated haematopoiesis regulator 1 (*LYL1)[9,10]*, *BHLHB1[11]*, LIM-only domain (LMO) genes (*LMO1, LMO2*)[12,13], *MYC[14]*, *MYB[15]*, *TAN1* [16], the T cell leukaemia homeobox 1(TLX1) and TLX3 [17,18], NK2 homeobox 1 (NKX2-1) and NKX2-2 [19] and homeobox A (HOXA) [20], that can function as oncogenes. Moreover, genetic alterations include transcription factor fusion oncogenes such as *PICALM/MLLT10/CALM-AF10 [21,22]*, *MLL-MLLT1/MLL-ENL [23,24]*, *SET/NUP214 [25]*, *NUP98-RAP1GDS1 [26,27]*; activation of signaling factors driving proliferation such as *LCK [28]*, *CCND2 [28-30]*, *JAK1 [31]*, *NUP214-ABL1 [32]*, *EML1-ABL1 [33]* and *NRAS [34]*.

Additional molecular alterations in T-ALL involve loss-of-function mutations and deletions in tumor suppressor genes such as Wilms tumour 1 (WT1) [35]; deletions and mutations in the *WT1* gene are present in about 10% of T-ALLs and are frequently associated with oncogenic expression of the *TLX1*, *TLX3*, or *HOXA* oncogenes [35,36]. Loss-of-function mutations in other tumor suppressor genes in T-ALL include: monoallelic or biallelic deletions involving the Lymphoid Enhancer Binding Factor 1 (*LEF1*) locus and mutations in the *LEF1* gene, that are present in about 15% of T-ALL cases [37]; ETS Variant 6 (*ETV6*) mutations, a transcriptional repressor strictly required for the development of hematopoietic stem cells, that produce truncated proteins with dominant-negative activity [38,39]; loss-of-function mutations and heterozygous deletions of B-Cell Chronic lymphocytic leukemia (CLL)/Lymphoma 11B (*BCL11B)[40]*; loss-of-function mutations in Runt-related transcription factor 1 (*RUNX1),* that can be found in immature T-ALL samples, suggesting a tumor suppressor role for *RUNX1* in T-cell transformation [41]; somatic GATA Binding Protein 3 (*GATA3)* missense

mutations, an important regulator of T cell differentiation, cluster in the zinc finger DNA-binding protein domain, and may be responsible for an early block in T-cell development [42].

Loss of tumor suppressor genes during T-cell transformation were identified in other important signaling pathways: rat sarcoma viral oncogene homolog (RAS)/MAPK [43], where cryptic deletions and/or mutations are present in the neurofibromatosis type 1 (*NF1*) gene, which encodes a negative regulator of the RAS pathway, occur in 3% of T-ALL [44], and phosphatidylinositol-4,5-bisphosphate 3-kinase (PI3K) [45], where nonsense, missense mutations or deletions of Phosphatase and Tensin homolog (PTEN), a critical negative regulator of the PI3K-AKT signaling pathway, occur in 10-20% of human T-ALL cases [46].

Moreover, alterations in epigenetic regulators and chromatin modifiers are reported in up to 25% of T-ALLs and involve the polycomb repressor complex 2 (*PRC2*) [47], including its core components embryonic ectoderm development (EED), Enhancer of zeste homolog 2 (EZH2) and suppressor of zeste 12 homolog (SUZ12), that mediates the repressive histone H3 lysine 27 trimethylation mark [48]; *KDM6A*, which encodes a histone demethylase [49]; and USP7, which encodes a deubiquitinating enzyme [50].

In particular, NOTCH1 activation was shown to specifically induce loss of the repressive *H3K27me3* mark by antagonizing PRC2 complex activity during T cell transformation, suggesting a dynamic interplay between oncogenic NOTCH1 activation and loss of PRC2 function in the pathogensis of T-ALL [47]. In addition, mutations and deletions in PHD Finger Protein 6 (*PHF6)* gene, which has a putative role in chromatin modification, are present in about 16% of pediatric and 38% of adult T-ALL cases[51].

Recently, Liu Y. et al. identified multiple new modalities of activation in known T-ALL driver genes, including sequence mutations (Pro44Leu; P44L) and enhancer alterations that deregulate MYCN, previously identified in neuroblastoma, novel rearrangements and mutations of MYB, rearrangements and complex mutations of ZFP36L2, and novel TAL1 enhancer mutations [52].

Classification of recurrent genetic alterations in T-ALL

Category	Gene target	Genetic rearrangement	Outcome (ref.)
NOTCH1 pathway	*NOTCH1*	t(7;9)(q34;p13)	NA
		Activating mutation	Good (51, 129)
			GPR (45, 49, 50)
			No impact (48)
	FBXW7	Inactivating mutation	NA
Cell cycle defects	*CDKN2A/2B*	9p21 deletion methylation	Good (60)
	CCND2	t(7;12)(q34;p13)	NA
		t(12;14)(p13;q11)	
	RB1	13q14 deletion	No impact (33)
	CDKN1B	12p13 deletion	NA
Cell growth transcription factor	*MYC*	t(8;14)(q24;q11)	NA
tumor suppressors	*WT1*	Inactivating mutation/deletion	No impact (80)
	LEF1	Inactivating mutation/deletion	NA
	ETV6	Inactivating mutation/deletion	No impact (33)
	BCL11B	Inactivating mutation/deletion	No impact (33)
	RUNX1	Inactivating mutation/deletion	No impact (33)
			Poor (101)
	GATA3	Inactivating mutation/deletion	Poor (33)
Signal transduction	PTEN	Inactivating mutation	No impact (106, 130)
		10q23 deletion	Poor (33)
	NUP214-ABL1	Episomal 9q34 amplification	Poor (108)
			No impact (131)
	EML1-ABL1	t(9;14)(q34;q32)	NA
	ETV6-ABL1	t(9;12)(q34;p13)	NA
	BCR-ABL1	t(9;22)(q34;q11)	Poor (132)
	NRAS	Activating mutation	No impact (33)
	NF1	Inactivating mutation/deletion	No impact (33)
	JAK1	Activating mutation	No impact (33)
	ETV6-JAK2	t(9;12)(p24;p13)	NA
	JAK3	activating mutation	No impact (33)
	FLT3	activating mutation	No impact (33)
	IL7R	activating mutation	No impact (33)
Chromatin remodeling	*EZH2*	Inactivating mutation/deletion	Poor (33)
	SUZ12	Inactivating mutation/deletion	No impact (33)
	EED	Inactivating mutation/deletion	No impact (33)
	PHF6	Inactivating mutation/deletion	No impact (81)

GPR, good prednisone response.

Table 1. Classification of recurrent genetic alterations in T-ALL [4].

Over the last years it has become increasingly apparent that RNA is involved in various forms of gene regulation. While much emphasis has been placed on the role of small non-coding RNAs, such as miRNAs, lncRNAs, and circular RNAs, in post-transcriptional modes of gene regulation it has become apparent that their involvement in normal development and disease, including cancer, are very complex. In the context of T-ALL, Mavrakis and colleagues [53] identified a cluster miR-17-92, composed of five microRNAs (miR-19b, miR-20a, miR-26a, miR-92, and miR-223), that cooperatively suppress a network of tumor suppressor genes, including *PHF6*, *PTEN*, *BIM*, and *FBXW7* in a NOTCH1-induced murine bone marrow transplant model of T-ALL. Another work showed how miR-19

plays a crucial role in promoting leukemogenesis in NOTCH1-induced T-ALL. Notably, dual translocations that simultaneously affect the 17-92 cluster, where miR-19 is located, and NOTCH, highlight the oncogenic importance of this interaction in T-ALL [54]. Moreover, using a mouse model of T-ALL, it was found that activated NOTCH1 leads to repression of miR-451 and miR-709 by inducing degradation of the E2a tumor suppressor, which transcriptionally activates the genes encoding miR-451 and miR-709. MiR-451, but not miR-709, was conserved in humans. T-ALL patients, carrying activating NOTCH1 mutations, were found to have decreased levels of miR-451 and increased MYC levels in comparison with T-ALLs with wild-type NOTCH1 [55].

Long non-coding RNAs (lncRNAs) have been reported to play important roles in the pathogenesis of some tumors, although their role in the pathogenesis of ALL or other hematological cancers remains poorly characterized [56]. Long non-coding RNAs are transcripts with a length of at least 200 nucleotides that lack protein-coding potential [57]. They primarily act together with chromatin modifier enzymes, guiding chromatin remodelers to their target sites, where they induce protein conformational changes and thereby activate/inactivate the interacting protein complex [58]. Trimarchi and colleagues were the first to identify a set of lncRNAs under control of aberrant NOTCH1 signaling in T-ALL [59]. In particular, they identified *LUNAR1* as an oncogenic lncRNA, localized in the nucleus, that is over-expressed in primary T-ALLs, with higher expression in T-ALL cases that harbor activating *NOTCH1* mutations. Another study showed how in vitro knockdown of *LUNAR1* significantly affected leukemic cell growth owing to decreased insulin-like growth factor receptor (IGF1R) signaling, suggesting that NOTCH signaling is also able to shape the lncRNA landscape in this disease [60]. These findings open the possibility that such previously uncharacterized transcripts are key modulators of cellular transformation, through their interaction with oncogenic and tumor suppressor programs in leukemia.

1.1.2 Classification of T-ALL

Acute Lymphoblastic Leukemias are an heterogeneous group of tumors differentially classified depending on immunophenotype, cytogenetics, molecular genetic abnormalities and clinical features including response to therapy.

T-cell markers are CD1a, CD2, CD3 (membrane and cytoplasm), CD4, CD5, CD7 and CD8, while CD2, CD5 and CD7 antigens are markers of the most immature T cells. The unequivocal diagnosis of T-ALL depends on the demonstration of surface/cytoplasmic CD3 [61]. Accordingly to the European Group for Immunological Characterization of Leukemias (EGIL), T-ALL is sub-classified on the base of their immunophenotype in four subgroups [61,62]:

- pro-T EGIL TI, this immature subgroup is defined by the expression of CD3, CD7;
- pre-T EGIL TII, is defined by the expression of CD3, CD7 and CD2 and/or CD5 and/or CD8;
- cortical T EGIL T-III is characterized by CD1a positivity;
- mature-T EGIL T-IV is characterized by the presence of CD3 and by the absence of CD1a on the cell surface.

Finally, a novel subgroup called ETP-ALL (Early-T Precursor-ALL) present characteristic immunophenotypic features, which include lack of CD1a and CD8 expression, weak CD5 expression, and expression of at least one myeloid and/or stem cell marker [63].

Molecular classification of T-ALL is associated with unique gene expression signatures that reflect thymocyte developmental arrest at different stages of differentiation. This classification identified three clinically relevant biological subgroups [64,65]:

- ETP-ALL present an arrest at the earliest stages of T-cell differentiation with lack of expression of both CD4 and CD8 and show stem-cell-like and myeloid-like features [63]. ETP-ALL show predominantly alterations that disrupt the activity of important transcription factors regulating haematopoietic and T cell-fate development, such as RUNX1, GATA3 and ETV6 and epigenetics regulators, such as isocitrate dehydrogenase 1

(IDH1), IDH2 and DNA methyltransferase 3A (DNMT3A), and mutations that activate signaling factors, for example NRAS and fms related tyrosine kinase 3 (FLT3) [66-68].

- T-ALLs arrested in the early stages of cortical thymocyte maturation show an CD4+CD8+CD1a+ immunophenotype [69] and recurrently present mutations in NOTCH1 and loss of CDKN2A. These leukemias are typically characterized by the activation of the transcription factors TLX1 and TLX3, NKX2-1 or NKX2-2 [1,70]. This subgroup can also contain genetic alterations including the nucleoporin 214 (NUP214)–ABL1 rearrangement [4] and mutations in PHF6 [51], WT1 [35] and protein tyrosine phosphatase non-receptor type 2 (PTPN2) [71].
- Late cortical leukemias present an arrest in mature late cortical thymocytes with $CD4^{+}CD8^{+}CD3^{+}$ immunophenotype. This subgroup typically present activation of the TAL1 oncogene, together with altered expression of LMO1 or LMO2. These leukaemias also frequently show mutations in NOTCH1 and CDKN2A, and a high prevalence of PTEN mutations and deletions [1].

The ETP-ALL subgroup initially associated with a very high risk of remission induction failure or relapse and significantly reduced overall survival, appears not to have such a dismal outcome following the implementation of current treatment intensification protocols [63,68,72,73]. On the other hand, T-ALLs with early cortical thymocyte immunophenotype present a favourable prognosis [2].

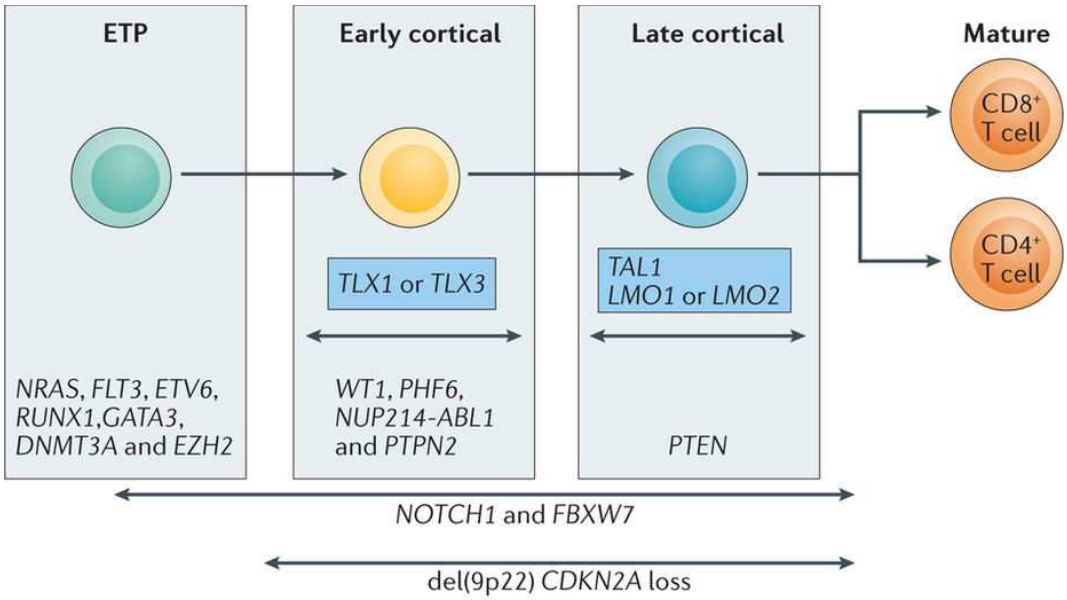

Figure 1. Oncogenic programmes and gene expression signatures define distinct molecular groups of T-ALL [2].

In a recent study, Yu Liu et al. constructed a network to link genetic alterations to T cell developmental stages and T-ALL subgroups, considering both gene–subgroup and gene–gene correlations [52]. From these analyses the pattern that emerged was consistent with a scenario where subtype-enriched genetic alterations reflect genes critical for a specific stage of T cell development. In fact, mutations in the Janus kinase/signal transducer and activator of transcription (JAK/STAT) or Ras signaling pathways, such as FLT3, NRAS and JAK3 were enriched in the LMO2/LYL1 and HOXA subgroups, while alterations in PI3K signaling pathway, for example PTEN and PIK3R1, were enriched in the TAL1 subgroup, suggesting a transition from early T cell development to later stages. USP7 alterations were enriched in the TAL1 subgroup, while CCCTC-binding factor (CTCF) alterations were prevalent in TLX3 cases, while Dynamin 2 (DNM2) and PHF6 mutations were enriched in TLX1/TLX3 cases, indicating that epigenetic regulators are mainly involved in the early versus late cortical stages of T cell development. Moreover, mutations in Ribosomal Protein L5 (RPL5) and LEF1 were most common in NKX2-1 cases, while changes in BCL11B or MYC were most common in TLX1 and RPL10 alterations were enriched in the TLX3 subgroups. MYB, interleukin 7 receptor (IL7R) and ABL1 were the most

frequently mutated genes that were not associated with a unique subtype, suggesting that they may drive signaling pathways in multiple stages of T cell maturation.

1.1.2.1 Notch signaling pathway

Notch signaling is an evolutionarily conserved pathway, that has been extensively characterized in many human systems as well as murine models. Notch signaling controls many cellular functions including cell differentiation, proliferation and apoptosis [74]. In thymus, Notch1 is essential for early T cell fate specification and thymocyte development [75,76].

The Notch proteins are heterodimeric Type I transmembrane receptors, which are composed of (Figure 2):

- an extracellular domain containing Epidermal growth factor (EGF)-like repeats, that mediate interactions with ligand, unique negative regulatory region (NRR) composed of three cysteine-rich Lin12-Notch repeats (LNR), that prevent receptor activation in the absence of ligand and a heterodimerization domain (HD);
- a single-pass transmembrane domain, which acts together with the cytoplasmatic region as transcription factor;
- an intracellular region containing the PEST domain that is targeted by proteasomal degradation to terminate NOTCH signaling.

In mammals there are four members (Notch1-4) of the Notch family of receptors and five Notch ligands (Delta-like 1, 3, 4 and Jagged 1, 2). In the canonical Notch signaling pathway Notch receptors, after binding with its ligands, undergo a conformational change, that leads to the proteolytic cleavage of the transmembrane-intracellular domain of the receptor, first by an A Disintegrin And Metalloprotease (ADAM), generating a truncated Notch intermediate [77], and subsequently by the γ -secretase complex [78]. This aspartyl protease cleaves Notch at a site within the cell membrane to release the activated intracellular

domains of Notch (ICN) into the cytosol. ICN translocates to the nucleus where it activates gene expression by association with CBF1, Suppressor of Hairless, Lag-1 (CSL) repressor complex (CBF in vertebrates, Su(H) in Drosophila, Lag-1 in C. elegans; also known as RBP-jκ) and coactivators of mastermind-like (MAML) family to form transcriptional complexes [79,80]. Notch signaling is tightly regulated through the action of the E3 ubiquitin ligase, FBXW7, which recognizes the PEST domain and targets ICN with polyubiquitination for proteosomal degradation [80] (Figure 2).

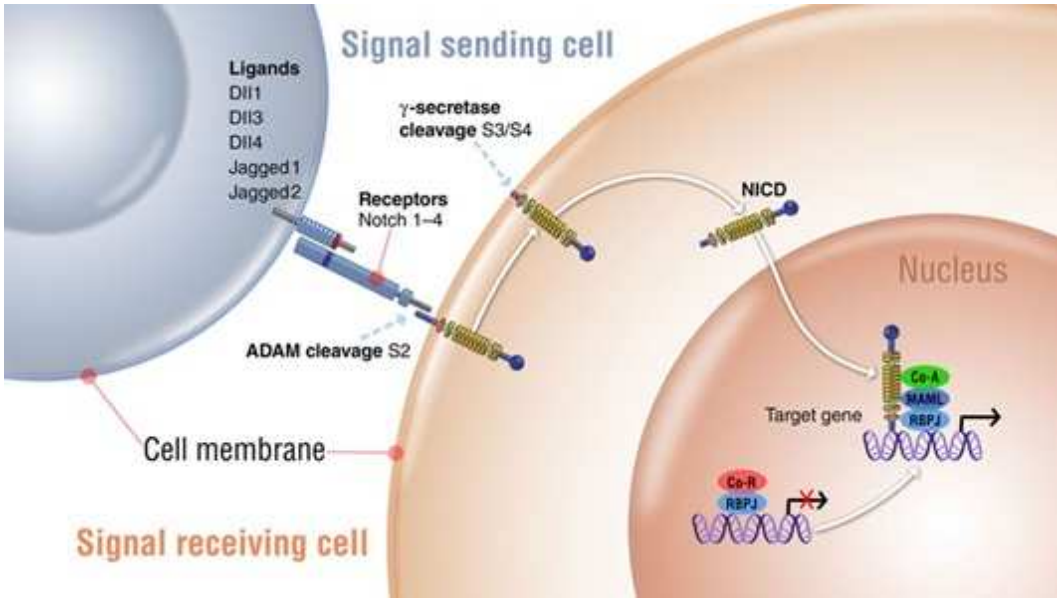

Figure 2. The Notch signaling pathway [81]. Co-A indicates coactivator; Co-R, corepressor; and MAML, Mastermind-like protein 1.

The Notch signaling pathway is involved in hematopoiesis both in the generation of cell diversity and in stem-cell maintenance [82]. Notch is already active in Hematopoietic stem cells (HSCs) in bone marrow to maintain their capacity to self-renewal [83]. Notch has a determinant role in T-cell lineage commitment and in suppressing B-lymphocyte development. In fact, the constitutive expression of active Notch1 in bone marrow (BM) progenitors causes a persistent block in early B-cell differentiation and the increase of immature CD4+CD8+ (double positive; DP) T cells [84]. Notch signaling simultaneously inhibits dendritic cell potential

in the spleen and in the lamina propria through the activation of Notch2 [85]. The pivotal role of Notch in T-cell fate continues in the thymus, where knockdown of Notch1 or inactivation of Notch pathway by RBP-J conditional knockdown *in vivo* induces the accumulation of B cells, in addition to the block of T-cell development at an early stage [75,76]. In vitro experiments demonstrated that Notch signals are necessary at each of the three early double negative (CD4-CD8-; DN) stages (DN1-3) [86] until the β-selection, which requires Notch/Delta interaction for the differentiation of only TCR-αβ-lineage thymocytes [87].
Consistenly, loss-of-function mutations or deletions of Notch signaling components have been linked to several human disorders, from developmental syndromes, such as Alagille syndrome, spondylocostal dysostosis, and cerebral autosomal dominant arteriopathy [88], to adult onset diseases, such as Cancer and Alzheimer's disease [89].

1.1.2.2 Notch1 signaling pathway in T-ALL

Activating mutations in the NOTCH1 ligand-activated transcription factor oncogene are found in over 60% of human T-ALLs cases [5] where they result in high levels of NOTCH1 signaling. A recent report using an integrated genomic approach in 264 T-ALL found an even higher frequency of NOTCH1 mutations (≈75%)[52]. The first identification of aberrant activation of the NOTCH1 signaling pathway in T-ALL showed rare t(7;9) (q34;q34.3) chromosomal translocation which determined the expression of a constitutively active form of NOTCH1 downstream of the TCRB promoter [90] (Figure 3b).
The most frequent mutations in NOTCH1 are HD mutations, which are found in approximately 40% of human T-ALLs. These mutations affect exons 26 and 27, which encode the N-terminal and C-terminal components of the heterodimerization domain, respectively (Figure 3). In normal conditions, in absence of Notch1 ligands the N-terminal and C-terminal subunits of the HD domain are closely associated with LNR repeats, which protect the

metalloprotease S2 cleavage site, holding them together [91]. Most of these mutations called HD mutations of class 1 (HD1) are usually single amino acid substitutions and small in-frame deletions and insertions (Figure 3c), which reduce the stability of the LNR-HD complex, resulting in ligand hypersensitivity or ligand-independent Notch1 activation. The other group of HD mutations class 2 (HD2) are composed of longer insertions located at the distal part of the HD domain encoded in exon 27, which relocate the S2 metalloprotease cleavage site out of reach of the protective LNR-HD complex, resulting in high levels of ligand-independent Notch1 activation [92] (Figure 3e).

Among LNR mutations there is the H1545P substitution, that induces a ligand-independent increase in Notch1 signaling, exposing the S2 cleavage site to metalloprotease [91] (Figure 3d). Juxtamembrane expansion mutants (JME NOTCH1) consist of internal tandem duplications in the 3' end of intron 27 and/or in the proximal region of exon 28, distancing the LNR-HD complex from the membrane without altering the primary structure of any of its components (Figure 3f). The Activation of this alleles requires ADAM and γ-secretase processing [93].

Another NOTCH1 mutational hotspot in T-ALL, present in 20% to 25% of patients, presents frameshift or nonsense nucleotide substitutions, which generate premature stop codons in the C-terminal region with loss of the PEST domain (Figure 3g). These alterations so-called ΔPEST impair degradation of the activated Notch1 by the proteasome, inducing increased levels of activated Notch1 signaling [94].

Similarly, FBXW7 mutations or deletions, found in 15% of T-ALL patients, involving three critical arginine residues in F-box domain, impair Notch1 recognition [95]. However, FBXW7 mutations result to have more diverse biological effects in leukemogenesis than NOTCH1Δ-PEST mutations, probably because Fbxw7 has different targets including proteins involved in cell metabolism, cell cycle progression and cell growth, such as c-MYC, JUN, Cyclin E and mTOR [96].

Notably, NOTCH1 HD mutations are present in about 25% of T-ALLs and are often found in association with ΔPEST (15%) in cis [5] or FBXW7 [95] mutations, inducing together ligand-independent activation and impaired

degradation of the activated receptor determining very high levels of NOTCH1 signaling.

The levels of active Notch1 are crucial to determinate leukemogenesis. In vivo strong Notch1 alleles, such as HD1-ΔPEST and HD2 mutations, drive ectopic T-cell transformation; while the more common weak mutations, such as HD1 and ΔPEST are inefficient to promote leukemia development, but can accelerate tumor progression collaborating with other leukemogenic events, such as activation of K-ras [97].

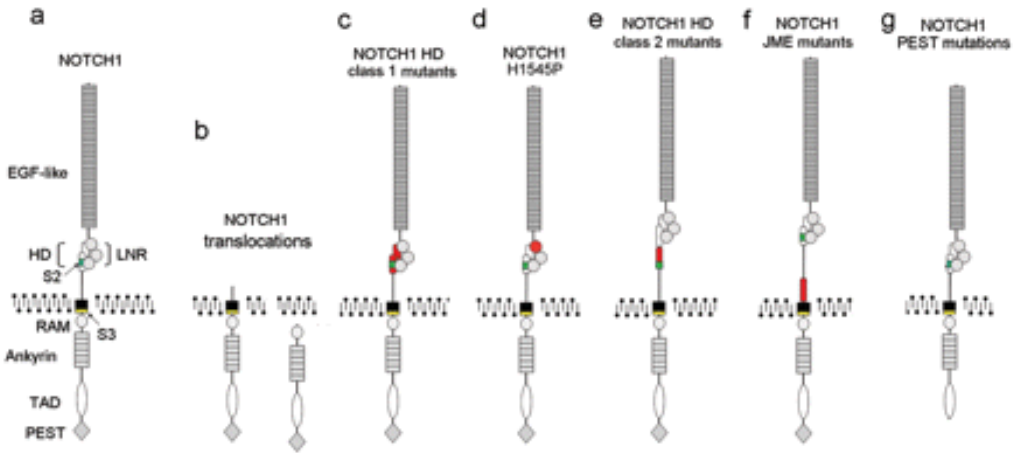

Figure 3. Oncogenic forms of NOTCH1 in T-ALL [98].

Notch1 oncogene promotes T-cell leukemic development, providing essential differentiation, proliferation, survival, and metabolic signals. During T-cell transformation, high levels of activated Notch1 in murine T-ALL models impair T-cells maturation of DP cells into both CD4 and CD8 mature single-positive (SP) cells [99], in addition to inhibiting B-cell development and promoting thymic-independent T-cell development [84]. In fact, Notch directly regulates numerous genes implicated in T-cell development such as pre-T-cell antigen receptor α (PTCRA) [100], IL7R [101] and IGF1R [66,67]. Moreover, Notch1 directly up-regulates genes of anabolic pathways and metabolism, including biosynthesis, protein translation and nucleotide and amino acid metabolism, mainly by transcriptional up-regulation of c-Myc [102,103]. This oncogene also mediates the

positive regulation of mTOR by Notch [104]. Notch also alters the cell cycle through the modulation of Cyclin D3 and Cyclin-dependent kinase 4 and 6 (CDK4 and CDK6) [105] and directly by the up-regulation of Cyclin-dependent kinase inhibitors CDKN2D and CDKN1B [106]. One of the most well know Notch1 targets is enhancer of split 1 homolog (HES1). This factor regulates cell cycle progression and contributes to activation of the PI3K/Akt pathway by transcriptionally down-regulating PTEN tumor suppressor expression. Notch1 can also activate the NF-κB pathway via up-regulation of the inhibitor of NF-κB (IkB)kinase (IKK) [107] and crosstalks with the WNT pathway [108].

1.1.3 T-ALL treatment

T-ALL is an aggressive hematologic tumor for which limited therapeutic options are available for patients with primary resistant or relapsed disease. Unfortunately, the specific mechanisms mediating escape from therapy, disease progression and leukemia relapse are still largely unknown.

High dose multi-agent chemotherapy for two or three years with or without cranial radiation [109] is the current standard therapy for T-ALL. This treatment is highly effective in the majority of childhood leukemias, reaching almost 85% survival rates at ten years. Unfortunately, the aggressive regiments are very often associated with acute toxicities and long-term side-effects at the level of bone development, central nervous system and fertility [107]. Moreover, at least 20% of pedriatic and 40% of adult T-ALL patients [108] still risk relapse, and this is associated with poor prognosis [109].

The current therapeutic treatment is composed of three phases (www.cancer.org/cancer/acute-lymphocytic-leukemia/treating/typical-treatment):

i. Remission (or remission induction) phase: the goal is to restore normal haematopoiesis, eradicating more than 99% of the initial bulk of leukaemic cells. Glucocorticoids are administered together with vincristine

and asparaginase or with anthracycline (or both). In children with high risk leukaemia or in adults, a fourth drug is often needed.

ii. Consolidation (intensification) phase: upon restoration of normal haematopoiesis, the aim is to eradicate drug-resistant leukemic cells to reduce the risk of relapse.

iii. Maintenance phase: patients undergo a continuative chemotherapeutic treatment for at least 2-2.5 years for the high risk of relapse in T-ALL.

The success of ALL treatment depends on the efficacy of central nervous system directed therapy. Glucocorticoids were the first drugs used for T-ALL treatment for their cytotoxic effect on lymphoid progenitor cells [110]. The elimination of prophylactic cranial irradiation has put glucocorticoids in a privileged position, as they can penetrate the central nervous system [111], but their efficacy is undermined by the high risk of infectious diseases for patients [112]. The resistance to glucocorticoid treatment is often associated with PTEN loss or AKT activation, the mechanism driving this pathway is in part due to the ability of AKT to phosphorylate the glucocorticoid receptor altering its intracellular localization [113].

Allogenic haematopoietic stem cell transplantation is contemplated in cases with poor response to treatment or high risk of relapse. This treatment improves the prognosis in adults having t(4;11) translocation, although benefits in infants with the same genotype are not confirmed. However, this procedure is associated with non-negligible morbidity and mortality risks [124].

Novel immunotherapeutic approaches against T-ALL include bispecific-T-cell engaging (BiTEs) antibodies and chimeric antigen receptor (CAR)- modified T-cells, that have two main aims: identification of a unique target present on T-ALL blasts and not on normal cells and fratricide, meaning that CAR-modified T-cell express their target on their own membrane leading to a reciprocal destruction between CAR T-lymphocytes [109].

In the last years several studies have elucidated numerous genetic defects that drive T-ALL, opening numerous opportunities for multiple targeted therapies. Therapy with tyrosine kinase inhibitors designed to target BCR-ABL, including imatinib, dasatinib and nilotinib, which inhibit proliferation and induce apoptosis in T-ALL cell lines [114], could be repurposed in T-ALL cases with documented

mutations, which induce JAK/STAT or ABL1 inactivation [115]. BCR-ABL translocations characterize approximately 6% of adults and children with T-ALL [32].

A number of inhibitors of JAK/STAT signaling are currently under clinical development, and the determination of their clinical activity against JAK1 mutated T-ALL will be of great interest. Gain-of- function mutations in IL7R are present in 10% of T-ALL cases and JAK1 or JAK3 gain-of-function mutations cause cytokine-independent receptor activation [116] and constitutive activation of JAK/STAT signaling [31], respectively .

Pharmacologic inhibition of BCL-2 has been suggested as a promising new therapeutic strategy in immature subtypes of human T-ALL, in particular in ETP-ALL [117]. In fact, recent studies indicated an increased sensitivity toward the highly specific BCL-2 inhibitor ABT-199 and synergistic cytotoxic effects between ABT-199 and conventional chemotherapeutics currently used in T-ALL [118,119].

The constitutive activation of the PI3K/AKT/ mTOR signal transduction pathway through deletions or mutations in PTEN [120,121] or PTEN post-transcriptional inactivation [122] suggests a novel therapeutic target in T-ALL. The mTOR inhibitor rapamycin showed promising results in preclinical models[123] and might modulate glucocorticoid resistance in T-ALL [124], but inhibition of mTOR can hyperactivate AKT by a feedback loop between mTOR, PI3K, and AKT [125]. Thus, dual PI3K/mTOR small-molecule inhibitors have been evaluated and demonstrated to have cytotoxic activity against T-ALL cell lines and lymphoblasts obtained from primary human leukemia patients [126].

Despite current T-ALL treatment results in favorable prognosis, approximately 20% of children and 50% of adult patients relapse within 5 years and have a poor prognosis. Relapsed disease is associated with secondary chemotherapy resistance and poor prognosis despite an intensified chemotherapeutic treatment [65].

In conclusion, the identification and molecular characterization of new oncogenes and tumor suppressors has uncovered several mechanisms involved in the pathogenesis of T-ALL and will aid in the design of more effective combination therapies for patients with poor prognosis.

1.1.3.1 NOTCH1-targeted therapy

The identification of activating NOTCH1 mutations in a large percentage of T-ALL patients created enormous interest in developing new targeted therapies for T-ALL and prompted the initiation of clinical trials to test the effectiveness of agents blocking NOTCH1 signaling [127]. Amongst the strategies proposed to target the NOTCH1 pathway are [128]:

- inhibitors of the proteolytic cleavage of the transmembrane NOTCH1 receptor by the presenilin/ γ-secretase complex using γ-secretase inhibitors (GSIs), alone or in combination with vincristine or dexamethasone [129-131]. γ-secretase inhibitors are being evaluated in different clinical trials, but unfortunately, this approach shows dose limiting gastrointestinal cytotoxicity due to goblet cell hyperplasia and low response rates [136]. Nevertheless, it seems that glucocorticoid treatment has a protective effect against gamma secretase inhibitor-induced gut cytotoxicity. The main player of this protective role has been identified in Ccnd2, as its absence leads to the loss of enteroprotection even in the presence of dexamethasone [126]. Combination therapy based on glucocorticoids and γ-secretase inhibitors shows high efficacy also in glucocorticoid resistant T-ALL: normally the transcriptional repressor HES1, upregulated by NOTCH1, binds the promoter of the glucocorticoid receptor resulting in glucocorticoid receptor repression; thus γ-secretase inhibition can lead to glucocorticoid sensitivity by inhibiting this response [126]. γ-secretase resistance is often associated with FBXW7 mutations, PTEN loss and consequent constitutive activation of PI3K/AKT pathway [93], therefore combination treatments of γ secretase inhibitors and PI3K-AKT-mTOR inhibitors have been proposed [101];
- specific antibodies for NOTCH1, that bind the negative regulatory region (NRR) of the NOTCH1 receptor [132,133]. The monoclonal antibodies against NOTCH1 ligand or receptor have shown antitumoral effects with limited gastrointestinal toxicity [137];
- stapled peptides, such as SAHM1, that target the NOTCH1 transcriptional complex [134];

- therapeutic targeting of downstream NOTCH pathway components, for example the inhibition of IGF1R, a direct NOTCH1 target gene, inhibits growth and viability of T-ALL cells [135]; perhexiline, an inhibitor of HES1, a critical downstream component of NOTCH1 signaling [136], used in the treatment of angina, reverted the HES1 gene signature, evoking a strong anti-leukemic response *in vitro* and *in vivo* [137];
- inhibition of sarcoplasmic/endoplasmic reticulum calcium ATPase (SERCA) channels with thapsigargin which impairs the surface expression of mature NOTCH1 protein with preferential suppression of mutant NOTCH1 receptors [138].

A recent review highlights that molecules such as the BRD4 inhibitor S-Tert-butyl2-(4-(4-chlorophenyl)-2,3,9-trimethyl-6H-thieno[3,2][1,2,4]triazolo[4,3-a][1,4]diazepin-6-yl)acetate(JQ1), may provide new opportunities for blocking oncogenic transcriptional networks [139] determined by aberrant expression of MYC [128]. MYC, a master transcriptional factor involved in catabolism and in numerous human cancers [140], controls cell growth downstream of NOTCH1 and pre-TCR signaling in early T-cell development [141].
The recent identification of massive binding of NOTCH1 at a distal enhancer near the MYC locus (NOTCH1-controlled MYC enhancer (N-Me)) has formally established a direct role for NOTCH1 in controlling MYC expression [141-143], and raised interest in targeting these super-enhancers through the use of BRD4 inhibitors also in T-ALL.

1.2 microRNA

Non-coding RNA (ncRNA) have been shown to play a crucial role in post-transcriptional gene regulation. Among ncRNAs there are the microRNAs (miRNAs), which regulate target mRNAs for degradation or translational repression. miRNAs were first described in 1993 by Lee et al. with the identification in C. elegans of lin-4, which was called as small temporal RNA [144]. Subsequently, studies concerning let-7 showed the wide conservation of these RNAs across other species including humans [145].
miRNAs are reported to regulate different biological processes including development, differentiation, and the homeostasis of both cells and organisms. In view of this, it is plausible to infer that miRNA dysregulation may be implicated in numerous disease states, including cancer [146].
Their discovery has added a new dimension to the understanding of complex gene regulatory networks in humans cancer.

1.2.1 Biogenesis and mechanism of action

The sequences of miRNA are located within different genomic contexts. The majority of miRNA are derived from the intronic regions of non-coding or protein-coding genes, while some miRNAs are derived from the exons of non-coding genes [147]. Some miRNA loci are in close proximity to each other to cluster together and so they are generally transcribed from a single polycistronic transcriptional unit. However, the individual miRNAs can then be post-transcriptionally regulated [148].

miRNA biogenesis can be classified into two different pathways: canonical and non-canonical mechanism.

(A) Canonical miRNA biogenesis pathway: miRNA transcription is principally performed by RNA Pol II, although some miRNAs, such as viral ones [149], are transcribed by RNA polymerase III [150]. Different transcription factors, such as p53, MYC, ZEB1-2, and MYOD1 [147,151] and epigenetic modifications, such as DNA methylation and histone modifications [152], can contribute to positively or negatively regulate miRNA expression. The primary transcript miRNA (pri-miRNA) is several kilobases long and presents local stem-loop structures (33-35bp), a terminal loop and single-stranded RNA fragments at both ends [153].

The maturation of pri-miRNA into a hairpin shaped precursor transcript (pre-miRNA) of about 65 nucleotides long is carry out by the nuclear RNase III Drosha together with its essential cofactor DiGeorge syndrome critical region 8 protein (DGCR8), costituing the complex Microprocessor [154,155]. Drosha is a nuclear protein of about 160 kDa, that belongs to a family of RNase III-type endonucleases. It presents a dsRNA-binding domain (dsRBD), that binds pri-miRNAs through the indispensable interaction with DGCR8 (90 kDa), and tandem RNase III domains (RIIIDs), that dimerize intramolecularly to form a core, where the two RIIID (RIIIDa-b) cut the 3′ and 5′ strand of the stem of pri-miRNA, generating sticky ends with 3′ overhangs [154,155]. Drosha removes the flanking segments and a 11 bp stem region to catalyze conversion of pri-miRNAs into pre-miRNAs [156].

Following Drosha processing, pre-miRNA is exported into the cytoplasm by protein exportin 5, that forms a heterocomplex with GTP-binding nuclear protein RanGTP [157,158]. Upon this translocation, GTP is hydrolysed, resulting in the disassembly of the complex and the release of the pre-miRNA into the cytosol. In the cytoplasm, pre-miRNA is processed by Dicer [159], an RNase III-type endonuclease of about 200 kDa that, similarly to Drosha, presents tandem RNase III domains, forming an intramolecular dimer to create a catalytic centre [160]. Dicer also has a helicase domain to facilitate recognition and processing of pre-miRNA [161,162]. Dicer is regulated by the interaction with dsRBD cofactors: TAR RNA-binding protein (TRBP) [163,164], that modulates the processing efficiency and the length of mature miRNAs [165,166] and/or PKR activating protein (PACT) [164,167]. The role of PACT is not clear, but TRBP and PACT were previously described as negative and positive regulators of dsRNA-

dependent protein kinase R (PKR), respectively [168]. However, the relation between the miRNA and PKR pathway is still unknown. Dicer cleaves pre-miRNA near the terminal loop, liberating a small RNA duplex [159] of about 21–25 nt long , with each strand bearing a 5' monophosphate, 3' hydroxyl group and a 3' 2-nt overhang. In more detail, human Dicer binds to the 5′ phosphorylated end of the pre-miRNA and cleaves it 22 nucleotides away from the 5′ end through its two basic pockets of PAZ domain, that are simultaneously occupied by the 5′ end and 3′ end of the pre-miRNA when the RNA has a two-nucleotide-long 3′ overhang [169,170]. This structural arrangement may explain at least in part the preference of human Dicer for a two-nucleotide-long 3′ overhang structure.

Following Dicer processing, the small RNA duplex is loaded onto an AGO protein to form an effector complex called RNA-induced silencing complex (RISC) [171]. The core component of RISC is a member of Argonaute (AGO) subfamily proteins. The AGO proteins are divided into three subclades: AGO, PIWI and worm-specific AGO proteins (WAGOs). Proteins of the AGO subclade are ubiquitously expressed and associate with miRNAs or siRNAs, whereas PIWI proteins are germ-cell-specific and interact with piRNAs. RISC assembly is composed of two main events: the loading of the RNA duplex and its subsequent unwinding.

All four human AGO paralog proteins (AGO1–4) can incorporate both siRNA and miRNA duplexes, with a preference for small RNA duplexes with central mismatches (nucleotide positions 8–11) [172].

Upon formation of the pre-RISC, composed of AGO proteins associated with loaded RNA duplexes, the passenger strand is quickly removed to generate a mature RISC. The slicing-competent AGO proteins, only AGO2 in humans, cut the passenger strand if the duplex is matched at the center [173,174], but in the majority of cases, where miRNA duplexes have central mismatches, prevent slicing (human AGO1, AGO3 and AGO4 do not have slicer activity) [172,175], the mismatches in the guide strand promote unwinding of miRNA duplexes [176].

RISC loading is not a simple binding between miRNA duplexes and AGO proteins, but rather an active process that requires ATP [177]; while the release of the passenger strand is ATP-independent [176]. The heat shock cognate 70 (HSC70)/heat shock protein 90 (HSP90) chaperone complex uses ATP and

mediates a conformational opening of AGO proteins, to permit the binding between AGO proteins and dsRNA [178]. Unwinding of the passenger strand does not require ATP; maybe due to the release of the structural tension introduced with opening incurred upon binding to AGO proteins during RISC loading [179].

Unwinding can be divided into slicer-dependent and slicer independent. As previously stated, in humans only AGO2 has cleavage activity and so it can facilitate unwinding by slicing the passenger strand [177]. On the other hand, most miRNA duplexes have central mismatches and thus present slicer-independent mechanism, in which mismatches in the guide strand at nucleotide positions 2–8 and/or 12–15 greatly enhance the unwinding efficiency by all four AGO proteins [176,177].

The guide strand is determined during the AGO loading step by the balance of at least three properties of a miRNA duplex [179]: the structure; the 5’ nucleotide identity, advancing 5'-terminal U [180]; and the thermodynamic [179]. Sometimes the strand that is not favored can also be selected, for example this has been noted in studies which compare miRNA isoforms sequenced from multiple tissue [181]. Thus the strand selection may not be completely strict.

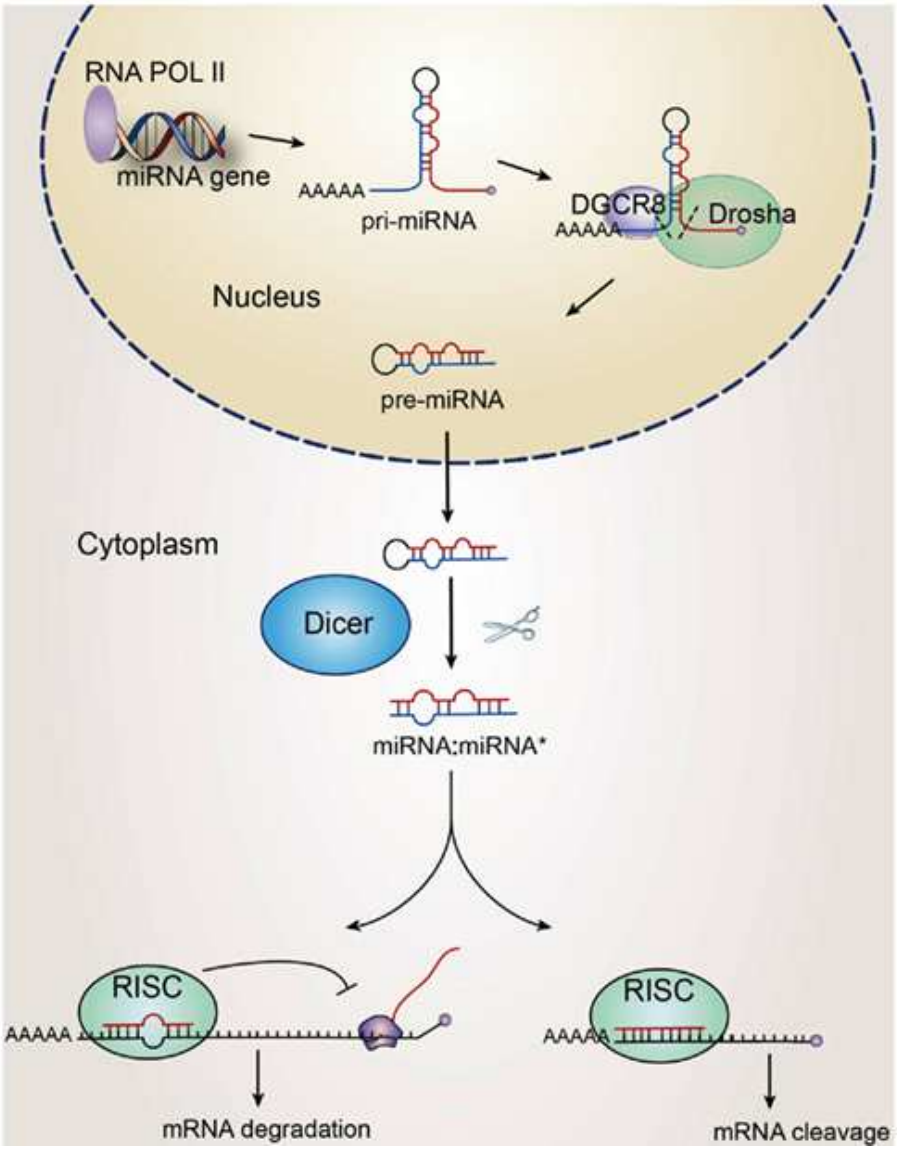

Figure 4. Canonical biosynthesis of miRNAs [182].

(B) On the other hand, the non-canonical pathways of miRNA biogenesis are mainly two:

I. bypass Drosha processing, for example, during mirtron production [183], in which the hairpin shaped pre-miRNAs are generated by mRNA splicing, or in the cases of small RNAs derived from endogenous short hairpin RNAs, which are generated directly through transcription [184];
II. bypass Dicer processing, in which pre-miRNA are directly loaded into RISC and miRNA maturation is obtained through the catalytic activity of AGO2 and, subsequently, by exonucleases activity [185].

Mature miRNAs, which are loaded into miRISC, mediate the post-transcriptional silencing of mRNAs presenting sequences, which are fully or partially complementary to the miRNA [186]. Most of miRNA target sites are located in the 3' UTR rather than in the 5' UTR or ORF, maybe because active translation will mechanistically impede RISC association with target mRNAs [187].

Usually, a target mRNA presents multiple binding sites for the same miRNA, such as for the HMGA2 repression, that dependends on multiple target sites of *let-7* in the 3′ UTR [188]. Moreover, different miRNAs can bind the same target mRNA, such as for the regulation of myotrophin (MTPN) by miR-375, miR-124 and let-7b, suggesting a cooperative microRNA control [189]. The silencing of mRNA is obtained by miRISC through two main ways, degradation or translation repression. The mode of silencing depends principally on two characteristics: the isoform of AGO protein that incorporates the mature miRNA and the total or partial complementarity between the miRNA and its target mRNA. Perfectly complementary mRNA targets are cleaved by AGO, but in humans only AGO2 has catalytic activity [190]; while, in the majority of cases, partially complementary and/or presence of other AGO proteins induce the recruitment of additional protein partners to mediate silencing [191]. Among the AGO factor partners, the Argonaute-bound GW182 plays a key role, acting as scaffold to assemble the multiprotein complex, composed of AGO proteins and silencing effectors, such as the cytoplasmic poly(A)-binding protein (PABP) and with the PAN2–PAN3 and CCR4–NOT deadenylase complexes [191,192].

The translational repression of mRNA targets by RISC can occur through multiple mechanisms:

- mRNA deadenylation and turnover, which consist of removal of the poly (A) tail from mRNAs by recruitment of the CCR4-NOT deadenylation complex, and subsequent degradation through 3' 5' exonucleases [193];
- blocking of translation initiation, in which miRISC through GW182 proteins prevent the binding of eIF4E to the 5' ends of capped mRNAs, where it is required for an eIF3-eIF4G-eIF4E interaction that recruits the 40S ribosomal subunits to the cap [194]. Further, to inhibit translation initiation, AGO2 through its methylated 5′ terminal structure (m^7G-cap) binding-like motif, can also compete with eIF4E for the interaction with the cap [195].

Moreover, AGO2 can interact with the antiassociation factor eIF6 [196] and prevent 60S subunit joining to translationally repressed mRNAs [196,197];

- blocking of translation elongation, that results by drop-off from the ribosome [198] or proteolysis of nascent peptides during translation [199];
- localizing to processing bodies (P-bodies), specific cytoplasmic foci containing mRNA degradation enzymes, in which mRNA targets are recruited by RISC [200].

These mechanisms of gene silencing are also proposed in a stepwise model, that combines translational repression, deadenylation, decapping and 5′-to-3′ mRNA degradation [201].

1.2.2 miRNAs in T-ALL

Numerous studies have demonstrated the fundamental importance of miRNA in normal development, differentiation and growth control, with their deregulated expression being reported in many human diseases, including cancer.

One of the mechanisms contributing to miRNA deregulation is the dysfunction of miRNA biogenesis factors, such as DROSHA and DICER. The down-regulation of these two key enzymes involved in miRNA biogenesis, has been reported in several cancers, including ovarian, lung, and breast cancers [202,203]. In addition, other genes involved in miRNA processing have been reported to be downregulated in cancer, such as Exportin-5, that prevents the export of precursor miRNAs to the cytoplasm, inducing an entrapment of pre-miRNAs in the nucleus [204]. Among the other mechanisms underlying deregulated miRNA expression, there is the transcriptional deregulation of genes, such as c-MYC and p53 transcription factors, which are known to regulate the transcription of a number of miRNA genes [205,206]. Moreover, single nucleotide polymorphisms (SNPs) are found in miRNA genes and sometimes affect their biogenesis and/or alter their target specificity [207]. Epigenetic changes, such as DNA methylation, can modulate the transcription of miRNA genes in cancer, for example the human

RNA methyltransferase BCDIN3D, that O-methylates the monophosphate of pre-mir-145 and pre-mir-23b, altering Dicer activity, resulted involved in tumorigenesis of breast cancer [208]. Also copy number abnormalities of miRNA genes contribute to miRNA deregulation in cancer, such as the deletion of miR-16 and miR15a present in 60% of Chronic Lymphocytic Leukemia (CLL) patients [204]. Finally, several miRNAs are regulated at the level of stability [209]. For example, the human polyribonucleotide nucleotidyltransferase 1 (PNPT1) degrades certain mature miRNAs in human melanoma cells without affecting pri- or pre-miRNA levels [210].

Cancer is a multistep complex disease, in which miRNAs can function as oncogenes or tumor suppressors. miRNAs overexpression can down-regulate tumor suppressors or other genes involved in cell differentiation, inducing tumor formation through increased proliferation, angiogenesis, and invasion. In this case, miRNAs are defined as oncogenes, while miRNAs that down-regulate proteins with oncogenic activity, are defined as tumor suppressors.

In T-ALL a miRNA network was identified, that included both oncogenes and tumor suppressors, involved in malignant T-cell transformation. Indeed, miR-19b, miR-20a/93, miR-26a, miR-92 and miR-223 were reported as multi-targeting regulators of T-ALL tumor suppressors such as *PTEN, BIM, NF1, FBXW7, IKZF1* and *PHF6*, promoting leukemia development *in vivo* [53]. In particular, among the targets of miR-19 action were genes that play a key role in lymphocyte survival, such as *BIM*, encoding a pro-apoptotic Bcl2 protein and known target of the 17–92 cluster, *PRKAA1*(encoding AMP-activated kinase), the tumour suppressor phosphatases *PP2A* and *PTEN* [54]. On the other hand, miR-193b-3p was identified as a tumor-suppressor that targets MYB oncogene, a leucine zipper transcription factor essential for normal and malignant hematopoiesis, and implicated in T-ALL development [211]. Moreover, miR-29, miR-31, miR-150, miR-155, and miR-200 were reported as tumor suppressors, whose inactivation promoted leukemogenesis. Notably, miR-150, miR-155 and miR-200 loss or decreased expression induced Myb activation in T-ALL samples. High mobility group box transcription factor (HBP1) was found to be a target of both miR-29 and miR-31, together with miR-155 and miR-200. In addition, it was

demonstrated that the reduced expression of these tumor suppressor miRNAs in T-ALL cells was a consequence of NOTCH and MYC activation [212].

In a recent study, the comparison of miRNA profiles from CD34+ cells, CD4+CD8+ DP thymocytes and T-ALL samples allowed the identification of unique miRNA expression signatures associated with distinct molecular subtypes of human T-ALL, identifying several novel miRNAs with putative oncogenic or tumor suppressor functions in T-ALL. Of these, miR-21-5p, miR-222-3p and miR-101-3p were significantly upregulated in the immature T-ALL samples compared to control CD34+ cells. On the other hand, the CD34+ cell subset resulted characterized by high levels of miR-222-3p, miR-146a-5p, mir-221-3p and hsa-miR-126-5p with respect to CD4+CD8+ DP cells, which presented up-regulation of miR-16-5p, miR-16-2-3p and miR-450b-5p. These miRNAs expression profiles most probably reflect the specific T-cell maturation arrest associated with the distinct molecular subtypes of T-ALL. Notably, miR-222-3p was significantly upregulated in the CD34+ subset, but its expression is higher in immature T-ALLs. Similarly, miR-182-5p, hsa-miR-29c-3p and hsa-miR-450b-5p showed significantly higher expression in the TAL-Rearranged T-ALLs as compared to their CD4+CD8+ DP normal counterparts.

Moreover, miR-486 both as miR-486-5p (reported as oncomiR in Down syndrome myeloid leukemias) and miR-486-3p (known to be linked to erythroid development downstream of MYB), was found to be more highly expressed in T-ALL samples compared to normal thymocytes [213].

1.2.2.1 miRNAs and NOTCH1

The highly conserved Notch signalling pathway regulates different developmental and homeostatic processes including cell proliferation, apoptosis, migration, invasion, and angiogenesis. miRNAs have been reported to play decisive roles in Notch signaling pathway [214].

In the context of T-cell leukemia, miR-19 was found to play a crucial role in promoting leukemogenesis in NOTCH1-induced T-ALL. Notably, dual translocations that simultaneously affect the 17-92 cluster, where miR-19 is located, and *NOTCH,* highlight the oncogenic importance of this interaction in T-ALL. In addition, other mechanisms, for example transcriptional activation by c-Myc and Notch1, are common causes of the increased miR-19 expression that is observed in T-ALL specimens. Thus, miR-19 contributes to leukemogenesis, regulating its target genes, such as BIM, encoding a pro-apoptotic BCL2 protein and target of the 17–92 cluster, and also PRKAA1, the tumour suppressor phosphatases PP2A (subunit Ppp2r5e) and PTEN [54]. Notably, it was reported that MYC, via miR-17-92 maintains a neoplastic state through the suppression of specific genes, such as four epigenetic regulatory genes Sin3b, Hbp1, Suv420h1, and Btg1and the pro-apoptotic protein Bim [215].

Recently, a study highlighted the importance of molecular tertiary structures of the miR-17-92 primary transcript in modulating the miRNA processing machinery. Although it does not totally explain the different patterns in expression of miR-17-92 components, RNA-binding proteins may play a role in selectively targeting and regulating miRNAs of the cluster during processing [216].

Another exciting study found that the use of anti-miR-17-92 via intravenous injection blocked tumor growth of allograft medulloblastoma tumors in immune-compromised mice, suggesting that future studies may permit the safe application of anti-miR-17-92 as a therapy and/or therapeutic adjuvant for cancer treatment [217].

miR-451 and miR-709 have been identified as potent suppressors that normally inhibit the initiation and maintenance of mouse Notch1-driven leukemogenesis *in vivo*. Using a mouse model of T-ALL, it was found that activated NOTCH1 leads to reduced levels of miR-451 and miR-709 by inducing degradation of the E2a tumor suppressor, which transcriptionally activates the genes encoding miR-451 and miR-709. Both miR-451 and miR-709 were found to directly repress Myc expression. In addition, miR-709 directly represses the expression of Akt and Ras-GRF1 oncogenes. However, only MiR-451, but not miR-709, was found to be conserved in humans. T-ALL patients, carrying activating *NOTCH1* mutations, were found to have decreased levels of miR-451 and increased MYC levels in

comparison with T-ALLs with wild-type NOTCH1, indicating that miR-451 influences MYC expression in human T-ALL bearing *NOTCH1* mutations [55].

Interestingly, a recent study found that Notch-1 mediates chemoresistance and supports proliferation in lung adenocarcinoma cells, partly by repressing of miR-451 through transcription factor AP-1. In addition, they found that MDR-1 is a direct target of miR-451, suggesting a novel Notch-1/AP-1/miR-451/MDR-1 signaling axis to use as a new therapeutic strategy in combination with Docetaxel (DTX) for the treatment of DTX-resistant lung adenocarcinoma [218].

Finally, the miR-223 was found to play an important role in T-ALL both in mouse and human T-ALL albeit with mixed results [219,220]. Indeed, after NOTCH1 inhibition through GSIs, miR223 was found either downregulated or upregulated in different T-ALL cell lines. One of the studies identified miR-223 as an oncogene regulated by Notch3. They showed that both Notch and NF-kB represent novel coregulatory signals for miR-223 expression, being able to activate cooperatively the transcriptional activity of miR-223 promoter, in part through a conserved RBPjk binding site. Moreover, they observed that the activation of miR-223 by NOTCH1 down-regulated FBXW7 expression in T-ALL cell lines. In addition, they found the existence of an inverse correlation between miR-223 and FBXW7 expression in a group of T-ALL patient-derived xenografts. Finally, they observed that specific inhibition of miR-223 restored GSI sensitivity in T-ALL cell lines resistant to GSI treatment, suggesting that miR-223 could be involved in regulating GSI sensitivity [219]. On the other hand, it was reported that the expression of miR-223 increases after GSI treatment, indicating that active Notch pathway signaling down-regulated the expression of miR-223. In addition, the IGF1R, previously reported as an important factor involved in T-ALL cell growth and leukemia-initiating activity, resulted negative regulated by miR-223.

It was also demonstrated that Notch1 pathway signaling can upregulate IGF1R in T-ALL cells by binding with CSL and Mastermind-like 1 to an IGF1R intronic enhancer element, suggesting that Notch signaling induces IGF1R expression directly by enhancing its transcription, and indirectly by repressing miR-223. Although miR-223 increases total IGF1R protein levels, surface IGF1R protein levels were unchanged, suggesting the activation of a compensatory mechanism to

restore cellular homeostasis (recycling and/or redistribution between intracellular pools and the cell surface), and no effect was observed on cell growth. These results support the notion that miR-223 contributes to IGF1R regulation, but probably in concert with other genes and/or microRNAs to alter T-ALL biology [220].

2 Aim

The discovery of activating mutations in NOTCH1 in about 60% of cases prompted scientists to direct efforts in the use of γ-secretase inhibitors (GSI) as a therapeutic options for a significant number of T-ALL patients. The use of GSI was supported by studies that showed their efficacy *in vitro* inducing cell cycle arrest in T-ALL cell lines [5]. Unfortunately, the treatment of patients with GSI showed minimal efficacy in early clinical trials [221]. Following on these results, many efforts have been focus on the development of new molecules that could directly inhibit NOTCH1 or combination therapies that could synergize with GSIs. In order to develop molecular therapies to use in combination with GSIs, it is imperative to better understand the downstream mechanisms mediating the response to NOTCH1 inhibition. Recently, it has been reported that microRNAs can play critical roles in the NOTCH signaling pathway. These microRNAs have been discovered using different approaches, from genetic screenings to microRNA profiling generated from the comparison of normal T cell subsets and NOTCH1-driven leukemia. However, little is currently known on the microRNAs that are regulated in the contest of NOTCH1 inhibition. A study of Gusscott and collaborators [220] analyzed the microRNAs regulated following NOTCH1 inhibition in JURKAT and P12 Ichikawa cell lines. They identified only a few microRNAs regulated upon GSI treatment and amongst these, the miR-223 resulted the most interesting in the context of T-ALL pathogenesis.

Our approach, made use of a mouse model of NOTCH1-induced leukemia that carries a NOTCH1 mutation recurrently found in human T-ALL patients. These tumors were primarily driven by oncogenic NOTCH1, constituting homogeneous pool of samples, in contrast to human primary T-ALL samples that are characterized by additional alterations and to human T-ALL cell lines that are even more complex due to additional alterations linked to prolonged *in vitro* culture. In addition, we treated murine NOTCH1-induced tumors *in vivo* thus recapitulating the biological effects derived from the microenvironment.

The following principal aims were pursued:

- ***Generation of microarray profiles of genes and microRNAs in T-ALL cells following in vivo inhibition of NOTCH1.***

To this end, we used a murine model of NOTCH1-induced leukemia, obtained by retrovirus-mediated overexpression of activated NOTCH1 alleles in hematopoietic lineage negative (Lin^-) progenitors. Forced expression of NOTCH1 in Lin^- progenitors induce primarily ectopic T cell development and subsequently T-cell leukemia [222]. We used an activated form of NOTCH1 that closely resembles human NOTCH1 mutated alleles: L1601P-ΔPEST allele that contains a mutation in the heterodimerization domain (HD) and a deletion in the PEST domain (HD-ΔPEST). We generated MicroRNA and gene expression profiles downstream of NOTCH1 inhibition upon *in vivo* treatment of secondary tumors with a highly active GSI.

- ***Functional validation of NOTCH1-regulated microRNAs and their targets in human T-ALL cells.***

  To this end, candidate microRNAs, that were significantly differentially regulated upon inhibition of NOTCH1 signaling in mouse T-leukemia cells, were selected among those that may have an interesting role in the pathogenesis of T-ALL. Thus, we examined their expression in human T-ALL cell lines and xenografts. In order to mechanistically link the role of a putative microRNA to the biology of human T-ALL, we tested if regulation of a specific microRNA could contribute to promote leukemogenesis *in vitro* and *in vivo*.

3 Materials & Methods

3.1 Mouse models of NOTCH1-induced T-ALL

NOTCH1-induced T-ALL tumors were generated in mice as previously described [97]. Briefly, bone marrow cells were collected from 6- to 12-week-old C57BL/6 mice (Charles River). Bone marrow progenitors (Lin-) were purified from bone marrow cells by negative selection using magnetic sorting (Miltenyi). The cells were cultured overnight in the presence of mIL-3 (10 ng/ml), mIL-6 (10 ng/ml), mFLT3L (50 ng/ml), mIL7 (100 ng/ml) and mSCF (50 ng/ml). The cells were then washed, resuspended in retroviral supernatant (empty vector or NOTCH1 L1601P-ΔPEST or ΔE), placed in the same cytokine cocktail containing polybrene (4 μg/ml), and centrifuged at 1,290 g for 90 minutes. A second round of spinoculation was performed the following day. After washing with PBS, approximately 50×10^4 $Lin^-/Sca1^+/GFP^+$ cells were injected i.v. into lethally irradiated (9 Gy) recipients (6–8-week-old C57BL/6 female mice). Tumor bearing mice were euthanized and primary tumor cells were extracted from their spleens. These tumor cells were then re-injected in sub-lethally irradiated mice (4 Gy) to generate secondary NOTCH1-induced T-ALL tumors. When these mice showed signs of leukemia development, groups of mice were randomized and injected i.p. with the potent GSI, Dibenzazepine (DBZ) (5mg/kg) or DMSO (vehicle) for three times every 8 hours. Each experimental group consisted of at least 3 animals. After this treatment, mice were sacrificed and T-leukemia cells were isolated from infiltrated spleens to perform molecular analyses. Procedures involving animals and their care conformed with institutional guidelines that comply 205 with national and international laws and policies (EEC Council Directive 86/609, OJ L 358, 12 206 December 1987). All mice were monitored daily and animals showing overt signs of disease or excessive weight loss were euthanized following Institutional Animal Care and Use Committee guidelines.

3.2 Plamids and constructs

pLenti-III-RFP and pLenti-III-GFP (m001, Applied Biological Materials) constructs were used as negative controls or with the sequence of pre-hsa-miR-22-3p (mh12804, Applied Biological Materials) to over-express the mature miRNA.
Migr1 vector was kindly provided by Prof. Warren Pear (University of Pennsylvania, Philadelphia, U.S.A). The Migr1-mCherry-Luc2 vector was obtained by sub-cloning the fusion protein between the red mCHERRY fluorescent protein and the luciferase Luc2 protein into ClaI and NcoI restriction sites present in the Migr1 vector, as already described [113]. Migr1 vectors expressing ΔE and HD ΔPEST (NOTCH1 L1601P-ΔPEST) mutant alleles were kindly provided by Prof. Raphael Kopan (Washington University, St. Louis, U.S.A.) and Prof. J. Aster (Brigham and Women's Hospital, Harvard Medical School, Boston, U.S.A.), respectively. The lentiviral vector expressing luciferase FUW-Luc-mCherry-puro was a kind gift from A.L. Kung (Pediatric Department, Columbia University Medical Center, New York, U.S.A.).

3.3 Retrovirus and lentivirus production

The production of retroviral and lentiviral particles was executed in human embryonic Kidney (HEK) 293T cells. These cells were plated in 10 cm culture dishes ($5x10^6$ cells) and transfected with a combination of the following vectors (i) packaging plasmids (retroviral or lentiviral; 2.7 µg) containing *gag*, *pol* and *rev* genes, (ii) plasmid encoding the envelope gene (Vesicular somatitis virus G glycoprotein; VSV-G; 300ng), (iii) retroviral (MigRI based) or lentiviral (pLenti-III-RFP or pLenti-III-GFP based) transfer plasmid (3 µg). 48 hours after transfection, the viral supernatants were collected and filtered. Infection of T-ALL cells or Lin^- progenitor cells was performed by spinoculation: cells were resuspended in medium containing virus and hexadimethrine bromide

(Polibrene®, Sigma) and distributed $2x10^6$ cells per well in 24 well plates. Plates were then centrifuged at 2200 rpm for 90 minutes at room temperature and subsequently placed over night at 37°C. Seventy-two hours post infection, cells were harvested and injected in mice or subjected to puromycin selection (1µg/ml; Sigma) for 3-5 days or sorted using a Beckman Coulter sorter.

3.4 Microarray expression profiling

Total RNA from the spleens of NOTCH1 (HD-ΔPEST) induced T-leukemia bearing mice treated with DBZ (n=3) or DMSO (n=3) was extracted using Trizol, as previously described. RNA concentration was determined using NanoDrop ND-1000 Spectrophotometer (NanoDrop Technologies Inc). The instrument provides the sample concentration in ng/µl and the absorbance of the sample at the wavelengths of 260nm and 280nm. The ratio (260/280) ranging from 1.8 to 2.1 indicated good quality of RNA (ratio < 1.8 indicates protein contamination and ratio > 2.1 RNA degradation and truncated transcripts). In addition, RNA quality and purity was assessed with the Agilent Bioanalyzer 2100 (Agilent Technologies) and executed at CRIBI Biotechnology Center. Only RNA samples that passed the high quality controls were used to perform gene expression profiling using SurePrint G3 Mouse GE 8x60K (Agilent Technologies). This chip allows the evaluation of the expression levels of 27000 genes and 4578 lncRNAs. MicroRNA expression profiling was performed using mouse miRNA 8x60K release 19.0 (Agilent Technologies), that allows the identification of 1247 mouse miRNAs. Arrays scanning was performed using an Agilent microarray scanner system (G2505C for gene and G2565CA for miRNA expression), following manufacturer's indications. Feature Extraction software version 10.7.3.1 (Agilent Technologies), with recommended settings (including the optimal grid file, 028005_D_F_20100804 for gene and 046065_D_F_20121223 for miRNA

expression microarrays) was used to quantify hybridization signals and produce QC reports and raw data for bioinformatic analyses.

3.5 Gene expression analysis methods

Bioinformatic analysis of gene expression microarray data was performed in the R/Bioconductor statistical environment using the limma package [223]. Data were pre-processed using the 'Normexp' background correction method with an offset of 16 and the normalization between arrays was executed with the quantile method. Differential expression analysis was performed by linear model, moderating the t-statistics by empirical Bayes shrinkage. The Benjamini and Hochberg's method [224] was used to correct for multiple testing, using a strict false discovery rate (FDR) cut-off of 0.01.

A gene set enrichment analysis (GSEA) was performed to evaluate the functional significance of curated gene sets. Genes were ranked by decreasing moderated t-statistics and GSEA pre-ranked was run with default parameters. Gene sets in the H collection of the Molecular Signatures Database (MSigDB) v6.0, consisting of 50 hallmark gene sets [225], were tested for significance.

3.6 MiRNA microarray analysis methods

Raw data were loaded and preprocessed in the R statistical environment using the AgiMicroRna Bioconductor library [226]. Preprocessing was performed using RMA algorithm to yield a summary measure of the microRNA expression using a linear model that accounts the probe affinity effect. As suggested by López-Romero [226,227] for microRNA arrays the background correction was omitted,

as it can increase the false positive detection of fold changes in low expressed microRNAs. Differential expression analysis was performed using the limma Bioconductor package [223], followed by multiple testing correction using the Benjamini and Hochberg's method [224] with FDR cut-off set at 0.10.

3.7 RNA extraction, reverse-transcription and quantitative Real Time PCR (qRT-PCR)

Total RNA was extracted by acid guanidinium thiocyanate-phenol-chloroform extraction method using TRIzol Reagent following manufacturers instructions.
cDNA was synthesized from 0.5 to 1 μg of total RNA using Super Script First-Strand Synthesis System (Life Technologies). Reverse transcription was followed by RT-qPCR reactions, which were performed using SensiMix SYBR Hi-ROX Kit (Bioline) and then the ABI Prism 7900 Sequence Detection System (Applied Biosystems). Relative gene expression levels were obtained using the ΔΔCt method [228] and normalizing with respect to β2M gene. Primer sequences used in the RT-qPCR are reported below:

Gene		**Sequence**
murine DELTEX	Forward	5'-AGCTGGTGCCCTACATCATC-3'
murine DELTEX	Reverse	5'-GATGGAGATGTCCATGTCGT-3'
human DELTEX	Forward	5'-GTGGGCTGATGCCTGTGAAT-3'
human DELTEX	Reverse	5'-CGAGCGTCCTCCTTCAGCAC-3'
human PGC1β	Forward	5'-CTGTTTSTGCCTCCCTCACACCTC-3'
human PGC1β	Reverse	5'-CTTCTTCCTCGTCTTCCTCCTCCT-3'
murine β2M	Forward	5'-GTATGCTATCCAGAAAACCC-3'
murine β2M	Reverse	5'-CTGAAGGACATATCTGACATC-3'
human β2M	Forward	5'-AAGGACTCGTCTTTCTATCTC-3'
human β2M	Reverse	5'-GATCCCACTTAACTATCTTGG-3'

On the other hand, to investigate microRNA expression levels, Reverse-Transcription (RT) of RNA into cDNA was performed using miRCURY LNA Universal RT microRNA PCR (Exiqon). This reaction allows miRNA polyadenylation and reverse transcription in a single reaction step, simplifying the procedure compared to systems that require miRNA-specific first-strand synthesis. This first step of universal reverse transcription was followed by real-time PCR amplification with locked nucleic acid (LNA)-enhanced primers. The miRCURY LNA miRNA PCR Assay system is a miRNA-specific, LNA-based system designed for sensitive and accurate detection of miRNAs by quantitative real-time PCR using SYBR Green, which allows quality control of the resulting PCR amplicon by melting curve analysis.

The universal reverse transcription combined with LNA-enhanced and melting temperature (Tm) -normalized primers allows accurate and reliable quantification of individual miRNAs from as little as 1 pg of total RNA. It enables accurate quantification of very low levels of miRNA without pre-amplification given its exceptional sensitivity and extremely low background, making it suitable for many types of samples, including serum, plasma and other biological fluids.

Relative microRNA expression levels were obtained using the ΔΔCt method [228]. For normalization the following control primer sets were used: U6 snRNA, SNORD48 and hsa-miR-25-3p. In order to chooce a stable endogenous reference miRNA that could be used also in human samples, mouse miRNA microarray data corresponding to 12 samples, 6 NOTCH1 HD-ΔPEST (3 DBZ treated and 3 DMSO treated) and 6 NOTCH1 ΔE (3 DBZ treated and 3 DMSO treated), were considered. Data were normalized all together using two different methods: 1) RMA normalization starting from the foreground signal; 2) quantile normalization, starting from the BG subtracted signal produced by Feature Extraction software together with the half option (to set at 1 the negative values). MiRNAs were then ranked according to the variability of their $\log_2$-expression across the 12 samples, leading to two different lists, one for each normalization method. The miRNA mmu-miR-25-3p was found among the most stable miRNAs in both lists and chosen as endogenous reference miRNA.

Primer sequences used in the RT-qPCR are reported below:

miRNA	Target Sequence
hsa-miR-17-5p	5'- CAAAGUGCUUACAGUGCAGGUAG-3'
hsa-miR-18a-5p	5'-UAAGGUGCAUCUAGUGCAGAUAG-3'
hsa-miR-20a-3p	5'- ACUGCAUUAUGAGCACUUAAAG -3'
hsa-miR-92a-3p	5'- UAUUGCACUUGUCCCGGCCUGU -3'
hsa-miR-199a-5p	5'-CCCAGUGUUCAGACUACCUGUUC-3'
hsa-miR-34a-5p	5'-UGGCAGUGUCUUAGCUGGUUGU-3'
hsa-miR-22-3p	5'-AAGCUGCCAGUUGAAGAACUGU-3'
hsa-miR-25-3p	5'-CAUUGCACUUGUCUCGGUCUGA-3'

3.8 Cell lines and drug treatments

T-ALL cell lines were cultured in RPMI 1640 (Euroclone) medium supplemented with 10% fetal bovine serum, 1% Ultraglutamine, 1% Na-Piruvate, 1% Hepes, 100U/ml penicillin G and 100 μg/ml streptomycin (Lonza) at 37°C in a humidified atmosphere under 5% CO_2.

For *in vitro* studies, cells were plated at a density of 0.25-0.3x10^6/mL in triplicate in 24 well-plates, for each experimental condition. The potent γ-secretase inhibitor, Dibenzazepine (DBZ) was dissolved in DMSO and added to the culture medium at the final concentration of 250nM. Control wells were treated with an equivalent percentage of DMSO (vehicle). After 72 hours of treatment, cells were pelleted and used to obtain RNA and protein lysates.

3.9 Cell viability assays

Cell viability analysis was performed by the bioluminescent method Vialight plus (Lonza) after 72h. The principle of this assay is based on bioluminescent detection of cellular ATP as a measure of cell viability. This test consists in quantification of light emission, produced by the oxidative reaction of the Luciferase enzyme on luciferin substrate, that require ATP. Briefly, 100µL of cell culture from each P24 well were transferred in duplicate in a dark 96-well plate and incubated for 5 minutes at room temperature. 50µL of Mammalian cell lysis solution was then added and incubated for 15 minutes at room temperature. Subsequently, 100µL of ATPlite substrate was added to each well and after 2 minutes of incubation, luminescence signal was detected with PerkinElmer's Victor plate reader.

3.10 Western blotting

Whole cell lysates were performed using Ripa Buffer (20mM Tris-HCl (pH 7.5), 15mM NaCl, 1mM Na2EDTA, 1mM EGTA, 1% NP-40, 1% sodium deoxycholate, 2.5mM sodium pyrophosphate, 1mM beta-glycerophosphate, 1mM Na3VO4, 1µg/ml leupeptin), supplemented with phosphatase (NaF 50mM, Na3OV4 1mM) and protease inhibitors (Sigma), for 30 minutes on ice. Lysates were then centrifuged at 13000 rpm for 30 minutes at 4°C, supernatants collected and stored at -80°C until use. Samples were quantified with the Micro BCA™ Protein Assay Kit (Thermo Scientific) according to manifacturers instructions. For Western blotting, approximately 20µg of proteins were separated on 4-12% gradient NuPAGE® Bis-Tris poly-acrylamide or 3-8% gradient NuPAGE® Tris-Acetate SDS-PAGE gels (Life Technologies) and then were transferred onto nitrocellulose membranes (Protran). Membranes were blocked in Dulbecco's Phosphate Buffer Saline-0.1%Tween-20 (PBS-T) containing 5% nonfat milk and then incubated over night at 4°C with primary antibodies. The following primary

antibodies were used: anti β-actin and anti-cleaved Notch1 (Val1744) from Cell Signaling Technologies; anti c-myc (9E10), anti α-tubulin from Santa Cruz Biotechnology and anti PGC1-beta from Abcam. The next morning, membranes were washed three times with PBS-T for ten minutes each, before incubation for 1 hour with the appropriate secondary antibodies conjugated with horseradish peroxidase (HRP). After the incubation with the secondary antibody, three washes of ten minutes each were performed before image acquisition. For immunodetection, nitrocellulose membranes were incubated with chemiluminescence reagent, obtained by mixing equal volumes of Western Lightning® Plus ECL Enhanced Luminol Reagent Plus and Western Lightning® Plus ECL Oxidizing Reagent Plus (PerkinElmer). Images were acquired with BioRad ChemiDoc XRS and analysed with Quantity One® 1-D analysis software.

3.11 Clonogenic assay

Colony forming unit (CFU) assays were performed by plating in 35x10mm Petri dishes an equivalent of 1000 T-ALL cells over-expressing hsa-miR-22 or empty vector control in 1ml of Methylcellulose Medium. This medium was composed of 40% Methocult H4100 (Stemcell Technologies) containing 2.6% methylcellulose in Iscove's Modified Dulbecco's Medium (IMDM), 20% fetal bovine serum and 40% RPMI 1640 medium, complemented with 1% Ultraglutamine, 1% Na-Piruvate, 1% Hepes, 100U/ml penicillin G and 100 μg/ml streptomycin (Lonza). Cultures were then incubated at 37°C in a humidified atmosphere of 5% CO2 in air. For each condition, triplicate dishes were prepared. After 7, 14 and 21 days, colonies were counted using an inverted microscope (Leica) and a 60mm gridded scoring dish.

3.12 Xenografts and *in vivo* treatment studies and imaging

Frozen T-ALL (PDTALL) xenograft cells were obtained from our collaborator Dr. Stefano Indraccolo (IOV, Padova). After thawing, $10x10^6$ viable T-ALL cells (in 400 µl PBS) were injected intra-venous (i.v.) in 6-8 week old NOD.Cg-*Prkdc*^{scid} *Il2rg*^{tm1Wjl}/SzJ (NSG) immunodeficient mice. Procedures involving animals and their care conformed with institutional guidelines that comply with national and international laws and policies (EEC Council Directive 86/609, OJ L 358, 12 December, 1987).

The degree of T-ALL engraftment in mice was monitored by periodic blood drawings and flow cytometric analysis of human CD45. When mice showed signs of leukemia development, they were randomized and injected intraperitoneally (i.p.) with either a potent GSI, Dibenzazepine (DBZ) (5mg/kg) or DMSO (vehicle) for three times every 8 hours. Each experimental group consisted of at least n=3 mice. After this treatment, mice were sacrificed and T-leukemia cells were isolated from fully infiltrated spleens to obtain RNA and protein lysates.

To evaluated the *in vivo* effects of miR-22-3p overexpressing, we transduced T-ALL cell lines (MOLT-4 and JURKAT E6), previously engineered to express luciferase reporter gene (FUW-Luc-mCherry-puro or MIGR1-mCherry-Luc2), with pLenti-III-GFP pre-hsa-mir-22 or an pLenti-III-GFP empty vector control. MOLT-4 T-ALL cells expressing luciferase were generated by infected them with FUW-Luc-mCherry-puro and subsequent selection *in vitro* with puromycin. Subsequently these cells were transduced with a lentiviral vector over-expressing pre-hsa-mir-22 or the empty vector, and sorted for green fluorescent protein (GFP) expression by flow cytometry. On the other hand, JURKAT T-ALL cells were initially infected with MIGR1-mCherry-Luc2 and sorted for mCherry fluorescent protein. Subsequently these cells were transduced with a lentiviral vector over-expressing pre-hsa-mir-22 or the empty lentiviral vector and selected *in vitro* with puromycin.

Before the execution of *in vivo* experiments with the above mentioned cells, we evaluated *in vitro* the expression levels of the luciferase reporter gene. To this

end, selected/sorted cells ($1x10^6$ cells) were collected and washed with PBS before cell lysis using the passive lysis buffer (Promega). Cell pellets were lysed in 100 µl of passive lysis buffer for 20 minutes at room temperature. Subsequently, cell lysates (10 µl per well) were added to a dark 96-well plate and luciferase assay reagent (50 µl) was added to each well. Firefly luciferase activity was measured with VICTOR™ X5 Multilabel Plate Reader (Perkin Elmer).

For *in vivo* experiments, we injected $5x10^6$ miR-22 over-expressing or control T-ALL cells expressing luciferase i.v. into 6–8-week-old female immunodeficient NOD.Cg-*Prkdc*^{scid} *Il2rg*^{tm1Wjl}/SzJ (NSG) mice. After a 7 day window for tumor engraftment, we evaluated disease progression by *in vivo* bioimaging with the *in vivo* Imaging System IVIS Spectrum (Xenogen). Briefly, for imaging studies, mice were anesthetized by isoflurane inhalation and injected with D-luciferin (Synchem) at 50 mg/kg intraperitoneum. After 5 minutes from luciferin injection, mice were imaged. Tumor bioluminescence was quantified by integrating the photonic flux (photons/s) or total counts through a region encircling each mouse as determined by the LIVING IMAGES software package (Xenogen).

All mice were monitored daily and animals showing overt signs of disease or excessive weight loss were euthanized following Institutional Animal Care and Use Committee guidelines.

Further, the effects of miR-22-3p overexpression *in vivo* were also evaluated using the Kaplan-Meier analysis to determine the impact on overall survival, human CD45 analysis by flow cytometry in the periphery together with spleen and liver weights to evaluate disease burden.

3.13 Mouse Cell Depletion

To enrich the human cells upon xenotransplantation, we used the Mouse Cell Depletion Kit (Miltenyi Biotec). Briefly, cells isolated from infiltrated spleens were resuspended in a specific buffer (PBS, 0.5% bovine serum albumin (BSA),

pH7.2) and added to Mouse Cell Depletion Cocktail, containing monoclonal antibodies conjugated with MicroBeads, which magnetically label mouse cells. After incubation at 4°C for 15 minutes, the cell suspension was loaded onto a MACS Column, that was placed in the magnetic field of a MACS Separator, and then the column was washed 2 times with the specific buffer. Thus, the magnetically labeled mouse cells were retained within the column, while the unlabeled cells ran through to collect the enriched human tumor cells.

3.14 Flow cytometric analysis

To evaluate the level of infiltration of the different mouse tissues by human T-ALL cells we performed flow cytometry (FACS). Briefly, cell suspensions were stained with a specific mouse anti-human CD45 (BD) allophycocyanin (APC) conjugated antibody according to manufacturer's instructions. Samples were collected on a FACSCalibur (BD Biosciences) flow cytometer, using Cell Quest software (BD Biosciences).

3.15 NOTCH1 and FBW7 mutational analysis

Genomic DNA was extracted from T-ALL cells derived from xenografts with easy DNA kit (Life Technologies). NOTCH1 and FBW7 mutation analysis was performed as previously described [133].

3.16 Meta-analysis

A large human T-ALL dataset (ArrayExpress accession number: E-GEOD-5827) was selected for meta-analysis. Processed data were loaded in the R statistical environment, log2-transformed, and differential gene expression analysis was performed using the Bioconductor limma package [223].
Functional analysis was performed using gene set enrichment analysis (GSEA) v3.0 [229]. Differentially expressed genes were ranked by decreasing moderated t-statistics and GSEA-Preranked was run with default parameters against the c3 collection of the Molecular Signatures Database (MSigDB) v6.0, containing gene sets representing potential targets of regulation by transcription factors or microRNAs. Additional gene sets with putative targets of miR-22 obtained from different microRNA target prediction softwares (DIANA-microT-CDS, TargetScan, miRDB) were included in a further analysis performed to identify miR-22 targets significantly down-regulated following GSI treatment.

3.17 Statistical analysis

Results were expressed as mean value ± standard deviation (SD). Statistical data analysis was performed using Student's t-test (two tailed, unpaired). Survival in animal experiments was represented with Kaplan-Meier curves and significance was estimated with the log-rank test (Prism GraphPad). Differences were considered statistically significant: *$p<0.05$, **$p<0.01$, ***$p<0.001$.

4 Results

4.1 NOTCH1-induced leukemias are highly sensitive to γ-secretase *in vivo*

We generated a mouse model of NOTCH1-induced leukemia by retrovirus-mediated overexpression of a constitutively active oncogenic mutant form of the NOTCH1 receptor (L1601P-ΔPEST) in hematopoietic Lin^- progenitors (Figure 1A upper panel), as previously reported [97]. Forced expression of NOTCH1 in Lin^- progenitors induce primarily ectopic T cell development and subsequently T-cell leukemia [230]. In details, we used the activated form of NOTCH1 L1601P-ΔPEST, that closely resembles human *NOTCH1* mutant alleles and contains a mutation in the heterodimerization domain (HD) and a deletion in the PEST domain (HD-ΔPEST), inducing ligand-independent activation of the receptor together with increased NOTCH1 activated protein stability. The *NOTCH1* L1601PΔPEST is considered a weak allele and transplanted mice, developed T-ALL in 3-5 months with a 20% penetrance.

In this way, we obtained a homogenous model where T-cell leukemia is highly dependent on NOTCH1 in contrast to human primary T-ALL samples that are characterized by additional alterations and to human T-ALL cell lines that are even more complex due to additional alterations linked to prolonged *in vitro* culture.

The NOTCH1-induced tumors (HD-ΔPEST) were treated with a potent γ-secretase inhibitor (GSI) to block NOTCH1 signaling. Briefly, we generated secondary NOTCH1-induced T-ALL injecting primary T-cell tumors into isogenic irradiated hosts and, when mice showed signs of leukemia development, we treated them with 5mg/kg of a potent GSI, Dibenzazepine (DBZ), for three times every 8 hours. In parallel, we treated mice with vehicle alone (DMSO) to generate a control group (Figure 1A, lower panel). The murine NOTCH1-induced T-ALLs resulted sensitive to DBZ, as demonstrated by strong down-regulation of Deltex, a direct NOTCH1 target gene, respect to vehicle treated mice ($P<0.001$; Figure 1B).

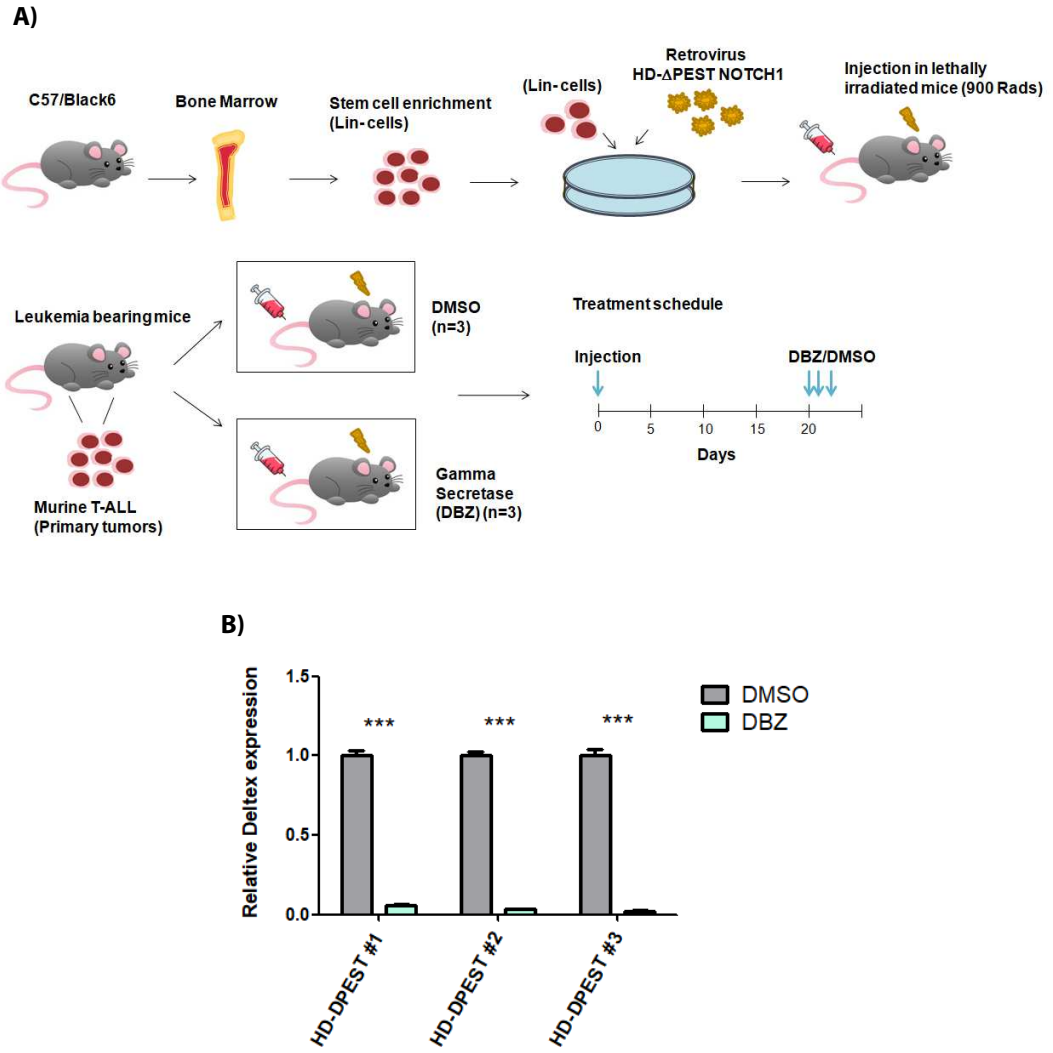

Figure 1. Treatment with a potent γ-secretase inhibitors, Dibenzazepine (DBZ), induces NOTCH1 pathway inhibition *in vivo*. (A) Schematic representation of the strategy used for the generation of primary T-ALL tumors by retrovirus-mediated overexpression of a constitutively active oncogenic mutant form of the NOTCH1 receptor (L1601P-ΔPEST) in hematopoietic lineage negative (Lin-) progenitors (upper panel). Secondary NOTCH1-induced T-ALL were obtained by injecting primary T-cell tumors into isogenic irradiated hosts; mice showing signs of leukemia development, were treated with vehicle only (DMSO) or with 5mg/kg of a potent GSI, Dibenzazepine (DBZ), for three times every 8 hours (lower panel). After this treatment, mice were sacrificed and T-leukemia cells were isolated from infiltrated spleens to obtain RNA and protein lysates. (B) qRT-PCR analysis of Deltex, a direct target of NOTCH1 (*** P<0.001; data is represented as Mean±SD. Assays were performed in triplicates).

We further analyzed the global effect of NOTCH1 inhibition using gene expression profiling analysis, SurePrint G3 Mouse GE 8x60K Agilent Microarray, that allow the study of the regulation of 27000 genes and 4578 lncRNAs. For this purpose, we extracted the RNA from the spleens of NOTCH1 induced T-leukemia bearing mice treated with DBZ (n=3) or DMSO (n=3), as previously described.

Differential expression analysis showed 728 significantly down-regulated and 878 significantly up-regulated genes upon DBZ treatment (FDR<0.01), see Supplementary Table 1 for the list of most differentially expressed genes (|FC|>4). Functional analysis using Gene Set Enrichment Analysis (GSEA) showed that the MSigDB hallmark gene sets related to NOTCH signaling and MYC targets were significantly down-regulated following NOTCH1 inhibition (Supplementary Table 2), as demonstrated in previous studies [102,103], confirming the validity of our experimental model.

4.2 Identification of differentially expressed microRNAs following *in vivo* NOTCH1 inhibition

In parallel to gene expression analysis, the murine NOTCH1-induced T-leukemia samples were hybridized on mouse miRNA 8x60K microarrays (release 19.0; Agilent), that allow the determination of 1247 mouse miRNAs. Microarray data analysis of NOTCH1 HD-ΔPEST tumors in the two experimental conditions (treatment with DBZ or with DMSO) was performed in the R/Bioconductor statistical environment (see Methods) and only microRNAs with FDR<0.10 were considered significant. Differential expression analysis revealed 68 differentially regulated microRNAs, of which 37 down-regulated and 31 up-regulated. At top of the list of NOTCH1 down-regulated miRNAs we found several components of the miR-17-92 cluster (Supplementary Table 3 and Figure 2), previously reported as highly expressed in T-ALL samples [53,54].

Amongst the up-regulated miRNAs we expected to find putative tumor suppressor miRNAs, that resulted lowly expressed in NOTCH1-induced T-ALLs and subsequently induced after DBZ treatment. Interestingly, we identified several microRNAs that have been previously reported as tumor suppressors in other

malignancies, such as miR-22 [231] and miR-34a [232], or, alternatively, linked to NOTCH1 signaling in other contexts, such as the miR-199a [233-235].

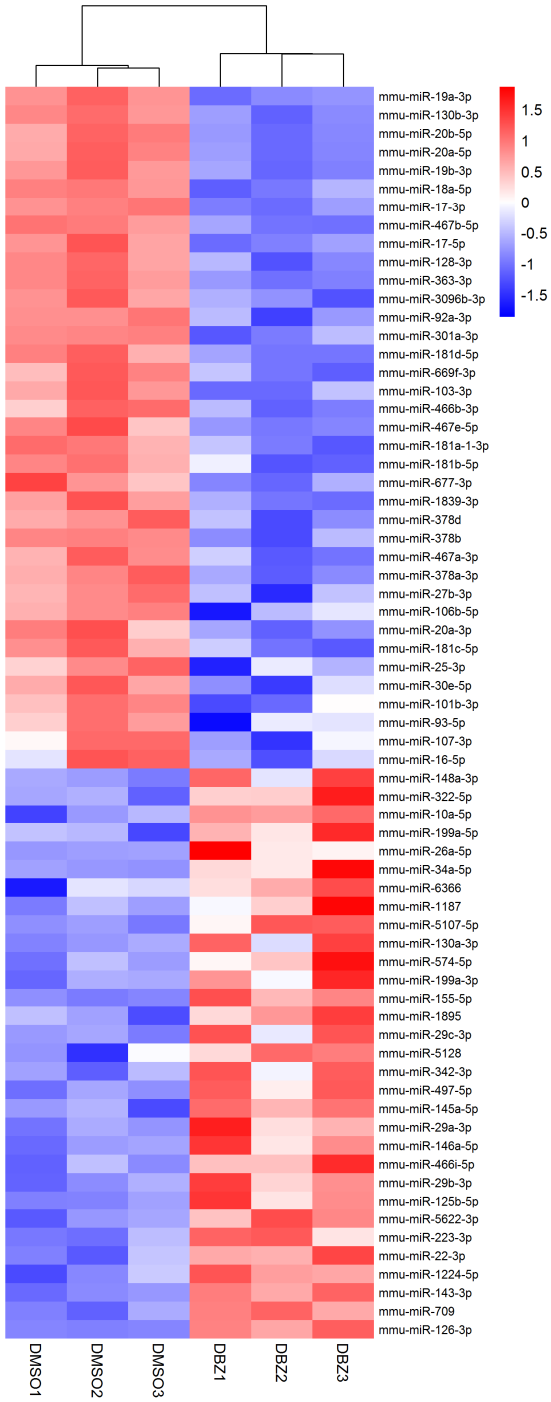

Figure 3. Heat map of microRNAs significantly regulated following NOTCH1 pathway inhibition *in vivo*. MicroRNA expression profiling was performed in three biological replicates of the same HD-ΔPEST NOTCH1 T-cell tumors treated *in vivo* with vehicle only (DMSO) or with 5mg/kg of a potent GSI, Dibenzazepine (DBZ), for three times every 8 hours. The heat map shows the significantly differentially expressed miRNAs (FDR < 0.10), ordered from the most down-regulated (top) to the most up-regulated (bottom) in DBZ-treated vs.control.

4.3 miR-17-92 is repressed following NOTCH1 inhibition in human T-ALL

The miR-17-92 cluster, containing six individual miRNAs miR-17, miR-18a, miR-19a, miR-19b-1, miR-19a, miR-20a and miR-92-1, was previously reported to be highly expressed in a murine model of NOTCH1-induced T-ALL [54], but the extent of their specific regulation in human T-ALL cells upon NOTCH1 inhibition has not been previously investigated.

In order to investigate this aspect, we treated different NOTCH1-mutated T-ALL cell lines (KOPTK1, CUTLL1, HPB-ALL, DND41, PF382, JURKAT E6, MOLT3, MOLT4, CCRF-CEM) *in vitro* for 72 hours with 250nM of DBZ or vehicle only (DMSO). We first assessed the efficacy of NOTCH1 inhibition following DBZ treatment using western blot analysis for activated NOTCH1 (ICN1) and c-MYC. This analysis confirmed the down-regulation of intracellular NOTCH1 (ICN1) and c-MYC, a direct target of NOTCH1 (Figure 4A). In addition, using qRT-PCR, we found that Deltex was also strongly repressed ($P<0.001$; Figure 4B).

We thus analyzed the expression of different components of the miR-17-92 cluster that resulted regulated in our murine microRNA expression profiling analysis: miR-17-5p, miR-18a-5p, miR-20a-3p and miR-92a-3p. To this end, we performed Exiqon qRT-PCR analysis, that consists in a single, universal reverse transcription reaction which serves as template for subsequent real-time PCR amplifications. This real-time PCR is based on SYBR Green with use of LNA-enhanced primers specific for the different miRNAs.

Two components of the 17-92-cluster resulted significantly down-regulated in several T-ALL cell lines after NOTCH1 pathway inhibition (Figure 4.C-F). More specifically, miR-20a-3p and miR-92a-3p resulted significantly down-regulated in several cell lines (in 6 and in 5 out of the 9 T-cell lines analyzed, respectively), indicating that these miRNA may have an important role downstream of NOTCH1 in human T-ALL. Notably, the regulation of the 17-92-cluster resulted particularly relevant in CCRF-CEM, DND41, MOLT4 and PF382 cell lines while, in other T-ALL cell lines (HPB-ALL, MOLT3, JURKAT E6 and CUTLL1), only

one or two components of the 17-92-cluster were regulated. On the other hand, KOPTK1 cells showed modest up-regulation of the 17-92-cluster following NOTCH1 inhibition.

Overall, these data showed that miR-17-92 cluster is mainly downregulated upon NOTCH1 inhibition in human T-ALL cells. However, although the role of the 17-92-cluster downstream NOTCH1 is relatively well known, the regulation of the specific components appear variable and cell context dependent.

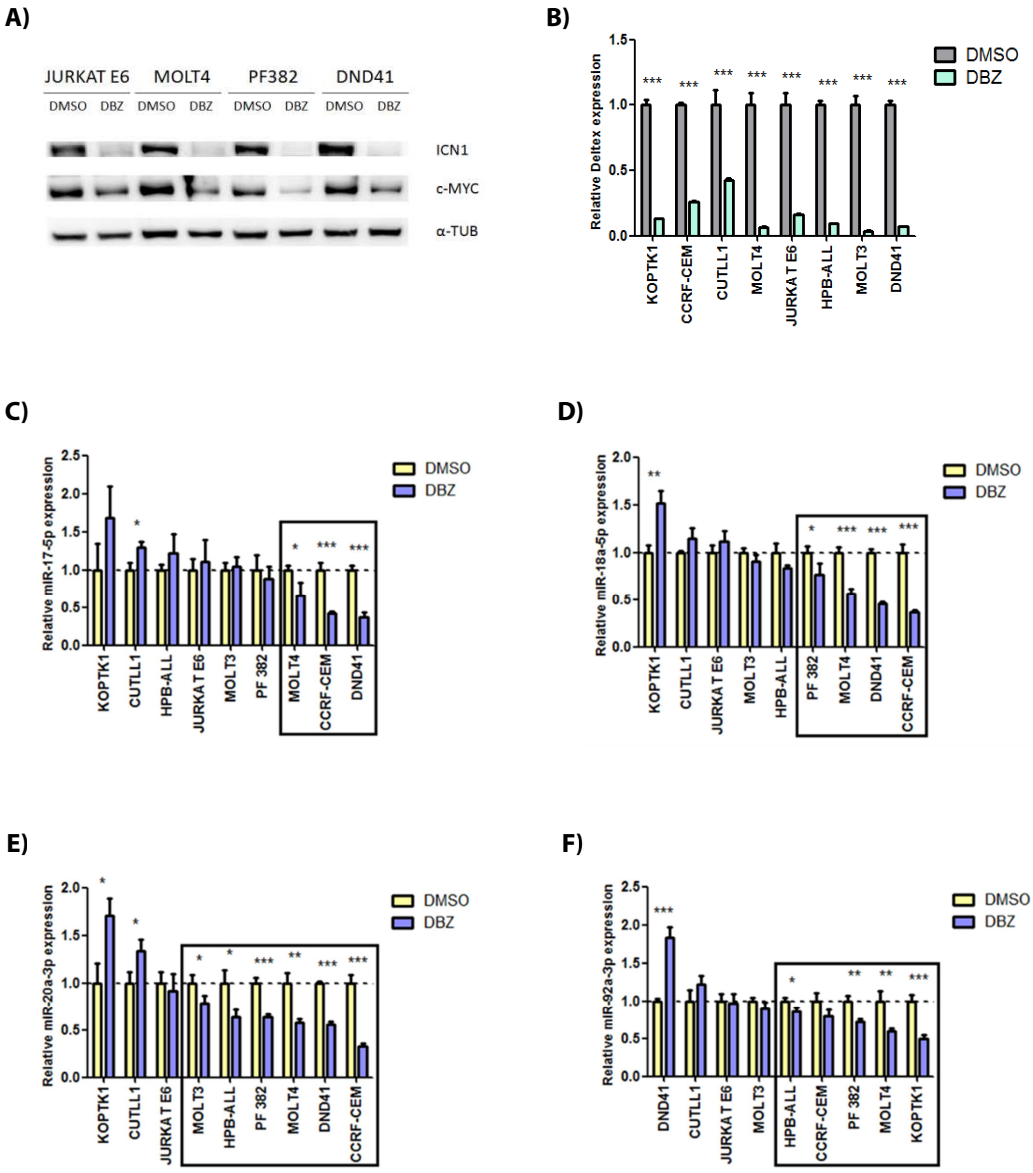

Figure 4. Down-regulation of miR-17-92 cluster after GSI treatment in human T-ALL cells. (A) Representative Western blot of Intracellular NOTCH1 (ICN1) and its direct target, c-Myc, in *NOTCH1* mutated T-ALL cell lines, treated *in vitro* with vehicle only (DMSO) or with 250nM of DBZ for 72 hours. (B) The same cell lines were investigated for the

regulation of Deltex, a direct target of NOTCH1 (*** P<0.001). Data is represented as Mean ± SD. Assays were performed in triplicate. (C-F) qRT-PCR analysis (miRCURY LNA microRNA; Exiqon) of miR-17-5p, miR-18a-5p, miR20a-3p and miR-92a-3p upon DBZ treatment (250nM, 72h) *in vitro* in NOTCH1 mutated T-ALL cell lines (KOPTK1, CUTLL1, HPB-ALL, DND41, PF382, JURKAT E6, MOLT3, MOLT4, CCRF-CEM) (* P<0.05; **P<0.01; *** P<0.001). Data is represented as Mean ± SD. Assays were performed in triplicate.

4.4 Validation of up-regulated microRNAs upon NOTCH1 inhibition in T-ALL cells

Among the putative tumor suppressor miRNAs, we identified miR-22a-3p, miR-34a-5p and miR-199a-5p, which have not been studied in the context of T-ALL and NOTCH1 inhibition.

In order to validate the regulation of these miRNAs, we extended our analysis to additional HD-ΔPEST T-tumors and to another model of murine NOTCH1-induced leukemia, that is based on the over-expression of the ΔE allele, presenting a deletion in EGF-like domain and which develop leukemia in 8-12 weeks with a 100% penetrance. This model closely resembles human T-ALL cases which present translocation of *NOTCH1* to the TCR locus [4,236]. Secondary transplants were treated with DBZ, as previously described for HD-ΔPEST T-tumors .

First of all, we confirmed the inhibition of NOTCH1 pathway in *NOTCH1* ΔE T-leukemia samples by western blot, that showed strong down-regulation of ICN1 expression in DBZ treated cells compared to DMSO treated cells (Figure 5A). In addition, Deltex, a direct target of NOTCH1, resulted significantly decreased, as demonstrated by RT-qPCR (P<0.001; Figure5B). NOTCH1 inhibition *in vivo* induced a significant up-regulation of miR-34a-5p both in HD-ΔPEST (P<0.001 and P<0.01, respectively in samples #1 and #2; Figure 5C) and in ΔE samples (P<0.01 and P<0.001, respectively in samples #1 and #2; Figure 5D). Similarly, miR-199a-5p resulted significantly up-regulated in the different samples analyzed after DBZ treatment (P<0.001, P<0.01, P<0.01and P<0.01 respectively in HD-ΔPEST #1 and #2 and ΔE #1 and #2; Figure 5D-E).

Overall, the regulation of miR-34a-5p and miR-199a-5p resulted consistent across different models of NOTCH1-induced leukemia, suggesting a role in murine NOTCH-induced T-ALL.

However, their function could not be validated in the human setting due to undetectable expression in human T-ALL cell lines and xenografts both in basal conditions and upon DBZ treatment.

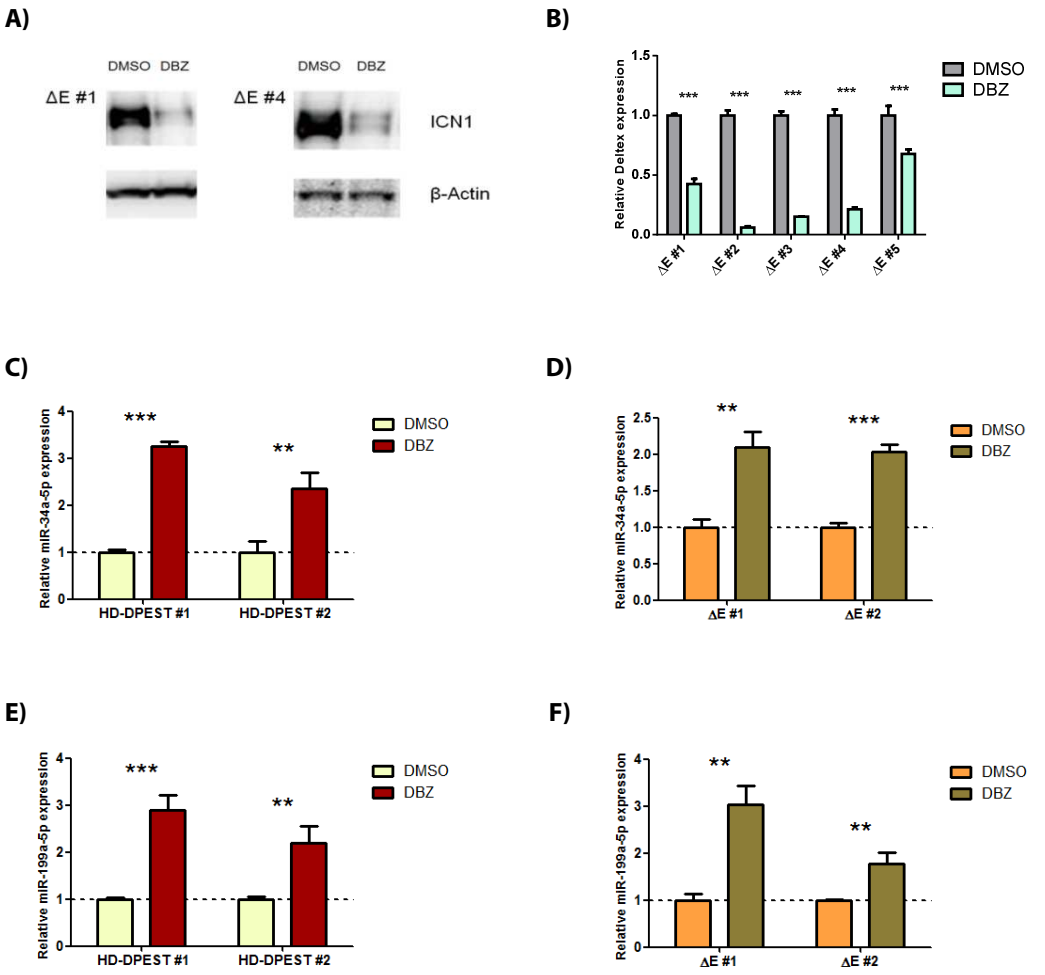

Figure 5. Up-regulation of miR-34a-5p and miR-199a-5p after GSI treatment in murine T-ALL. (A) Representative Western blot of Intracellular NOTCH1 (ICN1) in *NOTCH1* ΔE tumors, treated *in vivo* with vehicle only (DMSO) or with 5 mg/kg of DBZ for 3 times every 8 hours. (B) The same *NOTCH1* ΔE tumors were analyzed for the expression of Deltex, a direct target of NOTCH1 (*** P<0.001). Data is represented as Mean ± SD. Assays were performed in triplicate. (C-F) qRT-PCR analysis (miRCURY LNA microRNA; Exiqon) of miR-34a-5p and miR-199a-5p upon DBZ treatment *in vivo* in murine models of NOTH1-induced T-ALLs (HD-ΔPEST and in ΔE, respectively) (** P<0.01; *** P<0.001). Data were represent as Mean ± SD. Assays were performed in triplicate.

Another interesting NOTCH1-regulated microRNA resulted the miR-22a-3p. We first validated the expression of miR-22-3p in additional murine T-ALL tumors, where it resulted significantly up-regulated upon DBZ treatment in both HD-ΔPEST (n=3 samples) (Figure 6A) and ΔE (n=5 samples) (Figure 6B) NOTCH1-induced T-ALL samples.

We then assessed its regulation in human T-ALL cells. The *NOTCH1* mutated T-ALL cell lines, KOPTK1, CUTLL1, HPB-ALL, DND41, PF382, JURKAT E6, MOLT3, MOLT4, CCRF-CEM, previously investigated for miR-17-92 cluster, were tested for miR-22-3p expression upon *in vitro* DBZ treatment (250nM) for 72 hours. Amongst the different cell lines analyzed, we found that miR-22-3p resulted significantly up-regulated in 7 out of 9 cell lines (Figure 6C).

In order to check whether this regulation could also happen in patient samples, we used different patient-derived T-ALL (PDTALL) xenografts, previously derived in our Institute, that closely resemble primary T-ALL samples. The samples have been previously characterized for NOTCH1 and FBXW7 mutations (Table 1)[133]. To this end we expanded selected samples in immunodeficient mice NSG and when mice showed signs of leukemia, we treated them with 5mg/kg of DBZ for three times every eight hours. T-cell suspensions were obtained from spleens of sick mice, that were subsequently systematically depleted from murine cells using magnetic beads. This allowed us to restrict microRNAs analysis to only the human component, which resulted enriched from about 85% to 97%, as shown by flow cytometry analysis (Figure 6D). These tumors showed strongly down-regulation of ICN1 upon DBZ treatment, confirming the inhibition of NOTCH1 pathway (Figure 6E). Importantly, we found that miR-22-3p was significantly up-regulated upon GSI treatment in PDTALL samples that present strong *NOTCH1* alleles (PDTALL #25, #8 harbouring HD-ΔPEST mutations) or NOTCH1 and FBXW7 mutations (PDTALL #46, #47). PDTALL #12 was an exception because miR-22 expression remained constant after DBZ treatment, despite a strong mutation in *NOTCH1* (HD-ΔPEST). Differently, in xenografts with weak *NOTCH1* alleles (PDTALL #39, #11 having HD mutations) miR-22-3p was not consistently regulated (Figure 6F). Interestingly, PDTALL #9 and #48, classified as wild type for NOTCH1 and FBW7, did not regulated miR-22-3p upon DBZ treatment.

Thus, the regulation of miR-22 expression upon NOTCH1 inhibition in human PDTALL xenografts seems to depend on the NOTCH1 and FBW7 mutational status, with strong NOTCH1 signaling been associated with modulation of miR-22 expression following DBZ treatment, suggesting a possible interaction between NOTCH1 pathway and miR-22.

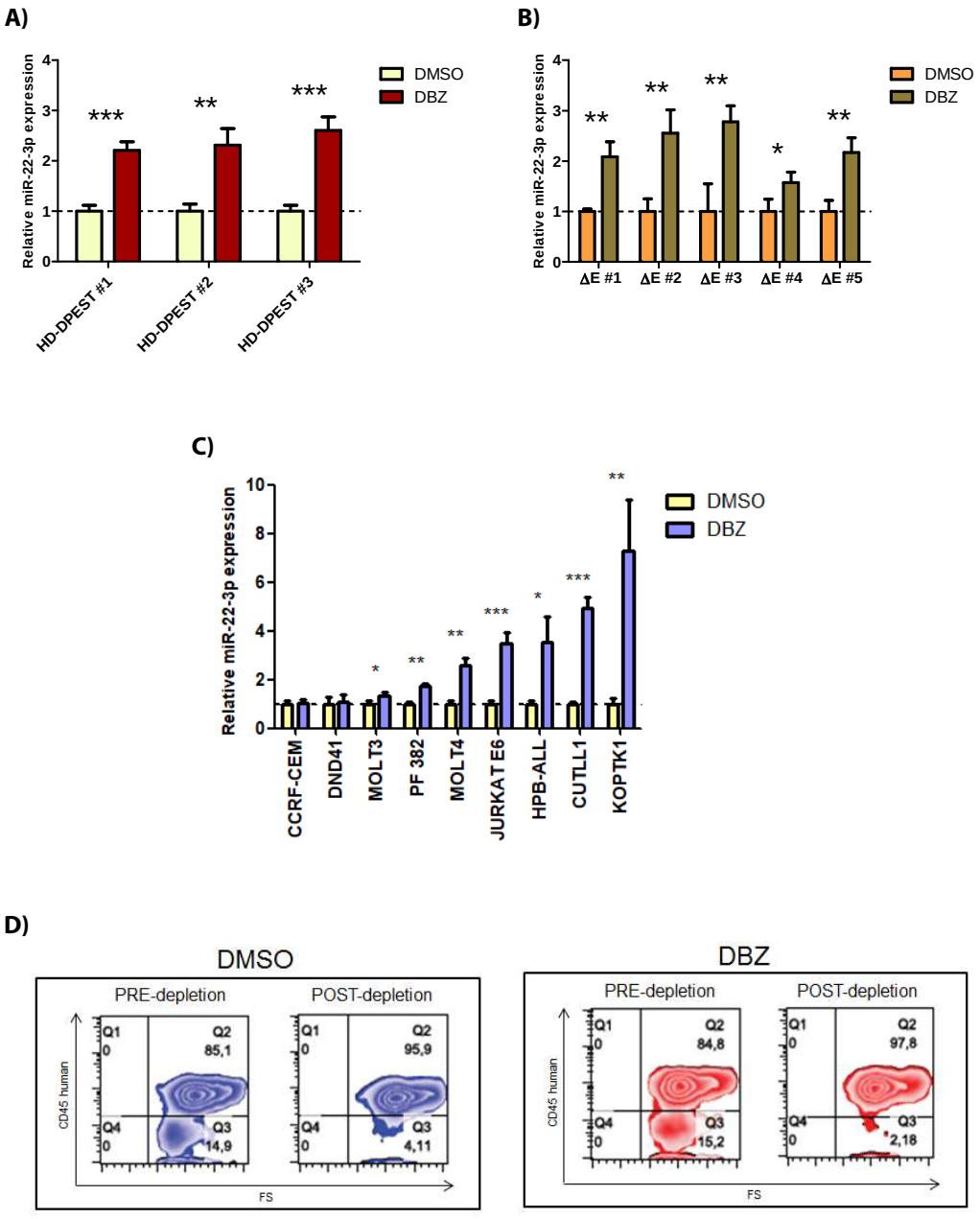

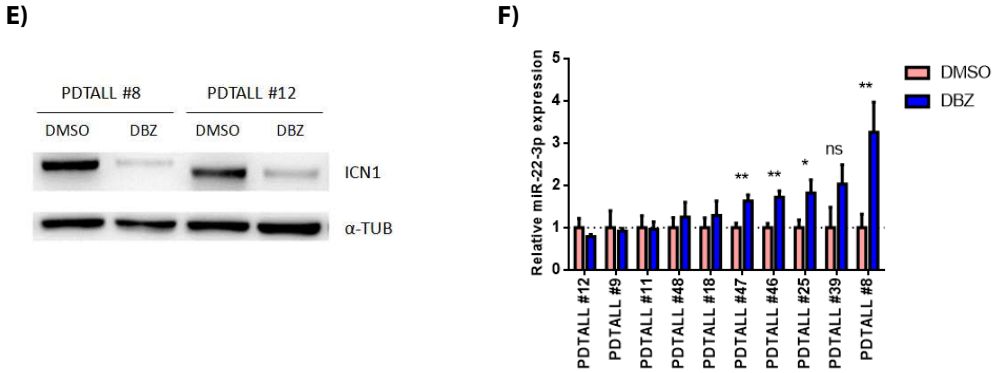

Figure 6. Up-regulation of miR-22-3p following γ-secretase inhibitor treatment in NOTCH1-induced T-ALL. (A-B) qRT-PCR analysis (miRCURY LNA microRNA; Exiqon) of miR-22-3p upon DBZ treatment *in vivo* in murine models of NOTCH1-induced T-ALLs (HD-ΔPEST and ΔE) (* P<0.05; ** P<0.01; *** P<0.001). Data is shown as Mean ± SD. Assays were performed in triplicate. (C) The same analysis was performed in NOTCH1 mutated T-ALL cell lines (KOPTK1, CUTLL1, HPB-ALL, DND41, PF382, JURKAT E6, MOLT3, MOLT4, CCRF-CEM) after treatment with 250nM of DBZ for 72h (* P<0.05; **P<0.01; *** P<0.001). Data is represented as Mean ± SD. Assays were performed in triplicate. (D) T-cell suspensions obtained from human T-ALL xenografts were systematically depleted from murine cells using magnetic beads (Mouse Cell Depletion Kit) to allow microRNA analysis of the human component. Representative dot plots are shown. (E) Representative Western blot of Intracellular NOTCH1 (ICN1) in patient-derived T-ALL (PDTALL), expanded in immune-deficient mice (NSG), treated *in vivo* with vehicle only (DMSO) or with 5mg/kg of DBZ for three times every eight hours. (F) The PDTALL #8, #9, #11, #12, #48, #18, #25, #39, #46, #47, following depletion of murine cells, were investigated by qRT-PCR for miR-22-3p expression. Data is represented as Mean ± SD. Assays were performed in triplicate.

PDTALL	***NOTCH1* status**	***FBW7* status**
8	HD-ΔPEST mutation	wild type
9	wild type	wild type
11	HD mutation	wild type
12	HD-ΔPEST mutation	wild type
18	JME mutation (exon 28)	wild type
25	HD-ΔPEST mutation	wild type
39	HD mutation	wild type
46	HD mutation	mutated
47	HD mutation	mutated
48	wild type	wild type

Table 1. Characteristics of T-ALL derived xenografts. List of patient-derived T-ALL (PDTALL), expanded in immune-deficient mice (NSG). NOTCH1 and FBXW7 mutational status are shown. Several of these xenografts have been previously described [133].

4.5 miR-22-3p results down-regulated in T-ALL cells respect to normal thymocytes

Our previous results showed that miR-22 was significantly down-regulated in murine NOTCH1-induced T-ALL cells upon inhibition of NOTCH1 signaling. Importantly, this result was also confirmed in human T-ALL cells treated *in vitro* and *in vivo* with γ-secretase inhibitors, suggesting a role of miR-22 in NOTCH1-induced leukemia, possibly as putative tumor suppressor. In addition, recent data showed that miR-22 has potent antitumor effects in acute myeloid cells (AML) [231].

In this scenario, we explored the role of miR-22 in human T-ALL cells. We first analyzed the expression of miR-22-3p in human T-ALL specimens (n=16, T-ALL cell lines) and we compared it with normal thymocytes (n=7). We analyzed a pool of T-ALL cell lines, composed both of NOTCH1-wild type (LOUCY, TALL1) and NOTCH1-mutated T-ALL (MOLT3, MOLT4, P12 ICHIKAWA, JURKAT E6, PF382, CUTLL1, ALL-SIL, KOPTK1, HPB-ALL, CCRF-CEM, KARPAS 45, KE 37, DND41, RPMI 8402, HSB2).

In accordance with the potential anti-tumor effects of miR-22 in T-ALL, miR-22-3p expression was significantly higher in normal human thymocytes compared to TALL cell lines ($P<0.01$; Figure 7A). Notably, the LOUCY and TALL1 cell lines, which were wild type for *NOTCH1*, presented an opposite trend respect to normal thymocytes (FC=2.18 and FC=0.18 respectively for LOUCY and TALL1). A similar trend was observed in PDTALL samples (n=10).

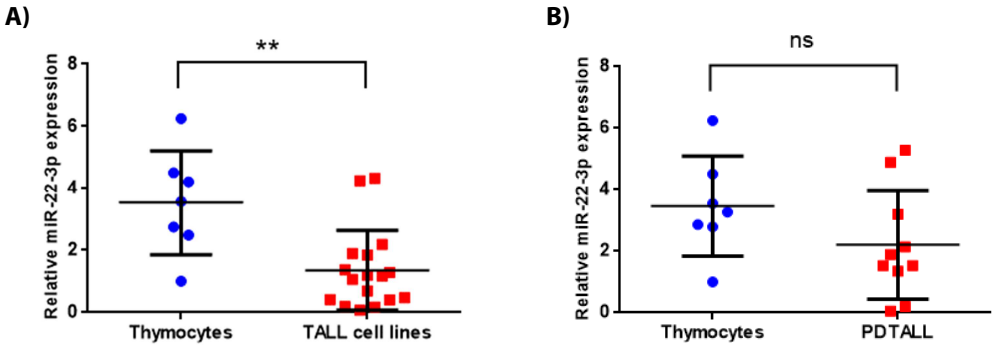

Figure 7. miR-22-3p results consistently downregulated in T-ALL cells compared to human thymocytes. (A-B) qRT-PCR analysis (miRCURY LNA microRNA; Exiqon) of hsa-miR-22 basal expression in human TALL cell lines and PDTALL samples, relative to human thymocytes (**, P<0,01).

4.6 miR-22-3p overexpression inhibits colony formation in T-ALL cells

The miR-22 has been recently reported as a tumor suppressor miRNA in acute myeloid leukemia (AML) [231]. We, thus, explored if miR-22 could be a potential tumor suppressor miR in NOTCH1-mutated T-ALL cells, infecting CCRF-CEM, JURKAT and MOLT4 T-ALL cells with the pLenti-pre-hsa-miR-22 overexpressing vector. The expression of miR-22-3p in T-ALL cells was evaluated following *in vitro* selection with puromycin. At the end of the selection, all the T-ALL cell lines significantly overexpressed miR-22 respect to control cells infected with the empty vector, as shown by quantitative PCR, (P<0.001; Figure 8A). We analyzed cell viability in the T-ALL cell lines which over-expressed hsa-miR-22 both under normal and stress culture conditions. The viability of MOLT4 cells over-expressing hsa-miR-22 appeared similar to control cells both under normal culture conditions (48 and 72 hours) and following glucose deprivation (48 hours), as shown in Figure 8B. Similar results were also reported for JURKAT E6 and CCRF-CEM cells.

In AML, the expression of miR-22 showed a significant inhibitory effect in colony forming assays [231]. We thus performed colony forming-unit (CFU) assays, that have been widely used as an *in vitro* method to monitor tumor cells

growth and proliferation. We plated the miR-22 over-expressing and control T-ALL cells in soft-agar medium (methylcellulose) at a concentration of 1000 cells/plate in triplicate. After 10-15 days, we evaluated the number of colonies in each of the replicate plates using an inverted microscope. For this assay, JURKAT E6, MOLT4 and CCRF-CEM cell lines were selected given their high transduction efficiency and their ability to form colonies *in vitro*. We found that miR-22 over-expression significantly affected colony formation in all the T-ALL cell lines analyzed ($P<0.05$, $P<0.001$ and $P<0.05$, respectively in JURKAT E6, MOLT4 and CCRF-CEM cells; Figure 8C). A representative image of control or miR-22 expressing CCRF-CEM cells is shown in Figure 8D, where it is possible to appreciate that miR-22 over-expression affects both the number and the size of the colonies.

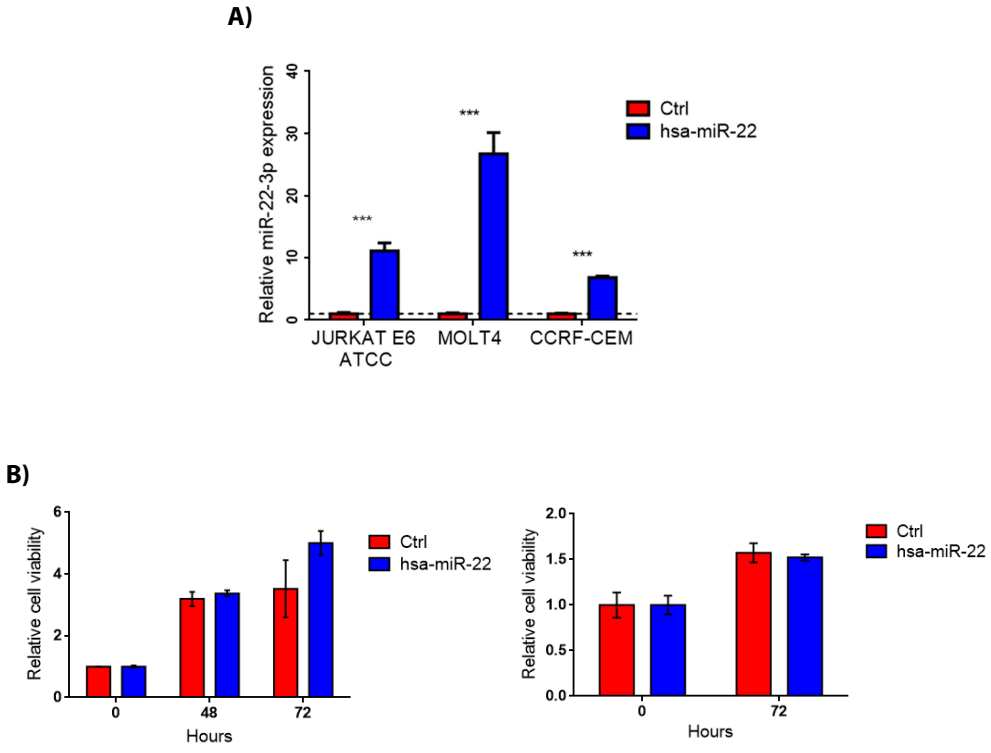

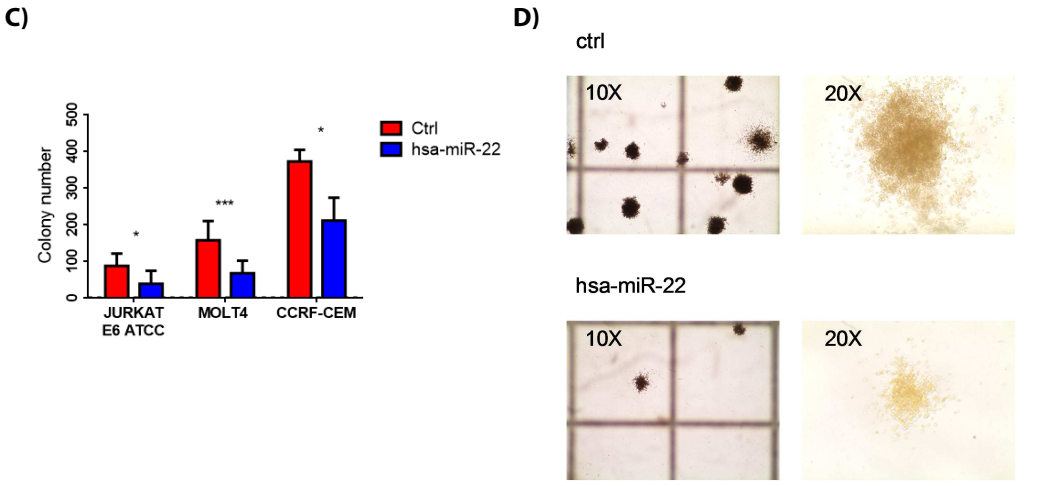

Figure 8. The over-expression of miR-22 in human T-ALL cells negatively affects growth in colony forming assays. (A) qRT-PCR analysis (miRCURY LNA microRNA; Exiqon) of hsa-miR-22 in NOTCH1-mutated T-ALL cell lines, which were infected with a lentiviral vector over-expressing pre-hsa-miR-22 or with empty vector, and subjected to puromycin selection (***, P<0.001). Data is represented as Mean ± SD. Assays were performed in triplicate. (B) Representative cell viability *in vitro* in MOLT4 T-ALL cells infected with vector empty (vector) or with vector over-expressing pre-hsa-miR-22-3p, at different time points (48h and 72h) in normal culture conditions (right panel) and following glucose deprivation (left panel). Data is represented as Mean ± SD. Assays were performed in triplicate (C-D) Effects of over-expression of hsa-miR-22 after 10 days in T cell lines in colony forming-unit (CFU) assays using methylcellulose-based medium (*, P<0.05; **, P<0.01; ***, P<0.001). Data is represented as Mean ± SD. Assays were performed in triplicate; representative images of CCRF-CEM colonies at 14 days, obtained by an inverted microscope at different magnification (10X and 20X).

4.7 miR-22-3p inhibits T-ALL cells growth *in vivo*

Since miR-22 over-expression *in vitro* determined a significant inhibitory effect on colony forming assays affecting both affecting the number and the size of the colonies, we asked whether miR-22 over-expression could influence *in vivo* growth of T-ALL cells.

We thus infected MOLT4 and JURKAT cells, previously engineered to express the luciferase reporter gene (Fuw-Luc-Cherry or MIGR1-mCherry-Luc2), with pLenti-III-GFP pre-hsa-mir-22, that allowed us to study tumor progression *in vivo*.

Cells expressing luciferase were infected with a lentiviral vector over-expressing pre-hsa-mir-22 or the empty vector as control. Subsequent selection was done with puromycin or sorting cells for GFP expression. Both MOLT4 and JURKAT E6 cells overexpressed significant levels of miR-22 respect to control cells (the empty vector), as shown by Exiqon quantitative PCR (Figure 9A) and, importantly, displayed similar levels luciferase activity, as shown by luciferase assay (Figure 9B).

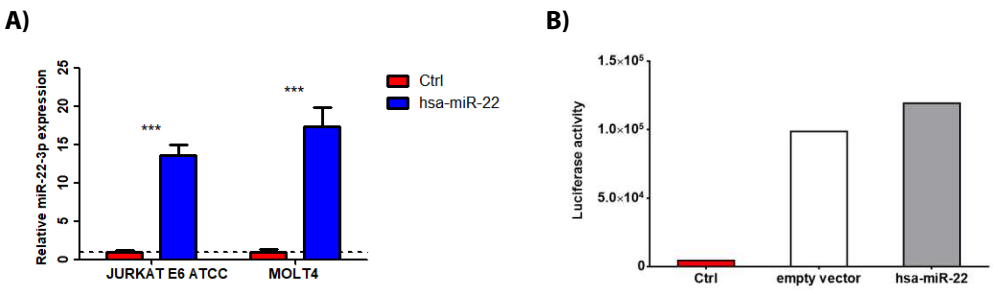

Figure 9. T-ALL cell lines stably expressing both miR-22 and luciferase. Human T-ALL cell lines expressing luciferase were engineered to stably express hsa-miR-22 or an empty vector (ctrl). (A) Exiqon qRT-PCR of hsa-miR-22 in T-ALL cells, expressing hsa-miR-22 or an empty vector (ctrl) (***, P<0.001; Data is represented as Mean ± SD. Assays were performed in triplicate). (B) JURKAT T-ALL cells were tested for Luciferase signal respect to control cells (untreated).

To generate tumors, we injected miR-22 overexpressing MOLT4 cells (n=6; $5x10^6$ cells/mouse) or MOLT4 cells infected with control vector (n=6; $5x10^6$ cells/mouse) in NSG mice. As previously described, we used the luciferase reporter gene system to quantify *in vivo* tumor growth. After 7 days from inoculation, we found that the luciferase activity signal was significantly reduced in mice injected with MOLT4 cells over-expressing hsa-miR-22 respect to the control group (Figure 10A). At day 21 post injection, most of the mice of the control group had lost weight, were sick and less active, indicating that the end-point of the experiment had been reached. We thus sacrificed the mice and evaluated the level of the infiltration of human T-ALL cells in the peripheral blood, staining cells with a specific antibody against human CD45 and analyzing samples by FACS analysis. This analysis revealed that the overexpression of miR-22-3p significantly reduced the percentage of tumor cells in the blood (**, p<0.01;

Figure 10B). Coherently, measuring the weight of the spleens and liver, we found that the over-expression of hsa-miR-22 significantly reduced their masses (***, P<0.001; Figure 10.C-D). Overall, these data indicated that the over-expression of miR-22 in MOLT4 strongly affected tumor progression *in vivo*.

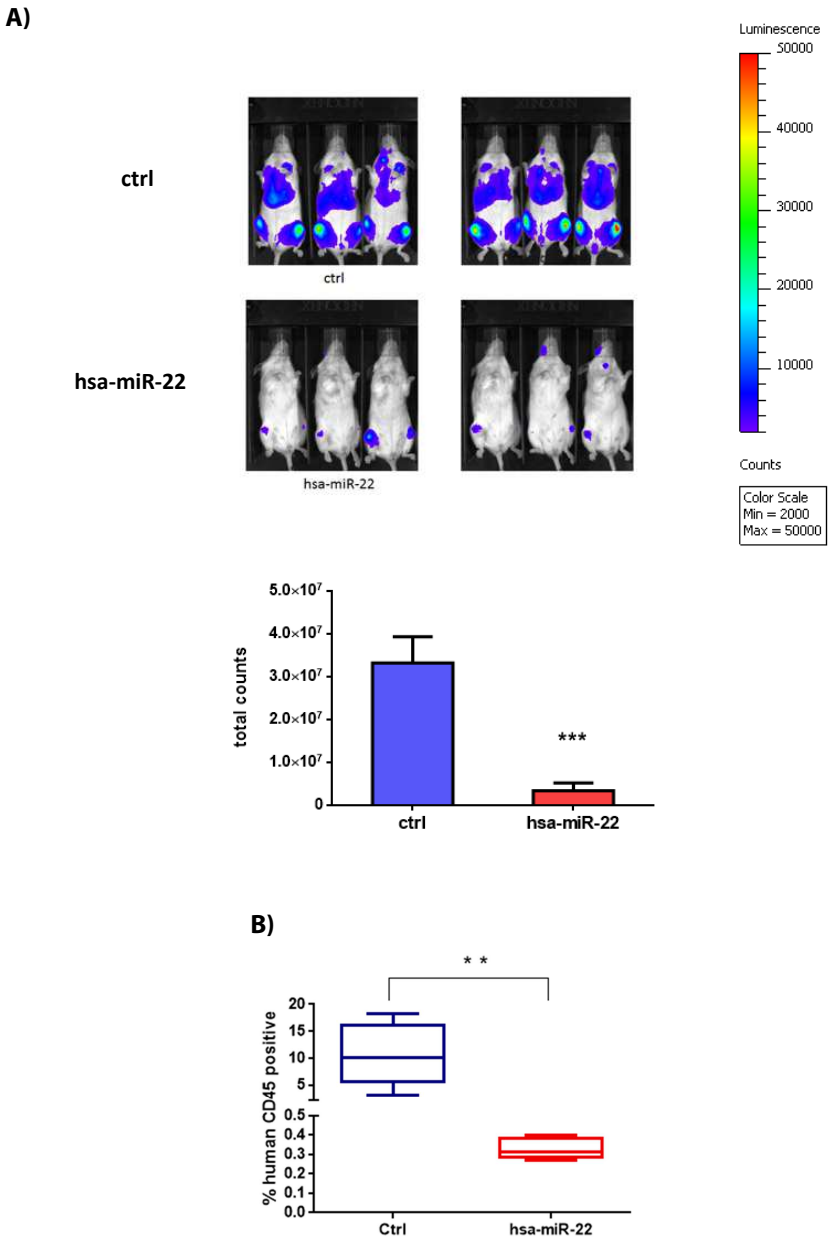

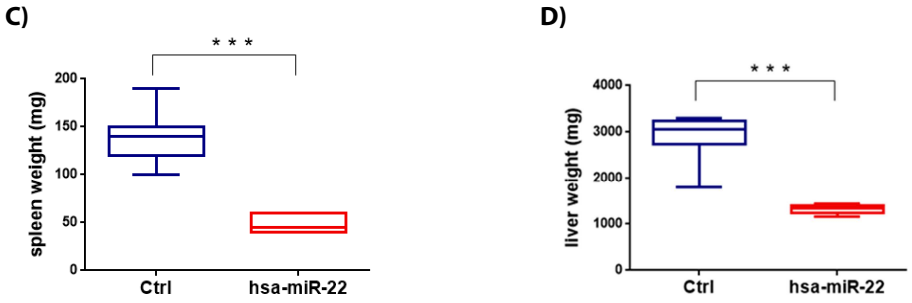

Figure 10. miR-22 inhibits MOLT4 T-ALL cells growth *in vivo*. MOLT4 cells expressing luciferase were engineered to stably express hsa-miR-22 or an empty vector (ctrl). These cells were injected to generate two different groups: "Ctrl" and "hsa-miR-22" (n=6). (A) Representative bioluminescence images of NSG mice at 7 days from the injection and luciferase activity quantification (***, P<0,001). (B) FACS analysis of human CD45 expression in the peripheral blood of NSG mice (**, P<0.01). (C-D) Quantification of spleen and liver weights at the moment of sacrifice (***, P<0,001).

We next evaluated whether miR-22 overexpression could affect overall survival. We thus established two groups of mice, by injecting MOLT4 cells, that express hsa-miR-22 (hsa-miR-22 group, n=10) or empty vector (Ctrl group, n=10). We used bioluminescence to follow disease progression. After 7 days, we observed a significant reduction in bioluminescence signal in mice over-expressing hsa-miR-22 (P<0.01) respect to the controls, similarly to the previous experiment (Figure 11A). Importantly, the Kaplan-Meier curves showed that the over-expression of hsa-miR-22 was associated with a significantly increased survival (P<0.001; Figure 11B).

These results further demonstrate that in T-ALL cells high hsa-miR-22 expression influences tumor progression, leading to slower disease progression.

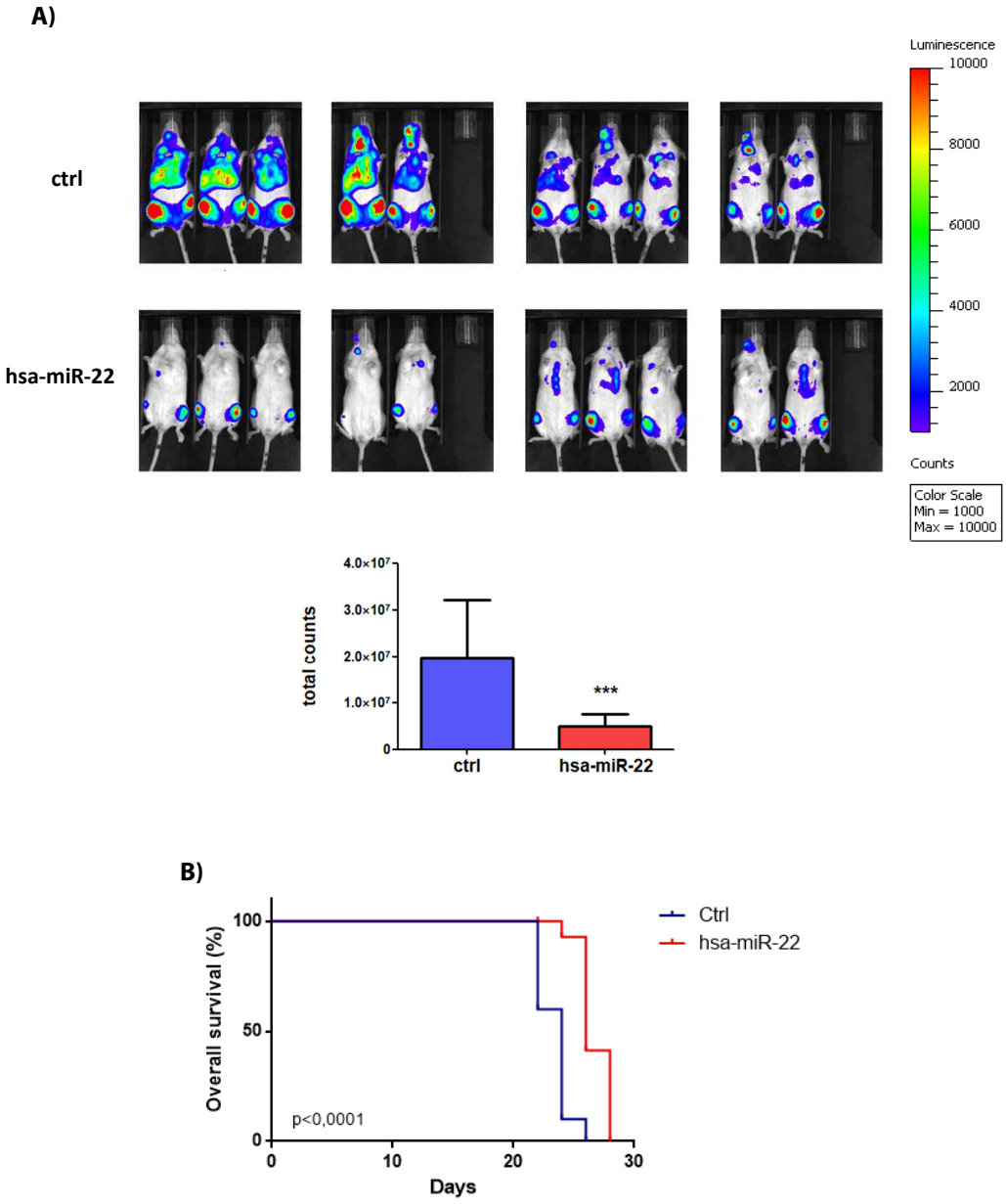

Figure 11. miR-22 over-expression increases survival *in vivo*. Human MOLT4 cells expressing luciferase were engineered to stably express hsa-miR-22 or an empty vector (ctrl). These cells were injected in NSG mice to generate two different groups: "Ctrl" and "hsa-miR-22" (n=10). (A) Representative bioluminescence images in NSG mice at 7 days from the injection are shown, together with luciferase activity quantification (**, P<0,01). (B) Kaplan-Meier analysis of survival in experimental groups.

We validated these results further using an additional cell line. Again, we established two groups of mice, injecting either JURKAT E6 cells expressing luciferase, that express hsa-miR-22 (hsa-miR-22 group, n=10) or empty vector (Ctrl group, n=10). At 14 days, we observed a similar effect, although less evident

than in MOLT4 cells. In fact there was a significant reduction in bioluminescence signal in the mice injected with JURKAT E6 cells over-expressing hsa-miR-22 respect to mice injected with JURKAT E6 cells infected with control vector (Figure 12).

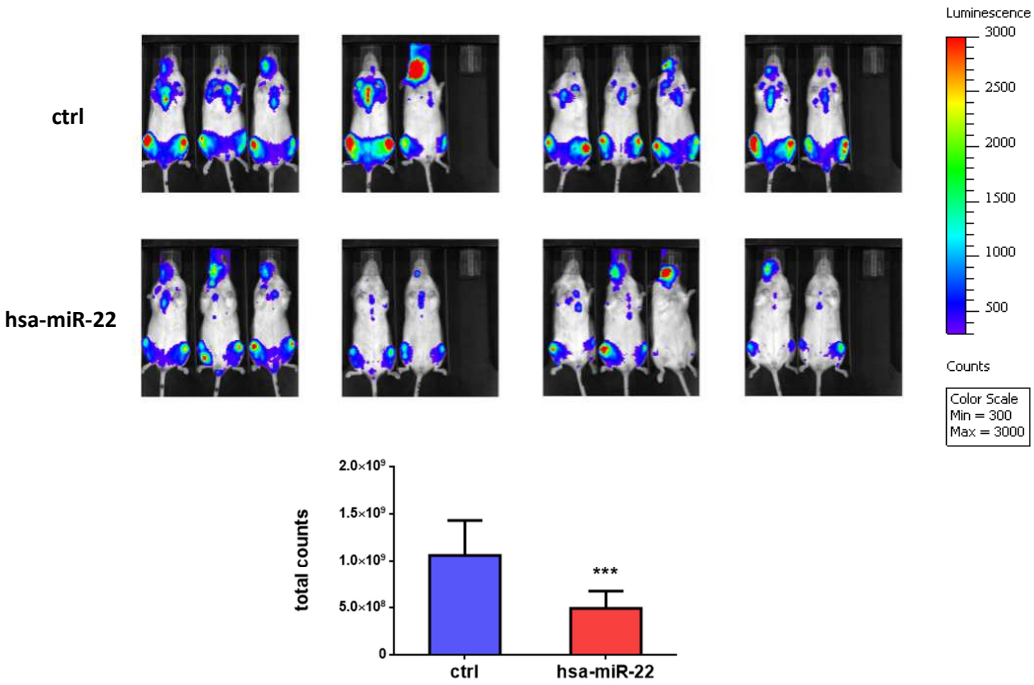

Figure 12. miR-22 over-expression inhibits JURKAT E6 T-ALL cells growth *in vivo*. JURKAT E6 cells expressing luciferase were engineered to stably express hsa-miR-22 or an empty vector (ctrl). These cells were injected to generate two different groups: "Ctrl" and "hsa-miR-22" (n=10). (A) Representative bioluminescence images in NSG mice at 14 days from the injection and luciferase activity quantification (***, P<0,001).

4.8 Meta-analysis of NOTCH1 regulated genes in human T-ALL cell lines

A large already published human T-ALL dataset, containing duplicate samples from 7 T-ALL cell lines harboring activating mutations in NOTCH1 treated with GSI (CompE) or vehicle (DMSO) for 24 [102], was selected for meta-analysis.

Gene set enrichment analysis (GSEA) was performed to see whether gene sets containing targets of transcription factors or miRNAs (C3 collection in the MSigDB v6.0) were significantly enriched in the list of differentially expressed genes in human T-ALL cell lines. Interestingly, among the significantly up-regulated gene sets, we found the targets of the microRNAs belonging to the miR-17/92 cluster. This result is in agreement with the murine microRNA differential expression analysis, presented in paragraph 2, in which we found components of miR-17/92 cluster to be strongly down-regulated, thus expecting an up-regulation of their target genes. Moreover, among the down-regulated gene sets we found numerous targets of the transcription factors MYC and MAX, both well known to be involved in T-ALL. In fact, MYC was previously reported as a developmentally regulated direct downstream target of Notch1 that contributes to the growth of T-ALL cells [102,103] and MAX, that antagonizes the action of c-myc, was reported to partially abrogate the growth advantage of ICN1 transduced cells [103].

Considering the crucial role of miR-22 in delaying T-ALL development *in vivo*, we performed further analysis on the human T-ALL dataset exploited before [102]. We ran GSEA against the C3 sub-collection of miR targets in the MSigDB v6.0, including also additional gene sets with putative targets of miR-22 obtained from different microRNA target prediction softwares. Since miR-22 was up-regulated in our experimental setting, we expected anti-correlated target genes and focused our attention on down-regulated gene sets containing putative targets of miR-22. None of them resulted significant. Thus, we selected the three negatively enriched gene sets obtained with the DIANA-microT-CDS software, TargetScan and miRDB for a leading edge analysis to determine the miR-22 targets that resulted down-regulated upon NOTCH1 inhibition in the human T-ALL cell lines

re-analyzed. We found 23 down-regulated genes that were consistently contributing to the negative enrichment of all the three selected gene sets of miR-22 targets (Supplementary Figure 1). Amongst these genes, we found Peroxisome Proliferator-Activated Receptor Gamma, Coactivator 1 Beta (*PGC-1β*), a component of the PGC-1 family, whose members are strong activators of mitochondrial metabolism. Notably, in the GSEA analysis run to discover targets of transcription factors significantly regulated upon treatment with GSI in human T-ALL cells, we found a gene set containing targets of the PPARG transcription factor (PPARG_01 gene set) as significantly down-regulated (FDR=0.014), indicating a possible crosstalk between miR-22 and PPARG pathway in this context.

4.9 Identification of *PGC-1β* as a putative target of miR-22-3p

In view of the previous meta-analysis of NOTCH1 regulated genes in human T-ALL cell lines, we focused on *PGC-1β* gene. The peroxisome proliferator-activated receptor γ (PPARγ) coactivator-1β (PGC-1β) belongs to the family of PGC-1 coactivators. The coactivators PGC-1α and PGC-1β share sequence similarities along their entire lengths and have a similar expression pattern, being highly expressed in tissues with an elevated mitochondrial energy metabolism, such as heart, skeletal muscle and brown adipose tissue [237]. PGC-1β sustains cell anabolism through de novo lipogenesis, while PGC-1α is primarily involved in gluconeogenesis [237].

We thus evaluated the expression of PGC-1β in human PDTALL samples using qRT-PCR. Interestingly, we found that PGC-1β was significantly down-regulated upon DBZ treatment *in vivo* in all the *NOTCH1* mutated PDTALL (Figure.13A), presenting both strong activated *NOTCH1* alleles (PDTALL #25, #8, #12 with HD-ΔPEST mutations) or NOTCH1 and FBXW7 mutations (PDTALL #46, #47)

and weak *NOTCH1* alleles (PDTALL #39). PDTALL #11 (HD *NOTCH1* mutation) was the only exception in which PGC-1β expression was not regulated following NOTCH1 inhibition (Figure.13A). Next, we asked if overexpression of hsa-miR-22 directly affected the expression of PGC-1β in human T-ALLs. Among three *NOTCH1* mutated T-ALL cell lines (MOLT4, DND41, JURKAT E6 ATCC), which were infected with pLenti-pre-hsa-miR-22 overexpressing vector, only MOLT4 cells showed a moderate but significant PGC-1β down-regulation compared to the control cells, infected with empty vector (Figure 13C). We further analyzed PGC-1β regulation at the protein level both in PDTALLs following DBZ treatment and in T-ALL cell lines that constitutively expressed high miR-22 levels. Western blot analysis showed that PGC-1β protein resulted highly expressed both in PDTALL and T-ALL cell lines, however this expression was not regulated following DBZ treatment or after miR-22 overexpression (Figure 13B-D). In conclusion, PGC-1β protein resulted abundant in T-ALL cells and NOTCH1 inhibition or miR-22 overexpression was not a sufficiently strong stimulus to modulate its expression at least in the panel of T-ALL cells we evaluated.

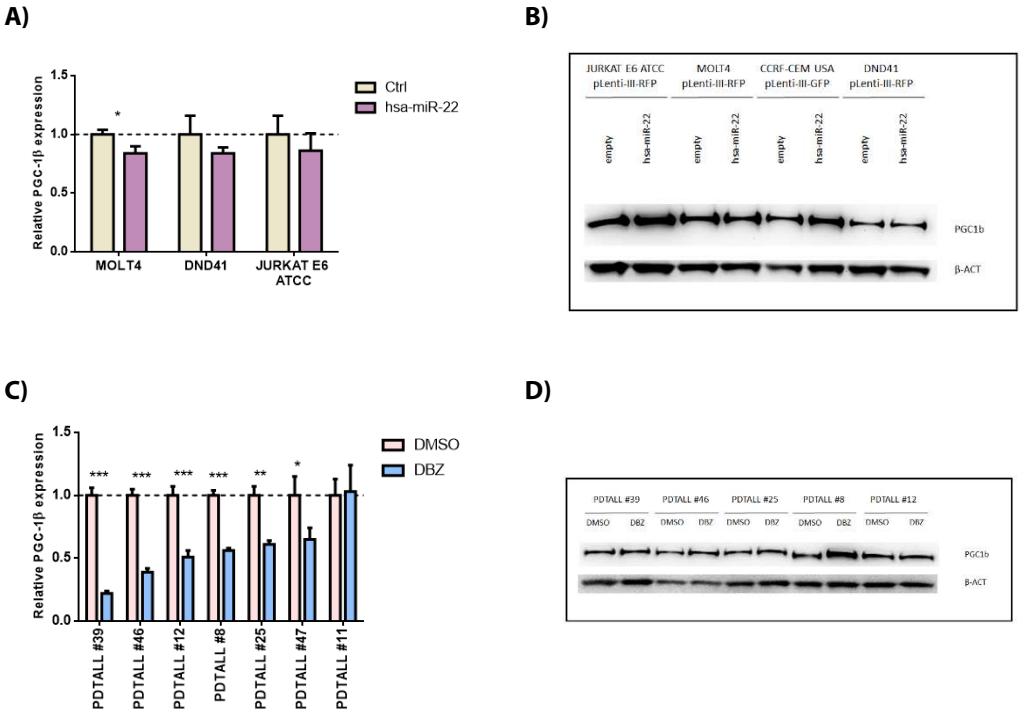

Figure 13. Down-regulation of PGC-1β in human T-ALL cells following GSI treatment or hsa-miR-22 overexpression. (A) qRT-PCR of PGC-1β, a putative miR-22 target gene, in human PDTALL #39, #46, #12, #8, #25, #47, #11 depleted from murine cells and treated *in vivo* with DBZ or with vehicle only (DMSO) (* P<0.05; ** P<0.01; *** P<0.001). Error bars represent ± SD of triplicate experiments. (B) PDTALL #39, #46, #25, #8, #12 were also investigated for the regulation of PGC-1β protein by Western blot after NOTCH1 inhibition. (C) qRT-PCR of PGC-1β in *NOTCH1* mutated TALL cell lines (MOLT4, DND41, JURKAT E6 ATCC), which were engineered to stably express hsa-miR-22 or an empty vector (ctrl) (* P<0.05; ** P<0.01; *** P<0.001). Data is represented as Mean ± SD. Assays were performed in triplicate. (B) *NOTCH1* mutated TALL cell lines expressing s hsa-miR-22 or an empty vector (ctrl), were investigated by Western blot for the regulation of PGC-1β protein.

5 Discussion

T-cell acute lymphoblastic leukemia (T-ALL) is an aggressive hematologic tumor that accounts for 10%–15% of pediatric and 25% of adult ALL cases. The introduction of intensive combination chemotherapy protocols has led to significant improvements in survival of this disease; however, the aggressive regiments are non-specific and very often associated with acute toxicities and patients suffer long-term side-effects.

Importantly, studies on oncogenic NOTCH1 resulted crucial not only for the high NOTCH1 mutational rate (> 60%) in T-ALL but also because γ-secretase inhibitors (GSIs) showed efficacy *in vitro* in numerous T-ALL cell lines [5]. In this scenario, several studies have focused on the identification of pathways that could synergize with NOTCH1 oncogene in order to identify molecular therapies to be used in combination with GSIs.

Among multiple and different functions of oncogenic NOTCH1, there are increasing evidences of the crucial role of non-coding RNAs in NOTCH-induced leukemia. However, little is currently known on the microRNAs that are regulated following NOTCH1 inhibition. Thus, the goal of this study was to analyze NOTCH1-regulated microRNAs following NOTCH1 inhibition in T-ALL cells in view of future therapies that may combine NOTCH1 inhibition with microRNA based therapy.

We first generated gene and microRNA expression profiling of murine NOTCH1-induced T-tumors treated *in vivo* with a highly active GSI. Gene expression analysis showed numerous genes significantly down-regulated and up-regulated upon DBZ treatment. In particular, Gene Set Enrichment Analysis (GSEA) showed that the MSigDB hallmark gene sets related to NOTCH signaling and MYC targets were significantly down-regulated following NOTCH1 inhibition, as previously demonstrated [102,103], confirming the efficacy of our experimental model.

MicroRNA expression profiling showed several components of the miR-17-92 cluster at the top of the list of NOTCH1 down-regulated miRNAs, in accordance with previously studies, which demonstrated this cluster is directly regulated by NOTCH1 in the context of T-ALL [53,54]. Dual translocations that simultaneously affect the 17-92 cluster, where miR-19 is located, and NOTCH1,

highlight the oncogenic importance of this interaction in T-ALL. Notably, from our analysis, the miR-19a resulted significantly up-regulated upon NOTCH1 inhibition occupying the top position of our microRNA list, further supporting its crucial role as oncomiR in NOTCH1-driven T-ALL [54].

Our data showed that the other members of the miR-17-92 cluster (miR-17-5p, miR-18a-5p, miR-20a-3p and miR-92a-3p) resulted generally down-regulated upon GSI treatment also in human T-ALL cells, even if the regulation of the specific components appear variable and cell context dependent.

Moreover, also miR-181a-1-3p resulted significantly down-regulated following NOTCH1 inhibition, suggesting a putative role as oncomiR in T-ALL. Our data resulted in accordance with a previous study, where the deletion of *mir-181a-1/b-1* expression inhibited the development of NOTCH1 oncogene-induced T-ALL by repressing multiple negative feedback regulators downstream of NOTCH and pre-TCR signaling pathways [238].

In addition, among the significantly up-regulated miRNAs following NOTCH1 inhibition, we found miR-223-3p, supporting a previous study of Kumar V. and collaborators, which reported that the expression of miR-223 increases after GSI treatment. Their results indicated that active NOTCH pathway signaling down-regulated the expression of miR-223, that in concert modulate the expression of IGFR1, which plays an important role in T-ALL contributing to leukemia-initiating activity [220]. However, the regulation of miR-223 in the context of NOTCH1 leukemia resulted controversial [219,220]. Indeed, miR-223 was found highly expressed in T-ALL and positively regulated by NOTCH3/NOTCH1, suggesting a complex modulation of miR-223 mainly due to the specific context analyzed [219].

Along with the oncomiRs, we also identified a few interesting putative tumor suppressor microRNA. For example, we found miR-709 to be significantly up-regulated following NOTCH1 inhibition. Our data are coherent with a previous study that for the first time analyzed the role of miR-709 in the context of NOTCH1-induced leukemia. In the latter study, miR-709 resulted significantly downregulated in murine NOTCH1-T-ALL respect to normal T-cells; in addition, they found that miR-709 could inhibit the initiation and maintenance of mouse

NOTCH1-driven leukemogenesis *in vivo* repressing Myc, a direct target of NOTCH1, and Akt and Ras-GRF1 oncogenes [55].

Interestingly, we identified some novel microRNAs up-regulated following NOTCH1 inhibition: mmu-miR-34a-5p, mmu-miR-199a-5p and mmu-miR-22-3p. miR-34a-5p is a highly conserved microRNA, that emerged as a key tumor suppressor in multiple tumor types [239-241], even if in CLL this miRNA resulted overexpressed [242]. The miR-34a-5p appeared particularly interesting because it entered in phase I clinical trials, with the compound MRX34, composed of a miR-34 mimic encapsulated in a lipid carrier [243], in patients with primary liver cancer, small cell lung cancer, lymphoma, melanoma, multiple myeloma or renal cell carcinoma. Another interesting microRNA was the miR-199a-5p because it was reported as tumor suppressor in several tumor types, such as head and neck squamous cell carcinoma [233], hepatocellular carcinoma [234] and triple-negative breast cancer [235]. Although, we found a consistent modulation of miR-34a-5p and miR-199a-5p in murine models of T-ALL, their role in human T-ALL cells was not further investigated due to undetectable expression both at basal conditions and upon NOTCH1 inhibition.

Differently from miR-34a-5p and miR-199a-5p, the modulation of miR-22a-3p upon NOTCH1 inhibition both in mouse and human T-ALL cells supported the hypothesis that it acts as a tumor suppressor both in mouse and human T-ALL cells carrying NOTCH1 activation. Considering the well-established role of NOTCH1 as transcriptional activator, it is plausible that the regulation of miR-22 downstream Notch1 is supported by a transcriptional repressor that is directly regulated by NOTCH1. Interestingly, we identified a N-box binding motif element that can potentially mediate transcriptional repression via HES1, which has already been shown to modulate several critical pathways downstream NOTCH1.

In the last couple of years, miR-22 is emerging as a crucial regulator of neoplastic progression. Initially, it was shown that miR-22 overexpressing transgenic mice were capable of developing a Myelodysplastic syndrome, which subsequently progressed to acute myeloid leukemia (AML). Mechanistically, miR-22 overexpression resulted in a significant downregulation of Tet2 and consequently

of its target genes [244]. Differently from these results, Jiang X and al. demonstrated that the forced expression of miR-22 significantly suppressed AML cell viability and growth *in vitro*, and substantially inhibited leukemia development and maintenance *in vivo* [231]. According to these results, miR-22 targeted multiple oncogenes, including CRTC1, FLT3 and MYCBP, and thus represses the CREB and MYC pathways [231]. In line with this data, another study showed that miR-22 is a tumor suppressor in AML induced by PU.1, an important transcription factor of monocyte/macrophage differentiation, and reintroduction of miR-22 in AML blasts relieved the differentiation block and the inhibition of cell growth [245].

However, the role of miR-22 in cancer appears complex and dependent on the cell context. In fact, miR-22 was found to act as a tumor suppressor miRNA in some tumors, such as in gastric cancer [246] or in Esophageal squamous cell carcinoma (ESCC), where its expression was much lower than that in normal cells. More specifically, miR-22 over-expression in ESCC cell lines could significantly inhibit cell proliferation, migration and invasion [247]. On the other hand, miR-22 was defined as an onco-miRNA in other tumors, such as in breast [248] and in prostate cancer, where its inhibition via an antagomiR negatively affected tumor cell behavior *in vitro* [249].

Our data suggest a tumor suppressor role for miR-22-3p in T-ALL. In fact, miR-22 resulted repressed in human TALL cell lines and PDTALL samples respect to normal thymocytes, in accordance with the potential tumor suppressor role of miR-22 in T-ALL. Interestingly, Ghisi M. and collaborators identified miR-22 amongst the microRNAs upregulated during normal T-cell development [250], suggesting a different regulation of miR-22 between normal and leukemic T-cells.

In order to mechanistically link the putative role of mir-22-3p to the biology of human T-ALL, we tested if its regulation could contribute to affect the growth of human T-ALL cells *in vitro*. Our data showed that miR-22 up-regulation did not affect growth and survival of T-ALL cells both under basal and after stress conditions (glucose deprivation). Conversely, overexpression of miR-22a-3p inhibited *in vitro* colony formation, affecting both the number and the size of the colonies, in T-ALL cell lines carrying constitutive NOTCH1 activation. This result, is in accordance with a recent study of miR-22 in AML [231], which

suggested a possible involvement of miR-22 as tumor suppressor in leukemia initiation. Moreover, miR-22-3p significantly impaired tumor growth *in vivo* when overexpressed in human T-ALL cells. We found that the over-expression of hsa-miR-22 induced a significant delay in tumor formation in mice, significantly reducing the percentage of tumor cells in the blood and the size and the weight of spleens and liver. Importantly, the Kaplan-Meier curves showed that the over-expression of hsa-miR-22 was significantly associated with increased survival. Overall, these data demonstrate that high hsa-miR-22 affects tumor progression, possibly reducing localization of leukemic cells to supportive niches (such as bone marrow) and so leading to slower tumor growth.

Considering the crucial role of miR-22 in delaying T-ALL development *in vivo*, we performed a meta-analysis on a human NOTCH1-mutated T-ALL dataset previously published [102], including also additional gene sets with putative targets of miR-22 obtained from different microRNA target prediction softwares. Amongst the 23 down-regulated genes, which were consistently contributing to the negative enrichment of miR-22 targets, we found the Peroxisome Proliferator-Activated Receptor Gamma (PPARγ) Coactivator 1 Beta (*PGC-1β*). PGC-1β belongs to the family of PGC-1 coactivators. The PGC-1 family, consisting of PGC-1α, PGC-1β and PGC-1-related coactivator (PRC), plays a key role in a regulatory network governing the transcriptional control of mitochondrial biogenesis and oxidative metabolism as well as of antioxidant defense [251]. The coactivators PGC-1α and PGC-1β share sequence similarities along their entire lengths and have a similar expression pattern, being highly expressed in tissues with an elevated mitochondrial energy metabolism, such as heart, skeletal muscle and brown adipose tissue [237]. PGC-1β sustains cell anabolism through de novo lipogenesis, while PGC-1α is primarily involved in gluconeogenesis [237]. Additionally, we ran a GSEA analysis to discover targets of transcription factors significantly regulated upon treatment with DBZ in human T-ALL cells and we found the PPARG_01 gene set, containing targets of the PPARγ transcription factor, significantly down-regulated, indicating a possible crosstalk between miR-22 and PPARG pathway in this context. Of note, the anti-infiammatory nuclear receptor gamma (PPARγ) was found both downregulated and induced by

NOCTH1 signaling in different contexts, suggesting a variegated role of PPARG pathway [252] [253].

Interestingly, among the significantly up-regulated gene sets, obtained from the previous GSEA analysis, we found targets of the microRNAs belonging to the miR-17/92 cluster. This result supported the murine microRNA differential expression analysis, in which we found components of the miR-17/92 cluster strongly down-regulated, confirming its key role in T-cell leukemia overexpressing NOTCH1. Moreover, among the down-regulated gene sets we found targets of the transcription factors MYC and MAX, both well known to have an involvement in T-ALL. MYC was previously reported as a developmentally regulated direct downstream target of Notch1 that contributes to the growth of T-ALL cells [102,103] and MAX, that antagonizes the action of c-myc, was reported to abrogate the growth advantage of ICN1 transduced cells [103].

Thus, we focused our attention on the role of PGC-1β in association with miR-22 in the context of NOTCH1-induced T-ALL. PGC-1β mRNA resulted significantly down-regulated following NOTCH1 inhibition *in vivo* in PDTALL xenografts and in one of three miR-22 overexpressing T-ALL cell lines. Notably, all of these human T-ALL samples were *NOTCH1* mutated. Conversely, Western Blot analysis of these same samples showed that the levels of PGC-1β protein were not regulated either following NOTCH1 inhibition or overexpression of miR-22-3p. In conclusion, our results demonstrate PGC-1β regulation at the transcriptional but not at the protein level. One possibility that could account for the discrepancy found, could lie in the high levels of PGC-1β protein present in the human T-ALL samples analyzed and to the subsequent difficulty to detect small variations using western blot analysis. Alternatively, the study of this protein may require more sophisticated analysis such protein fractionation and detection of post-translational modifications that may affect expression levels.

In conclusion, we found that miR-22-3p was down-regulated in T-ALL cells and its expression level could be restored following NOTCH1 inhibition. miR-22-3p over-expression affected *in vivo* tumor progression, reducing localization of leukemic cells to supportive niches (such as bone marrow) and so leading to

slower tumor growth, confirming its putative tumor suppressor role in T-ALL. Meta-analysis of NOTCH1 regulated genes in human T-ALL cell lines indicated PGC-1β as putative miR-22 target gene, but overexpression of miR-22 was not sufficient to consistently determine PGC-1β modulation.

We are currently investigating the putative NOTCH1/hsa.miR-22/PPARγ axis and additional putative miR-22 target genes, such as Max and IGF1R, that have a crucial role in the pathogenesis of T-ALL.

6 List of abbreviations

ABL1	abelson murine leukemia viral oncogene homolog 1
ADAM	A Disintegrin And Metalloprotease
AGO	Argonaute
ARF	ADP Ribosylation Factor
BCL11B	B-Cell CLL/Lymphoma 11B
bHLH	basic helix-loop-helix
BiTE	bispecific-T-cell engaging
BM	bone marrow
CAR	chimeric antigen receptor
CCND2	G1/S-specific cyclin-D2
CD	Cluster of Differentiation
CDK4	Cyclin-dependent kinase 4
CDK6	Cyclin-dependent kinase 6
CDKN2A	cyclin dependent kinase inhibitor 2A
CFU	Colony forming unit
CLL	Chronic Lymphocytic Leukemia
CSL	CBF1, Suppressor of Hairless, Lag-1
CTCF	CCCTC-Binding Factor
DBZ	Dibenzazepine
DGCR8	DiGeorge syndrome critical region 8
DMSO	Dimethyl sulfoxide
DNM2	Dynamin 2
DNMT3A	DNA methyltransferase 3A
dsRBD	dsRNA-binding domain
DTX	Docetaxel
EED	embryonic ectoderm development
EGF	Epidermal growth factor
EGIL	European Group for Immunological Characterization of Leukemias
ESCC	Esophageal squamous cell carcinoma
ETP	Early-T Precursor
ETV6	ETS Variant 6

EZH2	enhancer of zeste homolog 2
FBXW7	F-box/WD repeat-containing protein 7
FLT3	fms related tyrosine kinase 3
GATA3	GATA Binding Protein 3
GFP	green fluorescent protein
GSEA	gene set enrichment analysis
GSI	γ-secretase inhibitor
HBP1	High Mobility Group Box Transcription Factor 1
HD	heterodimerization domain
HEK	human embryonic Kidney
HES1	enhancer of split 1 homolog
HOXA	homeobox A
HRP	horseradish peroxidase
HSC70	heat shock cognate 70
HSCs	Hematopoietic stem cells
HSP90	heat shock protein 90
ICN1	intracellular domain of NOTCH1
IDH1	isocitrate dehydrogenase 1
IDH2	isocitrate dehydrogenase 2
IGF1R	Insulin Like Growth Factor 1 Receptor
IkB	inhibitor of NF-κB
IKK	inhibitor of NF-κB kinase
IL7R	interleukin-7 receptor
JAK	janus kinase
JAK3	janus kinase 3
JME	Juxtamembrane expansion mutants
KDM6A	lysine-specific demethylase 6A
LEF1	Lymphoid Enhancer Binding Factor 1
Lin-	lineage negative
LMO1	LIM-only domain 1
LMO2	LIM-only domain 2

lncRNA	long non-coding RNA
LNR	Lin12-Notch repeats
LUNAR1	Leukemia-Associated Non-Coding IGF1R Activator RNA 1
LYL1	lymphoblastic leukemia-derived sequence 1
MAML1	Mastermind Like Transcriptional Coactivator 1
MDM	Modified Dulbecco's Medium
miRNA	microRNA
MTPN	myotrophin
MYB	MYB Proto-Oncogene
MYC	MYC Proto-Oncogene
MYCN	MYCN Proto-Oncogene
ncRNA	non-coding RNA
NF1	neurofibromatosis type 1
NKX2-1	NK2 homeobox 1
NKX2-2	NK2 homeobox 2
NRAS	neuroblastoma RAS viral oncogene homolog
NRR	negative regulatory region
NUP214	nucleoporin 214
NUP98	nuclear pore complex protein Nup98-Nup96
PACT	PKR activating protein
P-bodies	processing bodies
PBS-T	Phosphate Buffer Saline-0.1%Tween-20
PGC-1β	Peroxisome Proliferator-Activated Receptor Gamma, Coactivator 1 Beta
PHF6	PHD Finger Protein 6
PI3K	phosphatidylinositol-4,5-bisphosphate 3-kinase
PICALM	phosphatidylinositol binding clathrin assembly protein
PIK3R1	Phosphoinositide-3-Kinase Regulatory Subunit 1
PKR	protein kinase R
PNPT1	polyribonucleotide nucleotidyltransferase 1

PPARγ	peroxisome proliferator-activated receptor γ
PRC	PGC-1-related coactivator
PRC2	polycomb repressor complex 2
pre-miRNA	precursor transcript miRNA
pri-miRNA	primary transcript miRNA
PTEN	phosphatase and tensin homolog
PTPN2	Protein Tyrosine Phosphatase, Non-Receptor Type 2
RAS	rat sarcoma viral oncogene homolog
RIIIDs	RNase III domains
RISC	RNA-induced silencing complex4
RPL10	60S ribosomal protein L10
RPL5	60S ribosomal protein L5
RUNX1	Runt-related transcription factor 1
SD	standard deviation
SERCA	sarcoplasmic/endoplasmic reticulum calcium ATPase
SNPs	single nucleotide polymorphisms
SP	single-positive
STAT	signal transducer and activator of transcription protein
SUZ12	suppressor of zeste 12 homolog
TAL1	T cell acute lymphocytic leukaemia 1
TAL2	T-cell acute lymphocytic leukemia 2
T-ALL	T-cell acute lymphoblastic leukemia
TLX1	T-cell leukemia homeobox protein 1
TLX3	T-cell leukemia homeobox protein 3
Tm	melting temperature
TRBP	TAR RNA-binding protein
USP7	PRC2ubiquitin-specific-processing protease 7
UTR	untranslated region
VSV-G	Vesicular somatitis virus G glycoprotein
WAGOs	worm-specific AGO proteins

WT1	Wilms’ tumor protein
ZFP36L2	ZFP36 Ring Finger Protein Like 2

7 References

1. Ferrando, A.A.; Neuberg, D.S.; Staunton, J.; Loh, M.L.; Huard, C.; Raimondi, S.C.; Behm, F.G.; Pui, C.H.; Downing, J.R.; Gilliland, D.G.*, et al.* Gene expression signatures define novel oncogenic pathways in t cell acute lymphoblastic leukemia. *Cancer Cell* **2002**, *1*, 75-87.
2. Belver, L.; Ferrando, A. The genetics and mechanisms of t cell acute lymphoblastic leukaemia. *Nat Rev Cancer* **2016**, *16*, 494-507.
3. Li, S.Y.; Ye, J.Y.; Meng, F.Y.; Li, C.F.; Yang, M.O. Clinical characteristics of acute lymphoblastic leukemia in male and female patients: A retrospective analysis of 705 patients. *Oncol Lett* **2015**, *10*, 453-458.
4. Van Vlierberghe, P.; Ferrando, A. The molecular basis of t cell acute lymphoblastic leukemia. *J Clin Invest* **2012**, *122*, 3398-3406.
5. Weng, A.P.; Ferrando, A.A.; Lee, W.; Morris, J.P.; Silverman, L.B.; Sanchez-Irizarry, C.; Blacklow, S.C.; Look, A.T.; Aster, J.C. Activating mutations of notch1 in human t cell acute lymphoblastic leukemia. *Science* **2004**, *306*, 269-271.
6. Aster, J.C.; Pear, W.S.; Blacklow, S.C. Notch signaling in leukemia. *Annu Rev Pathol* **2008**, *3*, 587-613.
7. Hebert, J.; Cayuela, J.M.; Berkeley, J.; Sigaux, F. Candidate tumor-suppressor genes mts1 (p16ink4a) and mts2 (p15ink4b) display frequent homozygous deletions in primary cells from t- but not from b-cell lineage acute lymphoblastic leukemias. *Blood* **1994**, *84*, 4038-4044.
8. Xia, Y.; Brown, L.; Yang, C.Y.; Tsan, J.T.; Siciliano, M.J.; Espinosa, R.; Le Beau, M.M.; Baer, R.J. Tal2, a helix-loop-helix gene activated by the (7;9)(q34;q32) translocation in human t-cell leukemia. *Proc Natl Acad Sci U S A* **1991**, *88*, 11416-11420.
9. Chen, Q.; Cheng, J.T.; Tasi, L.H.; Schneider, N.; Buchanan, G.; Carroll, A.; Crist, W.; Ozanne, B.; Siciliano, M.J.; Baer, R. The tal gene undergoes chromosome translocation in t cell leukemia and potentially encodes a helix-loop-helix protein. *EMBO J* **1990**, *9*, 415-424.
10. Mellentin, J.D.; Smith, S.D.; Cleary, M.L. Lyl-1, a novel gene altered by chromosomal translocation in t cell leukemia, codes for a protein with a helix-loop-helix dna binding motif. *Cell* **1989**, *58*, 77-83.
11. Wang, J.; Jani-Sait, S.N.; Escalon, E.A.; Carroll, A.J.; de Jong, P.J.; Kirsch, I.R.; Aplan, P.D. The t(14;21)(q11.2;q22) chromosomal translocation associated with t-cell acute lymphoblastic leukemia activates the bhlhb1 gene. *Proc Natl Acad Sci U S A* **2000**, *97*, 3497-3502.
12. Boehm, T.; Foroni, L.; Kaneko, Y.; Perutz, M.F.; Rabbitts, T.H. The rhombotin family of cysteine-rich lim-domain oncogenes: Distinct members are involved in t-cell translocations to human chromosomes 11p15 and 11p13. *Proc Natl Acad Sci U S A* **1991**, *88*, 4367-4371.
13. Royer-Pokora, B.; Loos, U.; Ludwig, W.D. Ttg-2, a new gene encoding a cysteine-rich protein with the lim motif, is overexpressed in acute t-cell leukaemia with the t(11;14)(p13;q11). *Oncogene* **1991**, *6*, 1887-1893.
14. Erikson, J.; Finger, L.; Sun, L.; ar-Rushdi, A.; Nishikura, K.; Minowada, J.; Finan, J.; Emanuel, B.S.; Nowell, P.C.; Croce, C.M. Deregulation of c-myc by translocation of the alpha-locus of the t-cell receptor in t-cell leukemias. *Science* **1986**, *232*, 884-886.
15. Clappier, E.; Cuccuini, W.; Kalota, A.; Crinquette, A.; Cayuela, J.M.; Dik, W.A.; Langerak, A.W.; Montpellier, B.; Nadel, B.; Walrafen, P.*, et al.* The c-myb locus is involved in chromosomal translocation and genomic duplications in human t-cell acute leukemia (t-all), the translocation defining a new t-all subtype in very young children. *Blood* **2007**, *110*, 1251-1261.

16. Palomero, T.; Barnes, K.C.; Real, P.J.; Glade Bender, J.L.; Sulis, M.L.; Murty, V.V.; Colovai, A.I.; Balbin, M.; Ferrando, A.A. Cutll1, a novel human t-cell lymphoma cell line with t(7;9) rearrangement, aberrant notch1 activation and high sensitivity to gamma-secretase inhibitors. *Leukemia* **2006**, *20*, 1279-1287.
17. Dubé, I.D.; Kamel-Reid, S.; Yuan, C.C.; Lu, M.; Wu, X.; Corpus, G.; Raimondi, S.C.; Crist, W.M.; Carroll, A.J.; Minowada, J. A novel human homeobox gene lies at the chromosome 10 breakpoint in lymphoid neoplasias with chromosomal translocation t(10;14). *Blood* **1991**, *78*, 2996-3003.
18. Hatano, M.; Roberts, C.W.; Minden, M.; Crist, W.M.; Korsmeyer, S.J. Deregulation of a homeobox gene, hox11, by the t(10;14) in t cell leukemia. *Science* **1991**, *253*, 79-82.
19. Przybylski, G.K.; Dik, W.A.; Grabarczyk, P.; Wanzeck, J.; Chudobska, P.; Jankowski, K.; von Bergh, A.; van Dongen, J.J.; Schmidt, C.A.; Langerak, A.W. The effect of a novel recombination between the homeobox gene nkx2-5 and the trd locus in t-cell acute lymphoblastic leukemia on activation of the nkx2-5 gene. *Haematologica* **2006**, *91*, 317-321.
20. Speleman, F.; Cauwelier, B.; Dastugue, N.; Cools, J.; Verhasselt, B.; Poppe, B.; Van Roy, N.; Vandesompele, J.; Graux, C.; Uyttebroeck, A.*, et al.* A new recurrent inversion, inv(7)(p15q34), leads to transcriptional activation of hoxa10 and hoxa11 in a subset of t-cell acute lymphoblastic leukemias. *Leukemia* **2005**, *19*, 358-366.
21. Dreyling, M.H.; Martinez-Climent, J.A.; Zheng, M.; Mao, J.; Rowley, J.D.; Bohlander, S.K. The t(10;11)(p13;q14) in the u937 cell line results in the fusion of the af10 gene and calm, encoding a new member of the ap-3 clathrin assembly protein family. *Proc Natl Acad Sci U S A* **1996**, *93*, 4804-4809.
22. Asnafi, V.; Radford-Weiss, I.; Dastugue, N.; Bayle, C.; Leboeuf, D.; Charrin, C.; Garand, R.; Lafage-Pochitaloff, M.; Delabesse, E.; Buzyn, A.*, et al.* Calm-af10 is a common fusion transcript in t-all and is specific to the tcrgammadelta lineage. *Blood* **2003**, *102*, 1000-1006.
23. Rubnitz, J.E.; Behm, F.G.; Curcio-Brint, A.M.; Pinheiro, R.P.; Carroll, A.J.; Raimondi, S.C.; Shurtleff, S.A.; Downing, J.R. Molecular analysis of t(11;19) breakpoints in childhood acute leukemias. *Blood* **1996**, *87*, 4804-4808.
24. Chervinsky, D.S.; Sait, S.N.; Nowak, N.J.; Shows, T.B.; Aplan, P.D. Complex mll rearrangement in a patient with t-cell acute lymphoblastic leukemia. *Genes Chromosomes Cancer* **1995**, *14*, 76-84.
25. Van Vlierberghe, P.; van Grotel, M.; Tchinda, J.; Lee, C.; Beverloo, H.B.; van der Spek, P.J.; Stubbs, A.; Cools, J.; Nagata, K.; Fornerod, M.*, et al.* The recurrent set-nup214 fusion as a new hoxa activation mechanism in pediatric t-cell acute lymphoblastic leukemia. *Blood* **2008**, *111*, 4668-4680.
26. Hussey, D.J.; Nicola, M.; Moore, S.; Peters, G.B.; Dobrovic, A. The (4;11)(q21;p15) translocation fuses the nup98 and rap1gds1 genes and is recurrent in t-cell acute lymphocytic leukemia. *Blood* **1999**, *94*, 2072-2079.
27. Mecucci, C.; La Starza, R.; Negrini, M.; Sabbioni, S.; Crescenzi, B.; Leoni, P.; Di Raimondo, F.; Krampera, M.; Cimino, G.; Tafuri, A.*, et al.* T(4;11)(q21;p15) translocation involving nup98 and rap1gds1 genes: Characterization of a new subset of t acute lymphoblastic leukaemia. *Br J Haematol* **2000**, *109*, 788-793.
28. Tycko, B.; Smith, S.D.; Sklar, J. Chromosomal translocations joining lck and tcrb loci in human t cell leukemia. *J Exp Med* **1991**, *174*, 867-873.
29. Clappier, E.; Cuccuini, W.; Cayuela, J.M.; Vecchione, D.; Baruchel, A.; Dombret, H.; Sigaux, F.; Soulier, J. Cyclin d2 dysregulation by chromosomal translocations to tcr loci in t-cell acute lymphoblastic leukemias. *Leukemia* **2006**, *20*, 82-86.

30. Karrman, K.; Andersson, A.; Björgvinsdóttir, H.; Strömbeck, B.; Lassen, C.; Olofsson, T.; Nguyen-Khac, F.; Berger, R.; Bernard, O.; Fioretos, T.*, et al.* Deregulation of cyclin d2 by juxtaposition with t-cell receptor alpha/delta locus in t(12;14)(p13;q11)-positive childhood t-cell acute lymphoblastic leukemia. *Eur J Haematol* **2006**, *77*, 27-34.
31. Flex, E.; Petrangeli, V.; Stella, L.; Chiaretti, S.; Hornakova, T.; Knoops, L.; Ariola, C.; Fodale, V.; Clappier, E.; Paoloni, F.*, et al.* Somatically acquired jak1 mutations in adult acute lymphoblastic leukemia. *J Exp Med* **2008**, *205*, 751-758.
32. Graux, C.; Cools, J.; Melotte, C.; Quentmeier, H.; Ferrando, A.; Levine, R.; Vermeesch, J.R.; Stul, M.; Dutta, B.; Boeckx, N.*, et al.* Fusion of nup214 to abl1 on amplified episomes in t-cell acute lymphoblastic leukemia. *Nat Genet* **2004**, *36*, 1084-1089.
33. De Keersmaecker, K.; Graux, C.; Odero, M.D.; Mentens, N.; Somers, R.; Maertens, J.; Wlodarska, I.; Vandenberghe, P.; Hagemeijer, A.; Marynen, P.*, et al.* Fusion of eml1 to abl1 in t-cell acute lymphoblastic leukemia with cryptic t(9;14)(q34;q32). *Blood* **2005**, *105*, 4849-4852.
34. Bar-Eli, M.; Ahuja, H.; Foti, A.; Cline, M.J. N-ras mutations in t-cell acute lymphocytic leukaemia: Analysis by direct sequencing detects a novel mutation. *Br J Haematol* **1989**, *72*, 36-39.
35. Tosello, V.; Mansour, M.R.; Barnes, K.; Paganin, M.; Sulis, M.L.; Jenkinson, S.; Allen, C.G.; Gale, R.E.; Linch, D.C.; Palomero, T.*, et al.* Wt1 mutations in t-all. *Blood* **2009**, *114*, 1038-1045.
36. Renneville, A.; Kaltenbach, S.; Clappier, E.; Collette, S.; Micol, J.B.; Nelken, B.; Lepelley, P.; Dastugue, N.; Benoît, Y.; Bertrand, Y.*, et al.* Wilms tumor 1 (wt1) gene mutations in pediatric t-cell malignancies. *Leukemia* **2010**, *24*, 476-480.
37. Gutierrez, A.; Sanda, T.; Ma, W.; Zhang, J.; Grebliunaite, R.; Dahlberg, S.; Neuberg, D.; Protopopov, A.; Winter, S.S.; Larson, R.S.*, et al.* Inactivation of lef1 in t-cell acute lymphoblastic leukemia. *Blood* **2010**, *115*, 2845-2851.
38. Van Vlierberghe, P.; Ambesi-Impiombato, A.; Perez-Garcia, A.; Haydu, J.E.; Rigo, I.; Hadler, M.; Tosello, V.; Della Gatta, G.; Paietta, E.; Racevskis, J.*, et al.* Etv6 mutations in early immature human t cell leukemias. *J Exp Med* **2011**, *208*, 2571-2579.
39. Poggi, M.; Canault, M.; Favier, M.; Turro, E.; Saultier, P.; Ghalloussi, D.; Baccini, V.; Vidal, L.; Mezzapesa, A.; Chelghoum, N.*, et al.* Germline variants in etv6 underlie reduced platelet formation, platelet dysfunction and increased levels of circulating cd34+ progenitors. *Haematologica* **2017**, *102*, 282-294.
40. Nagel, S.; Kaufmann, M.; Drexler, H.G.; MacLeod, R.A. The cardiac homeobox gene nkx2-5 is deregulated by juxtaposition with bcl11b in pediatric t-all cell lines via a novel t(5;14)(q35.1;q32.2). *Cancer Res* **2003**, *63*, 5329-5334.
41. Grossmann, V.; Kern, W.; Harbich, S.; Alpermann, T.; Jeromin, S.; Schnittger, S.; Haferlach, C.; Haferlach, T.; Kohlmann, A. Prognostic relevance of runx1 mutations in t-cell acute lymphoblastic leukemia. *Haematologica* **2011**, *96*, 1874-1877.
42. Ho, I.C.; Tai, T.S.; Pai, S.Y. Gata3 and the t-cell lineage: Essential functions before and after t-helper-2-cell differentiation. *Nat Rev Immunol* **2009**, *9*, 125-135.
43. Kawamura, M.; Ohnishi, H.; Guo, S.X.; Sheng, X.M.; Minegishi, M.; Hanada, R.; Horibe, K.; Hongo, T.; Kaneko, Y.; Bessho, F.*, et al.* Alterations of the p53, p21, p16, p15 and ras genes in childhood t-cell acute lymphoblastic leukemia. *Leuk Res* **1999**, *23*, 115-126.
44. Balgobind, B.V.; Van Vlierberghe, P.; van den Ouweland, A.M.; Beverloo, H.B.; Terlouw-Kromosoeto, J.N.; van Wering, E.R.; Reinhardt, D.; Horstmann, M.;

Kaspers, G.J.; Pieters, R.*, et al.* Leukemia-associated nf1 inactivation in patients with pediatric t-all and aml lacking evidence for neurofibromatosis. *Blood* **2008**, *111*, 4322-4328.

45. Gutierrez, A.; Sanda, T.; Grebliunaite, R.; Carracedo, A.; Salmena, L.; Ahn, Y.; Dahlberg, S.; Neuberg, D.; Moreau, L.A.; Winter, S.S.*, et al.* High frequency of pten, pi3k, and akt abnormalities in t-cell acute lymphoblastic leukemia. *Blood* **2009**, *114*, 647-650.
46. Palomero, T.; Dominguez, M.; Ferrando, A.A. The role of the pten/akt pathway in notch1-induced leukemia. *Cell Cycle* **2008**, *7*, 965-970.
47. Ntziachristos, P.; Tsirigos, A.; Van Vlierberghe, P.; Nedjic, J.; Trimarchi, T.; Flaherty, M.S.; Ferres-Marco, D.; da Ros, V.; Tang, Z.; Siegle, J.*, et al.* Genetic inactivation of the polycomb repressive complex 2 in t cell acute lymphoblastic leukemia. *Nat Med* **2012**, *18*, 298-301.
48. Ntziachristos, P.; Tsirigos, A.; Welstead, G.G.; Trimarchi, T.; Bakogianni, S.; Xu, L.; Loizou, E.; Holmfeldt, L.; Strikoudis, A.; King, B.*, et al.* Contrasting roles of histone 3 lysine 27 demethylases in acute lymphoblastic leukaemia. *Nature* **2014**, *514*, 513-517.
49. Van der Meulen, J.; Sanghvi, V.; Mavrakis, K.; Durinck, K.; Fang, F.; Matthijssens, F.; Rondou, P.; Rosen, M.; Pieters, T.; Vandenberghe, P.*, et al.* The h3k27me3 demethylase utx is a gender-specific tumor suppressor in t-cell acute lymphoblastic leukemia. *Blood* **2015**, *125*, 13-21.
50. Huether, R.; Dong, L.; Chen, X.; Wu, G.; Parker, M.; Wei, L.; Ma, J.; Edmonson, M.N.; Hedlund, E.K.; Rusch, M.C.*, et al.* The landscape of somatic mutations in epigenetic regulators across 1,000 paediatric cancer genomes. *Nat Commun* **2014**, *5*, 3630.
51. Van Vlierberghe, P.; Palomero, T.; Khiabanian, H.; Van der Meulen, J.; Castillo, M.; Van Roy, N.; De Moerloose, B.; Philippé, J.; González-García, S.; Toribio, M.L.*, et al.* Phf6 mutations in t-cell acute lymphoblastic leukemia. *Nat Genet* **2010**, *42*, 338-342.
52. Liu, Y.; Easton, J.; Shao, Y.; Maciaszek, J.; Wang, Z.; Wilkinson, M.R.; McCastlain, K.; Edmonson, M.; Pounds, S.B.; Shi, L.*, et al.* The genomic landscape of pediatric and young adult t-lineage acute lymphoblastic leukemia. *Nat Genet* **2017**.
53. Mavrakis, K.J.; Van Der Meulen, J.; Wolfe, A.L.; Liu, X.; Mets, E.; Taghon, T.; Khan, A.A.; Setty, M.; Setti, M.; Rondou, P.*, et al.* A cooperative microrna-tumor suppressor gene network in acute t-cell lymphoblastic leukemia (t-all). *Nat Genet* **2011**, *43*, 673-678.
54. Mavrakis, K.J.; Wolfe, A.L.; Oricchio, E.; Palomero, T.; de Keersmaecker, K.; McJunkin, K.; Zuber, J.; James, T.; Khan, A.A.; Leslie, C.S.*, et al.* Genome-wide rna-mediated interference screen identifies mir-19 targets in notch-induced t-cell acute lymphoblastic leukaemia. *Nat Cell Biol* **2010**, *12*, 372-379.
55. Li, X.; Sanda, T.; Look, A.T.; Novina, C.D.; von Boehmer, H. Repression of tumor suppressor mir-451 is essential for notch1-induced oncogenesis in t-all. *J Exp Med* **2011**, *208*, 663-675.
56. Wang, Y.; Wu, P.; Lin, R.; Rong, L.; Xue, Y.; Fang, Y. Lncrna nalt interaction with notch1 promoted cell proliferation in pediatric t cell acute lymphoblastic leukemia. *Sci Rep* **2015**, *5*, 13749.
57. Guttman, M.; Rinn, J.L. Modular regulatory principles of large non-coding rnas. *Nature* **2012**, *482*, 339-346.
58. Panzeri, I.; Rossetti, G.; Abrignani, S.; Pagani, M. Long intergenic non-coding rnas: Novel drivers of human lymphocyte differentiation. *Front Immunol* **2015**, *6*, 175.

59. Trimarchi, T.; Bilal, E.; Ntziachristos, P.; Fabbri, G.; Dalla-Favera, R.; Tsirigos, A.; Aifantis, I. Genome-wide mapping and characterization of notch-regulated long noncoding rnas in acute leukemia. *Cell* **2014**, *158*, 593-606.
60. Durinck, K.; Wallaert, A.; Van de Walle, I.; Van Loocke, W.; Volders, P.J.; Vanhauwaert, S.; Geerdens, E.; Benoit, Y.; Van Roy, N.; Poppe, B.*, et al.* The notch driven long non-coding rna repertoire in t-cell acute lymphoblastic leukemia. *Haematologica* **2014**, *99*, 1808-1816.
61. Chiaretti, S.; Zini, G.; Bassan, R. Diagnosis and subclassification of acute lymphoblastic leukemia. *Mediterr J Hematol Infect Dis* **2014**, *6*, e2014073.
62. Graux, C.; Cools, J.; Michaux, L.; Vandenberghe, P.; Hagemeijer, A. Cytogenetics and molecular genetics of t-cell acute lymphoblastic leukemia: From thymocyte to lymphoblast. *Leukemia* **2006**, *20*, 1496-1510.
63. Coustan-Smith, E.; Mullighan, C.G.; Onciu, M.; Behm, F.G.; Raimondi, S.C.; Pei, D.; Cheng, C.; Su, X.; Rubnitz, J.E.; Basso, G.*, et al.* Early t-cell precursor leukaemia: A subtype of very high-risk acute lymphoblastic leukaemia. *Lancet Oncol* **2009**, *10*, 147-156.
64. Ferrando, A.A.; Department of Pediatric Oncology, B., MA 02142 USA; Neuberg, D.S.; Department of Biostatistical Science, D.-F.C.I.a.H.M.S., Boston, MA 02115 USA; Staunton, J.; Whitehead Institute/Massachusetts Institute of Technology Center for Genome Research, C., MA 02142 USA; Loh, M.L.; Department of Medicine, B.a.W.s.H., Boston, MA 02115 USA; Huard, C.; Whitehead Institute/Massachusetts Institute of Technology Center for Genome Research, C., MA 02142 USA*, et al.* Gene expression signatures define novel oncogenic pathways in t cell acute lymphoblastic leukemia. *Cancer Cell* **2002**, *1*, 75-87.
65. Belver, L.; Ferrando, A. The genetics and mechanisms of t cell acute lymphoblastic leukaemia. *Nature Reviews Cancer* **2016**, *16*, 494-507.
66. Van Vlierberghe, P.; Ambesi-Impiombato, A.; De Keersmaecker, K.; Hadler, M.; Paietta, E.; Tallman, M.S.; Rowe, J.M.; Forne, C.; Rue, M.; Ferrando, A.A. Prognostic relevance of integrated genetic profiling in adult t-cell acute lymphoblastic leukemia. *Blood* **2013**, *122*, 74-82.
67. Zhang, J.; Ding, L.; Holmfeldt, L.; Wu, G.; Heatley, S.L.; Payne-Turner, D.; Easton, J.; Chen, X.; Wang, J.; Rusch, M.*, et al.* The genetic basis of early t-cell precursor acute lymphoblastic leukaemia. *Nature* **2012**, *481*, 157-163.
68. Haydu, J.E.; Ferrando, A.A. Early t-cell precursor acute lymphoblastic leukaemia. *Curr Opin Hematol* **2013**, *20*, 369-373.
69. Niehues, T.; Kapaun, P.; Harms, D.O.; Burdach, S.; Kramm, C.; Körholz, D.; Janka-Schaub, G.; Göbel, U. A classification based on t cell selection-related phenotypes identifies a subgroup of childhood t-all with favorable outcome in the coall studies. *Leukemia* **1999**, *13*, 614-617.
70. Homminga, I.; Pieters, R.; Langerak, A.W.; de Rooi, J.J.; Stubbs, A.; Verstegen, M.; Vuerhard, M.; Buijs-Gladdines, J.; Kooi, C.; Klous, P.*, et al.* Integrated transcript and genome analyses reveal nkx2-1 and mef2c as potential oncogenes in t cell acute lymphoblastic leukemia. *Cancer Cell* **2011**, *19*, 484-497.
71. Kleppe, M.; Soulier, J.; Asnafi, V.; Mentens, N.; Hornakova, T.; Knoops, L.; Constantinescu, S.; Sigaux, F.; Meijerink, J.P.; Vandenberghe, P.*, et al.* Ptpn2 negatively regulates oncogenic jak1 in t-cell acute lymphoblastic leukemia. *Blood* **2011**, *117*, 7090-7098.
72. Patrick, K.L.; Snowden, J.A.; Wilson, G.; Collins, N.; Dalley, C.D. Long term lympho-haematopoietic reconstitution by umbilical cord blood stem cells following primary graft failure and autologous rescue. *Br J Haematol* **2012**, *158*, 419-420.

73. Wood, B.; Winter, S.; Dunsmore, K.; Devidas, M.; Chen, S.; Asselin, B.; Esiashvili, N.; Loh, M.; Winick, N.; Carroll, W*., et al.* T-lymphoblastic leukemia (t-all) shows excellent outcome, lack of significance of the early thymic precursor (etp) immunophenotype, and validation of the prognostic value of end-induction minimal residual disease (mrd) in children's oncology group (cog) study aall0434. *Blood* **2014**, *124*.
74. Capaccione, K.M.; Pine, S.R. The notch signaling pathway as a mediator of tumor survival. *Carcinogenesis* **2013**, *34*, 1420-1430.
75. Radtke, F.; Wilson, A.; Stark, G.; Bauer, M.; van Meerwijk, J.; MacDonald, H.R.; Aguet, M. Deficient t cell fate specification in mice with an induced inactivation of notch1. *Immunity* **1999**, *10*, 547-558.
76. Han, H.; Tanigaki, K.; Yamamoto, N.; Kuroda, K.; Yoshimoto, M.; Nakahata, T.; Ikuta, K.; Honjo, T. Inducible gene knockout of transcription factor recombination signal binding protein-j reveals its essential role in t versus b lineage decision. *Int Immunol* **2002**, *14*, 637-645.
77. Brou, C.; Logeat, F.; Gupta, N.; Bessia, C.; LeBail, O.; Doedens, J.R.; Cumano, A.; Roux, P.; Black, R.A.; Israël, A. A novel proteolytic cleavage involved in notch signaling: The role of the disintegrin-metalloprotease tace. *Mol Cell* **2000**, *5*, 207-216.
78. Mumm, J.S.; Schroeter, E.H.; Saxena, M.T.; Griesemer, A.; Tian, X.; Pan, D.J.; Ray, W.J.; Kopan, R. A ligand-induced extracellular cleavage regulates gamma-secretase-like proteolytic activation of notch1. *Mol Cell* **2000**, *5*, 197-206.
79. Bray, S.J. Notch signalling: A simple pathway becomes complex. *Nat Rev Mol Cell Biol* **2006**, *7*, 678-689.
80. Fryer, C.J.; White, J.B.; Jones, K.A. Mastermind recruits cycc:Cdk8 to phosphorylate the notch icd and coordinate activation with turnover. *Mol Cell* **2004**, *16*, 509-520.
81. Nakano, T.; Fukuda, D.; Koga, J.; Aikawa, M. Delta-like ligand 4-notch signaling in macrophage activation. *Arterioscler Thromb Vasc Biol* **2016**, *36*, 2038-2047.
82. Bigas, A.; D'Altri, T.; Espinosa, L. The notch pathway in hematopoietic stem cells. *Curr Top Microbiol Immunol* **2012**, *360*, 1-18.
83. Liu, N.; Zhang, J.; Ji, C. The emerging roles of notch signaling in leukemia and stem cells. *Biomark Res* **2013**, *1*, 23.
84. Pui, J.C.; Allman, D.; Xu, L.; DeRocco, S.; Karnell, F.G.; Bakkour, S.; Lee, J.Y.; Kadesch, T.; Hardy, R.R.; Aster, J.C*., et al.* Notch1 expression in early lymphopoiesis influences b versus t lineage determination. *Immunity* **1999**, *11*, 299-308.
85. Radtke, F.; MacDonald, H.R.; Tacchini-Cottier, F. Regulation of innate and adaptive immunity by notch. *Nat Rev Immunol* **2013**, *13*, 427-437.
86. Schmitt, T.M.; Ciofani, M.; Petrie, H.T.; Zúñiga-Pflücker, J.C. Maintenance of t cell specification and differentiation requires recurrent notch receptor-ligand interactions. *J Exp Med* **2004**, *200*, 469-479.
87. Taghon, T.; Yui, M.A.; Pant, R.; Diamond, R.A.; Rothenberg, E.V. Developmental and molecular characterization of emerging beta- and gammadelta-selected pre-t cells in the adult mouse thymus. *Immunity* **2006**, *24*, 53-64.
88. Gridley, T. Notch signaling and inherited disease syndromes. *Hum Mol Genet* **2003**, *12 Spec No 1*, R9-13.
89. Louvi, A.; Artavanis-Tsakonas, S. Notch signalling in vertebrate neural development. *Nat Rev Neurosci* **2006**, *7*, 93-102.
90. Ellisen, L.W.; Bird, J.; West, D.C.; Soreng, A.L.; Reynolds, T.C.; Smith, S.D.; Sklar, J. Tan-1, the human homolog of the drosophila notch gene, is broken by

chromosomal translocations in t lymphoblastic neoplasms. *Cell* **1991**, *66*, 649-661.
91. Gordon, W.R.; Roy, M.; Vardar-Ulu, D.; Garfinkel, M.; Mansour, M.R.; Aster, J.C.; Blacklow, S.C. Structure of the notch1-negative regulatory region: Implications for normal activation and pathogenic signaling in t-all. *Blood* **2009**, *113*, 4381-4390.
92. Malecki, M.J.; Sanchez-Irizarry, C.; Mitchell, J.L.; Histen, G.; Xu, M.L.; Aster, J.C.; Blacklow, S.C. Leukemia-associated mutations within the notch1 heterodimerization domain fall into at least two distinct mechanistic classes. *Mol Cell Biol* **2006**, *26*, 4642-4651.
93. Sulis, M.L.; Williams, O.; Palomero, T.; Tosello, V.; Pallikuppam, S.; Real, P.J.; Barnes, K.; Zuurbier, L.; Meijerink, J.P.; Ferrando, A.A. Notch1 extracellular juxtamembrane expansion mutations in t-all. *Blood* **2008**, *112*, 733-740.
94. Thompson, B.J.; Buonamici, S.; Sulis, M.L.; Palomero, T.; Vilimas, T.; Basso, G.; Ferrando, A.; Aifantis, I. The scffbw7 ubiquitin ligase complex as a tumor suppressor in t cell leukemia. *J Exp Med* **2007**, *204*, 1825-1835.
95. O'Neil, J.; Grim, J.; Strack, P.; Rao, S.; Tibbitts, D.; Winter, C.; Hardwick, J.; Welcker, M.; Meijerink, J.P.; Pieters, R.*, et al.* Fbw7 mutations in leukemic cells mediate notch pathway activation and resistance to gamma-secretase inhibitors. *J Exp Med* **2007**, *204*, 1813-1824.
96. Minella, A.C.; Clurman, B.E. Mechanisms of tumor suppression by the scf(fbw7). *Cell Cycle* **2005**, *4*, 1356-1359.
97. Chiang, M.Y.; Xu, L.; Shestova, O.; Histen, G.; L'heureux, S.; Romany, C.; Childs, M.E.; Gimotty, P.A.; Aster, J.C.; Pear, W.S. Leukemia-associated notch1 alleles are weak tumor initiators but accelerate k-ras-initiated leukemia. *J Clin Invest* **2008**, *118*, 3181-3194.
98. Ferrando, A.A. The role of notch1 signaling in t-all. *Hematology Am Soc Hematol Educ Program* **2009**, 353-361.
99. Izon, D.J.; Punt, J.A.; Xu, L.; Karnell, F.G.; Allman, D.; Myung, P.S.; Boerth, N.J.; Pui, J.C.; Koretzky, G.A.; Pear, W.S. Notch1 regulates maturation of cd4+ and cd8+ thymocytes by modulating tcr signal strength. *Immunity* **2001**, *14*, 253-264.
100. Reizis, B.; Leder, P. Direct induction of t lymphocyte-specific gene expression by the mammalian notch signaling pathway. *Genes Dev* **2002**, *16*, 295-300.
101. González-García, S.; García-Peydró, M.; Martín-Gayo, E.; Ballestar, E.; Esteller, M.; Bornstein, R.; de la Pompa, J.L.; Ferrando, A.A.; Toribio, M.L. Csl-maml-dependent notch1 signaling controls t lineage-specific il-7r{alpha} gene expression in early human thymopoiesis and leukemia. *J Exp Med* **2009**, *206*, 779-791.
102. Palomero, T.; Lim, W.K.; Odom, D.T.; Sulis, M.L.; Real, P.J.; Margolin, A.; Barnes, K.C.; O'Neil, J.; Neuberg, D.; Weng, A.P.*, et al.* Notch1 directly regulates c-myc and activates a feed-forward-loop transcriptional network promoting leukemic cell growth. *Proc Natl Acad Sci U S A* **2006**, *103*, 18261-18266.
103. Weng, A.P.; Millholland, J.M.; Yashiro-Ohtani, Y.; Arcangeli, M.L.; Lau, A.; Wai, C.; Del Bianco, C.; Rodriguez, C.G.; Sai, H.; Tobias, J.*, et al.* C-myc is an important direct target of notch1 in t-cell acute lymphoblastic leukemia/lymphoma. *Genes Dev* **2006**, *20*, 2096-2109.
104. Chan, S.M.; Weng, A.P.; Tibshirani, R.; Aster, J.C.; Utz, P.J. Notch signals positively regulate activity of the mtor pathway in t-cell acute lymphoblastic leukemia. *Blood* **2007**, *110*, 278-286.
105. Joshi, I.; Minter, L.M.; Telfer, J.; Demarest, R.M.; Capobianco, A.J.; Aster, J.C.; Sicinski, P.; Fauq, A.; Golde, T.E.; Osborne, B.A. Notch signaling mediates g1/s

cell-cycle progression in t cells via cyclin d3 and its dependent kinases. *Blood* **2009**, *113*, 1689-1698.
106. Rao, S.S.; O'Neil, J.; Liberator, C.D.; Hardwick, J.S.; Dai, X.; Zhang, T.; Tyminski, E.; Yuan, J.; Kohl, N.E.; Richon, V.M.*, et al.* Inhibition of notch signaling by gamma secretase inhibitor engages the rb pathway and elicits cell cycle exit in t-cell acute lymphoblastic leukemia cells. *Cancer Res* **2009**, *69*, 3060-3068.
107. Song, L.L.; Peng, Y.; Yun, J.; Rizzo, P.; Chaturvedi, V.; Weijzen, S.; Kast, W.M.; Stone, P.J.; Santos, L.; Loredo, A.*, et al.* Notch-1 associates with ikkalpha and regulates ikk activity in cervical cancer cells. *Oncogene* **2008**, *27*, 5833-5844.
108. Weerkamp, F.; van Dongen, J.J.; Staal, F.J. Notch and wnt signaling in t-lymphocyte development and acute lymphoblastic leukemia. *Leukemia* **2006**, *20*, 1197-1205.
109. Raetz, E.A.; Teachey, D.T. T-cell acute lymphoblastic leukemia. *Hematology Am Soc Hematol Educ Program* **2016**, *2016*, 580-588.
110. Pui, C.H.; Evans, W.E. Treatment of acute lymphoblastic leukemia. *N Engl J Med* **2006**, *354*, 166-178.
111. Pui, C.H.; Howard, S.C. Current management and challenges of malignant disease in the cns in paediatric leukaemia. *Lancet Oncol* **2008**, *9*, 257-268.
112. Hurwitz, C.A.; Silverman, L.B.; Schorin, M.A.; Clavell, L.A.; Dalton, V.K.; Glick, K.M.; Gelber, R.D.; Sallan, S.E. Substituting dexamethasone for prednisone complicates remission induction in children with acute lymphoblastic leukemia. *Cancer* **2000**, *88*, 1964-1969.
113. Piovan, E.; Yu, J.; Tosello, V.; Herranz, D.; Ambesi-Impiombato, A.; Da Silva, A.C.; Sanchez-Martin, M.; Perez-Garcia, A.; Rigo, I.; Castillo, M.*, et al.* Direct reversal of glucocorticoid resistance by akt inhibition in acute lymphoblastic leukemia. *Cancer Cell* **2013**, *24*, 766-776.
114. Quintás-Cardama, A.; Cortes, J. Nilotinib: A phenylamino-pyrimidine derivative with activity against bcr-abl, kit and pdgfr kinases. *Future Oncol* **2008**, *4*, 611-621.
115. Girardi, T.; Vicente, C.; Cools, J.; De Keersmaecker, K. The genetics and molecular biology of t-all. *Blood* **2017**, *129*, 1113-1123.
116. Zenatti, P.P.; Ribeiro, D.; Li, W.; Zuurbier, L.; Silva, M.C.; Paganin, M.; Tritapoe, J.; Hixon, J.A.; Silveira, A.B.; Cardoso, B.A.*, et al.* Oncogenic il7r gain-of-function mutations in childhood t-cell acute lymphoblastic leukemia. *Nat Genet* **2011**, *43*, 932-939.
117. Peirs, S.; Matthijssens, F.; Goossens, S.; Van de Walle, I.; Ruggero, K.; de Bock, C.E.; Degryse, S.; Canté-Barrett, K.; Briot, D.; Clappier, E.*, et al.* Abt-199 mediated inhibition of bcl-2 as a novel therapeutic strategy in t-cell acute lymphoblastic leukemia. *Blood* **2014**, *124*, 3738-3747.
118. Chonghaile, T.N.; Roderick, J.E.; Glenfield, C.; Ryan, J.; Sallan, S.E.; Silverman, L.B.; Loh, M.L.; Hunger, S.P.; Wood, B.; DeAngelo, D.J.*, et al.* Maturation stage of t-cell acute lymphoblastic leukemia determines bcl-2 versus bcl-xl dependence and sensitivity to abt-199. *Cancer Discov* **2014**, *4*, 1074-1087.
119. Anderson, M.A.; Huang, D.; Roberts, A. Targeting bcl2 for the treatment of lymphoid malignancies. *Semin Hematol* **2014**, *51*, 219-227.
120. Palomero, T.; Sulis, M.L.; Cortina, M.; Real, P.J.; Barnes, K.; Ciofani, M.; Caparros, E.; Buteau, J.; Brown, K.; Perkins, S.L.*, et al.* Mutational loss of pten induces resistance to notch1 inhibition in t-cell leukemia. *Nat Med* **2007**, *13*, 1203-1210.
121. Zuurbier, L.; Petricoin, E.F.; Vuerhard, M.J.; Calvert, V.; Kooi, C.; Buijs-Gladdines, J.G.; Smits, W.K.; Sonneveld, E.; Veerman, A.J.; Kamps, W.A.*, et al.* The

significance of pten and akt aberrations in pediatric t-cell acute lymphoblastic leukemia. *Haematologica* **2012**, *97*, 1405-1413.
122. Silva, A.; Yunes, J.A.; Cardoso, B.A.; Martins, L.R.; Jotta, P.Y.; Abecasis, M.; Nowill, A.E.; Leslie, N.R.; Cardoso, A.A.; Barata, J.T. Pten posttranslational inactivation and hyperactivation of the pi3k/akt pathway sustain primary t cell leukemia viability. *J Clin Invest* **2008**, *118*, 3762-3774.
123. Avellino, R.; Romano, S.; Parasole, R.; Bisogni, R.; Lamberti, A.; Poggi, V.; Venuta, S.; Romano, M.F. Rapamycin stimulates apoptosis of childhood acute lymphoblastic leukemia cells. *Blood* **2005**, *106*, 1400-1406.
124. Wei, G.; Twomey, D.; Lamb, J.; Schlis, K.; Agarwal, J.; Stam, R.W.; Opferman, J.T.; Sallan, S.E.; den Boer, M.L.; Pieters, R.*, et al.* Gene expression-based chemical genomics identifies rapamycin as a modulator of mcl1 and glucocorticoid resistance. *Cancer Cell* **2006**, *10*, 331-342.
125. Easton, J.B.; Kurmasheva, R.T.; Houghton, P.J. Irs-1: Auditing the effectiveness of mtor inhibitors. *Cancer Cell* **2006**, *9*, 153-155.
126. Chiarini, F.; Falà, F.; Tazzari, P.L.; Ricci, F.; Astolfi, A.; Pession, A.; Pagliaro, P.; McCubrey, J.A.; Martelli, A.M. Dual inhibition of class ia phosphatidylinositol 3-kinase and mammalian target of rapamycin as a new therapeutic option for t-cell acute lymphoblastic leukemia. *Cancer Res* **2009**, *69*, 3520-3528.
127. Sanchez-Martin, M.; Ferrando, A. The notch1-myc highway toward t-cell acute lymphoblastic leukemia. *Blood* **2017**, *129*, 1124-1133.
128. Bongiovanni, D.; Saccomani, V.; Piovan, E. Aberrant signaling pathways in t-cell acute lymphoblastic leukemia. *Int J Mol Sci* **2017**, *18*.
129. Real, P.J.; Tosello, V.; Palomero, T.; Castillo, M.; Hernando, E.; de Stanchina, E.; Sulis, M.L.; Barnes, K.; Sawai, C.; Homminga, I.*, et al.* Gamma-secretase inhibitors reverse glucocorticoid resistance in t cell acute lymphoblastic leukemia. *Nat Med* **2009**, *15*, 50-58.
130. Yoon, S.O.; Zapata, M.C.; Singh, A.; Jo, W.S.; Spencer, N.; Choi, Y.S. Gamma secretase inhibitors enhance vincristine-induced apoptosis in t-all in a notch-independent manner. *Apoptosis* **2014**, *19*, 1616-1626.
131. Samon, J.B.; Castillo-Martin, M.; Hadler, M.; Ambesi-Impiobato, A.; Paietta, E.; Racevskis, J.; Wiernik, P.H.; Rowe, J.M.; Jakubczak, J.; Randolph, S.*, et al.* Preclinical analysis of the γ-secretase inhibitor pf-03084014 in combination with glucocorticoids in t-cell acute lymphoblastic leukemia. *Mol Cancer Ther* **2012**, *11*, 1565-1575.
132. Wu, Y.; Cain-Hom, C.; Choy, L.; Hagenbeek, T.J.; de Leon, G.P.; Chen, Y.; Finkle, D.; Venook, R.; Wu, X.; Ridgway, J.*, et al.* Therapeutic antibody targeting of individual notch receptors. *Nature* **2010**, *464*, 1052-1057.
133. Agnusdei, V.; Minuzzo, S.; Frasson, C.; Grassi, A.; Axelrod, F.; Satyal, S.; Gurney, A.; Hoey, T.; Seganfreddo, E.; Basso, G.*, et al.* Therapeutic antibody targeting of notch1 in t-acute lymphoblastic leukemia xenografts. *Leukemia* **2014**, *28*, 278-288.
134. Moellering, R.E.; Cornejo, M.; Davis, T.N.; Del Bianco, C.; Aster, J.C.; Blacklow, S.C.; Kung, A.L.; Gilliland, D.G.; Verdine, G.L.; Bradner, J.E. Direct inhibition of the notch transcription factor complex. *Nature* **2009**, *462*, 182-188.
135. Medyouf, H.; Gusscott, S.; Wang, H.; Tseng, J.C.; Wai, C.; Nemirovsky, O.; Trumpp, A.; Pflumio, F.; Carboni, J.; Gottardis, M.*, et al.* High-level igf1r expression is required for leukemia-initiating cell activity in t-all and is supported by notch signaling. *J Exp Med* **2011**, *208*, 1809-1822.

136. Schnell, S.A.; Ambesi-Impiombato, A.; Sanchez-Martin, M.; Belver, L.; Xu, L.; Qin, Y.; Kageyama, R.; Ferrando, A.A. Therapeutic targeting of hes1 transcriptional programs in t-all. *Blood* **2015**, *125*, 2806-2814.
137. Wendorff, A.A.; Koch, U.; Wunderlich, F.T.; Wirth, S.; Dubey, C.; Brüning, J.C.; MacDonald, H.R.; Radtke, F. Hes1 is a critical but context-dependent mediator of canonical notch signaling in lymphocyte development and transformation. *Immunity* **2010**, *33*, 671-684.
138. Roti, G.; Carlton, A.; Ross, K.N.; Markstein, M.; Pajcini, K.; Su, A.H.; Perrimon, N.; Pear, W.S.; Kung, A.L.; Blacklow, S.C*., et al.* Complementary genomic screens identify serca as a therapeutic target in notch1 mutated cancer. *Cancer Cell* **2013**, *23*, 390-405.
139. Delmore, J.E.; Issa, G.C.; Lemieux, M.E.; Rahl, P.B.; Shi, J.; Jacobs, H.M.; Kastritis, E.; Gilpatrick, T.; Paranal, R.M.; Qi, J*., et al.* Bet bromodomain inhibition as a therapeutic strategy to target c-myc. *Cell* **2011**, *146*, 904-917.
140. Dang, C.V. Myc on the path to cancer. *Cell* **2012**, *149*, 22-35.
141. Dose, M.; Khan, I.; Guo, Z.; Kovalovsky, D.; Krueger, A.; von Boehmer, H.; Khazaie, K.; Gounari, F. C-myc mediates pre-tcr-induced proliferation but not developmental progression. *Blood* **2006**, *108*, 2669-2677.
142. Herranz, D.; Ambesi-Impiombato, A.; Palomero, T.; Schnell, S.A.; Belver, L.; Wendorff, A.A.; Xu, L.; Castillo-Martin, M.; Llobet-Navás, D.; Cordon-Cardo, C*., et al.* A notch1-driven myc enhancer promotes t cell development, transformation and acute lymphoblastic leukemia. *Nat Med* **2014**, *20*, 1130-1137.
143. Yashiro-Ohtani, Y.; Wang, H.; Zang, C.; Arnett, K.L.; Bailis, W.; Ho, Y.; Knoechel, B.; Lanauze, C.; Louis, L.; Forsyth, K.S*., et al.* Long-range enhancer activity determines myc sensitivity to notch inhibitors in t cell leukemia. *Proc Natl Acad Sci U S A* **2014**, *111*, E4946-4953.
144. Lee, R.C.; Feinbaum, R.L.; Ambros, V. The c. Elegans heterochronic gene lin-4 encodes small rnas with antisense complementarity to lin-14. *Cell* **1993**, *75*, 843-854.
145. Pasquinelli, A.E.; Reinhart, B.J.; Slack, F.; Martindale, M.Q.; Kuroda, M.I.; Maller, B.; Hayward, D.C.; Ball, E.E.; Degnan, B.; Müller, P*., et al.* Conservation of the sequence and temporal expression of let-7 heterochronic regulatory rna. *Nature* **2000**, *408*, 86-89.
146. Friedman, R.C.; Farh, K.K.; Burge, C.B.; Bartel, D.P. Most mammalian mrnas are conserved targets of microrna s. *Genome Res* **2009**, *19*, 92-105.
147. Kim, V.N.; Han, J.; Siomi, M.C. Biogenesis of small rnas in animals. *Nat Rev Mol Cell Biol* **2009**, *10*, 126-139.
148. Altuvia, Y.; Landgraf, P.; Lithwick, G.; Elefant, N.; Pfeffer, S.; Aravin, A.; Brownstein, M.J.; Tuschl, T.; Margalit, H. Clustering and conservation patterns of human microrna s. *Nucleic Acids Res* **2005**, *33*, 2697-2706.
149. Pfeffer, S.; Sewer, A.; Lagos-Quintana, M.; Sheridan, R.; Sander, C.; Grässer, F.A.; van Dyk, L.F.; Ho, C.K.; Shuman, S.; Chien, M*., et al.* Identification of microrna s of the herpesvirus family. *Nat Methods* **2005**, *2*, 269-276.
150. Borchert, G.M.; Lanier, W.; Davidson, B.L. Rna polymerase iii transcribes human microrna s. *Nat Struct Mol Biol* **2006**, *13*, 1097-1101.
151. Krol, J.; Loedige, I.; Filipowicz, W. The widespread regulation of microrna biogenesis, function and decay. *Nat Rev Genet* **2010**, *11*, 597-610.
152. Davis-Dusenbery, B.N.; Hata, A. Mechanisms of control of microrna biogenesis. *J Biochem* **2010**, *148*, 381-392.
153. Lee, Y.; Kim, M.; Han, J.; Yeom, K.H.; Lee, S.; Baek, S.H.; Kim, V.N. Microrna genes are transcribed by rna polymerase ii. *EMBO J* **2004**, *23*, 4051-4060.

154. Han, J.; Lee, Y.; Yeom, K.H.; Kim, Y.K.; Jin, H.; Kim, V.N. The drosha-dgcr8 complex in primary microrna processing. *Genes Dev* **2004**, *18*, 3016-3027.
155. Gregory, R.I.; Yan, K.P.; Amuthan, G.; Chendrimada, T.; Doratotaj, B.; Cooch, N.; Shiekhattar, R. The microprocessor complex mediates the genesis of microrna. *Nature* **2004**, *432*, 235-240.
156. Lee, Y.; Ahn, C.; Han, J.; Choi, H.; Kim, J.; Yim, J.; Lee, J.; Provost, P.; Rådmark, O.; Kim, S*., et al.* The nuclear rnase iii drosha initiates microrna processing. *Nature* **2003**, *425*, 415-419.
157. Lund, E.; Güttinger, S.; Calado, A.; Dahlberg, J.E.; Kutay, U. Nuclear export of microrna precursors. *Science* **2004**, *303*, 95-98.
158. Bohnsack, M.T.; Czaplinski, K.; Gorlich, D. Exportin 5 is a rangtp-dependent dsrna-binding protein that mediates nuclear export of pre-mirnas. *RNA* **2004**, *10*, 185-191.
159. Hutvágner, G.; McLachlan, J.; Pasquinelli, A.E.; Bálint, E.; Tuschl, T.; Zamore, P.D. A cellular function for the rna-interference enzyme dicer in the maturation of the let-7 small temporal rna. *Science* **2001**, *293*, 834-838.
160. Zhang, H.; Kolb, F.A.; Jaskiewicz, L.; Westhof, E.; Filipowicz, W. Single processing center models for human dicer and bacterial rnase iii. *Cell* **2004**, *118*, 57-68.
161. Gu, S.; Jin, L.; Zhang, Y.; Huang, Y.; Zhang, F.; Valdmanis, P.N.; Kay, M.A. The loop position of shrnas and pre-mirnas is critical for the accuracy of dicer processing in vivo. *Cell* **2012**, *151*, 900-911.
162. Tsutsumi, A.; Kawamata, T.; Izumi, N.; Seitz, H.; Tomari, Y. Recognition of the pre-mirna structure by drosophila dicer-1. *Nat Struct Mol Biol* **2011**, *18*, 1153-1158.
163. Haase, A.D.; Jaskiewicz, L.; Zhang, H.; Lainé, S.; Sack, R.; Gatignol, A.; Filipowicz, W. Trbp, a regulator of cellular pkr and hiv-1 virus expression, interacts with dicer and functions in rna silencing. *EMBO Rep* **2005**, *6*, 961-967.
164. Kok, K.H.; Ng, M.H.; Ching, Y.P.; Jin, D.Y. Human trbp and pact directly interact with each other and associate with dicer to facilitate the production of small interfering rna. *J Biol Chem* **2007**, *282*, 17649-17657.
165. Fukunaga, R.; Han, B.W.; Hung, J.H.; Xu, J.; Weng, Z.; Zamore, P.D. Dicer partner proteins tune the length of mature mirnas in flies and mammals. *Cell* **2012**, *151*, 533-546.
166. Lee, H.Y.; Doudna, J.A. Trbp alters human precursor microrna processing in vitro. *RNA* **2012**, *18*, 2012-2019.
167. Lee, Y.; Hur, I.; Park, S.Y.; Kim, Y.K.; Suh, M.R.; Kim, V.N. The role of pact in the rna silencing pathway. *EMBO J* **2006**, *25*, 522-532.
168. García, M.A.; Meurs, E.F.; Esteban, M. The dsrna protein kinase pkr: Virus and cell control. *Biochimie* **2007**, *89*, 799-811.
169. Park, J.E.; Heo, I.; Tian, Y.; Simanshu, D.K.; Chang, H.; Jee, D.; Patel, D.J.; Kim, V.N. Dicer recognizes the 5' end of rna for efficient and accurate processing. *Nature* **2011**, *475*, 201-205.
170. Tian, Y.; Simanshu, D.K.; Ma, J.B.; Park, J.E.; Heo, I.; Kim, V.N.; Patel, D.J. A phosphate-binding pocket within the platform-paz-connector helix cassette of human dicer. *Mol Cell* **2014**, *53*, 606-616.
171. Hammond, S.M.; Boettcher, S.; Caudy, A.A.; Kobayashi, R.; Hannon, G.J. Argonaute2, a link between genetic and biochemical analyses of rnai. *Science* **2001**, *293*, 1146-1150.
172. Liu, J.; Carmell, M.A.; Rivas, F.V.; Marsden, C.G.; Thomson, J.M.; Song, J.J.; Hammond, S.M.; Joshua-Tor, L.; Hannon, G.J. Argonaute2 is the catalytic engine of mammalian rnai. *Science* **2004**, *305*, 1437-1441.

173. Diederichs, S.; Haber, D.A. Dual role for argonautes in microrna processing and posttranscriptional regulation of microrna expression. *Cell* **2007**, *131*, 1097-1108.
174. Rand, T.A.; Petersen, S.; Du, F.; Wang, X. Argonaute2 cleaves the anti-guide strand of sirna during risc activation. *Cell* **2005**, *123*, 621-629.
175. Meister, G.; Landthaler, M.; Patkaniowska, A.; Dorsett, Y.; Teng, G.; Tuschl, T. Human argonaute2 mediates rna cleavage targeted by mirnas and sirnas. *Mol Cell* **2004**, *15*, 185-197.
176. Kawamata, T.; Seitz, H.; Tomari, Y. Structural determinants of mirnas for risc loading and slicer-independent unwinding. *Nat Struct Mol Biol* **2009**, *16*, 953-960.
177. Yoda, M.; Kawamata, T.; Paroo, Z.; Ye, X.; Iwasaki, S.; Liu, Q.; Tomari, Y. Atp-dependent human risc assembly pathways. *Nat Struct Mol Biol* **2010**, *17*, 17-23.
178. Iwasaki, S.; Kobayashi, M.; Yoda, M.; Sakaguchi, Y.; Katsuma, S.; Suzuki, T.; Tomari, Y. Hsc70/hsp90 chaperone machinery mediates atp-dependent risc loading of small rna duplexes. *Mol Cell* **2010**, *39*, 292-299.
179. Kawamata, T.; Tomari, Y. Making risc. *Trends Biochem Sci* **2010**, *35*, 368-376.
180. Hu, H.Y.; Yan, Z.; Xu, Y.; Hu, H.; Menzel, C.; Zhou, Y.H.; Chen, W.; Khaitovich, P. Sequence features associated with microrna strand selection in humans and flies. *BMC Genomics* **2009**, *10*, 413.
181. Chiang, H.R.; Schoenfeld, L.W.; Ruby, J.G.; Auyeung, V.C.; Spies, N.; Baek, D.; Johnston, W.K.; Russ, C.; Luo, S.; Babiarz, J.E*., et al.* Mammalian microrna: Experimental evaluation of novel and previously annotated genes. *Genes Dev* **2010**, *24*, 992-1009.
182. Barca-Mayo, O.; Lu, Q.R. Fine-tuning oligodendrocyte development by microrna. *Front Neurosci* **2012**, *6*, 13.
183. Berezikov, E.; Chung, W.J.; Willis, J.; Cuppen, E.; Lai, E.C. Mammalian mirtron genes. *Mol Cell* **2007**, *28*, 328-336.
184. Chong, M.M.; Zhang, G.; Cheloufi, S.; Neubert, T.A.; Hannon, G.J.; Littman, D.R. Canonical and alternate functions of the microrna biogenesis machinery. *Genes Dev* **2010**, *24*, 1951-1960.
185. Cheloufi, S.; Dos Santos, C.O.; Chong, M.M.; Hannon, G.J. A dicer-independent mirna biogenesis pathway that requires ago catalysis. *Nature* **2010**, *465*, 584-589.
186. Ameres, S.L.; Zamore, P.D. Diversifying microrna sequence and function. *Nat Rev Mol Cell Biol* **2013**, *14*, 475-488.
187. Gu, S.; Jin, L.; Zhang, F.; Sarnow, P.; Kay, M.A. Biological basis for restriction of microrna targets to the 3' untranslated region in mammalian mrnas. *Nat Struct Mol Biol* **2009**, *16*, 144-150.
188. Lee, Y.S.; Dutta, A. The tumor suppressor microrna let-7 represses the hmga2 oncogene. *Genes Dev* **2007**, *21*, 1025-1030.
189. Krek, A.; Grün, D.; Poy, M.N.; Wolf, R.; Rosenberg, L.; Epstein, E.J.; MacMenamin, P.; da Piedade, I.; Gunsalus, K.C.; Stoffel, M*., et al.* Combinatorial microrna target predictions. *Nat Genet* **2005**, *37*, 495-500.
190. Ipsaro, J.J.; Joshua-Tor, L. From guide to target: Molecular insights into eukaryotic rna-interference machinery. *Nat Struct Mol Biol* **2015**, *22*, 20-28.
191. Fabian, M.R.; Sonenberg, N. The mechanics of mirna-mediated gene silencing: A look under the hood of mirisc. *Nat Struct Mol Biol* **2012**, *19*, 586-593.
192. Braun, J.E.; Huntzinger, E.; Izaurralde, E. The role of gw182 proteins in mirna-mediated gene silencing. *Adv Exp Med Biol* **2013**, *768*, 147-163.

193. Parker, R.; Song, H. The enzymes and control of eukaryotic mrna turnover. *Nat Struct Mol Biol* **2004**, *11*, 121-127.
194. Rehwinkel, J.; Behm-Ansmant, I.; Gatfield, D.; Izaurralde, E. A crucial role for gw182 and the dcp1:Dcp2 decapping complex in mirna-mediated gene silencing. *RNA* **2005**, *11*, 1640-1647.
195. Kiriakidou, M.; Tan, G.S.; Lamprinaki, S.; De Planell-Saguer, M.; Nelson, P.T.; Mourelatos, Z. An mrna m7g cap binding-like motif within human ago2 represses translation. *Cell* **2007**, *129*, 1141-1151.
196. Chendrimada, T.P.; Finn, K.J.; Ji, X.; Baillat, D.; Gregory, R.I.; Liebhaber, S.A.; Pasquinelli, A.E.; Shiekhattar, R. Microrna silencing through risc recruitment of eif6. *Nature* **2007**, *447*, 823-828.
197. Wang, B.; Yanez, A.; Novina, C.D. Microrna-repressed mrnas contain 40s but not 60s components. *Proc Natl Acad Sci U S A* **2008**, *105*, 5343-5348.
198. Petersen, C.P.; Bordeleau, M.E.; Pelletier, J.; Sharp, P.A. Short rnas repress translation after initiation in mammalian cells. *Mol Cell* **2006**, *21*, 533-542.
199. Nottrott, S.; Simard, M.J.; Richter, J.D. Human let-7a mirna blocks protein production on actively translating polyribosomes. *Nat Struct Mol Biol* **2006**, *13*, 1108-1114.
200. Liu, J.; Valencia-Sanchez, M.A.; Hannon, G.J.; Parker, R. Microrna-dependent localization of targeted mrnas to mammalian p-bodies. *Nat Cell Biol* **2005**, *7*, 719-723.
201. Huntzinger, E.; Izaurralde, E. Gene silencing by microrna: Contributions of translational repression and mrna decay. *Nat Rev Genet* **2011**, *12*, 99-110.
202. Merritt, W.M.; Lin, Y.G.; Han, L.Y.; Kamat, A.A.; Spannuth, W.A.; Schmandt, R.; Urbauer, D.; Pennacchio, L.A.; Cheng, J.F.; Nick, A.M.*, et al.* Dicer, drosha, and outcomes in patients with ovarian cancer. *N Engl J Med* **2008**, *359*, 2641-2650.
203. Karube, Y.; Tanaka, H.; Osada, H.; Tomida, S.; Tatematsu, Y.; Yanagisawa, K.; Yatabe, Y.; Takamizawa, J.; Miyoshi, S.; Mitsudomi, T.*, et al.* Reduced expression of dicer associated with poor prognosis in lung cancer patients. *Cancer Sci* **2005**, *96*, 111-115.
204. Melo, S.A.; Moutinho, C.; Ropero, S.; Calin, G.A.; Rossi, S.; Spizzo, R.; Fernandez, A.F.; Davalos, V.; Villanueva, A.; Montoya, G.*, et al.* A genetic defect in exportin-5 traps precursor microrna s in the nucleus of cancer cells. *Cancer Cell* **2010**, *18*, 303-315.
205. Bommer, G.T.; Gerin, I.; Feng, Y.; Kaczorowski, A.J.; Kuick, R.; Love, R.E.; Zhai, Y.; Giordano, T.J.; Qin, Z.S.; Moore, B.B.*, et al.* P53-mediated activation of mirna34 candidate tumor-suppressor genes. *Curr Biol* **2007**, *17*, 1298-1307.
206. He, L.; He, X.; Lim, L.P.; de Stanchina, E.; Xuan, Z.; Liang, Y.; Xue, W.; Zender, L.; Magnus, J.; Ridzon, D.*, et al.* A microrna component of the p53 tumour suppressor network. *Nature* **2007**, *447*, 1130-1134.
207. Ryan, B.M.; Robles, A.I.; Harris, C.C. Genetic variation in microrna networks: The implications for cancer research. *Nat Rev Cancer* **2010**, *10*, 389-402.
208. Xhemalce, B.; Robson, S.C.; Kouzarides, T. Human rna methyltransferase bcdin3d regulates microrna processing. *Cell* **2012**, *151*, 278-288.
209. Rüegger, S.; Großhans, H. Microrna turnover: When, how, and why. *Trends Biochem Sci* **2012**, *37*, 436-446.
210. Das, S.K.; Sokhi, U.K.; Bhutia, S.K.; Azab, B.; Su, Z.Z.; Sarkar, D.; Fisher, P.B. Human polynucleotide phosphorylase selectively and preferentially degrades microrna-221 in human melanoma cells. *Proc Natl Acad Sci U S A* **2010**, *107*, 11948-11953.

211. Mets, E.; Van der Meulen, J.; Van Peer, G.; Boice, M.; Mestdagh, P.; Van de Walle, I.; Lammens, T.; Goossens, S.; De Moerloose, B.; Benoit, Y.*, et al.* Microrna-193b-3p acts as a tumor suppressor by targeting the myb oncogene in t-cell acute lymphoblastic leukemia. *Leukemia* **2015**, *29*, 798-806.
212. Sanghvi, V.R.; Mavrakis, K.J.; Van der Meulen, J.; Boice, M.; Wolfe, A.L.; Carty, M.; Mohan, P.; Rondou, P.; Socci, N.D.; Benoit, Y.*, et al.* Characterization of a set of tumor suppressor micrornas in t cell acute lymphoblastic leukemia. *Sci Signal* **2014**, *7*, ra111.
213. Wallaert, A.; Van Loocke, W.; Hernandez, L.; Taghon, T.; Speleman, F.; Van Vlierberghe, P. Comprehensive mirna expression profiling in human t-cell acute lymphoblastic leukemia by small rna-sequencing. *Sci Rep* **2017**, *7*, 7901.
214. Wang, Z.; Li, Y.; Kong, D.; Ahmad, A.; Banerjee, S.; Sarkar, F.H. Cross-talk between mirna and notch signaling pathways in tumor development and progression. *Cancer Lett* **2010**, *292*, 141-148.
215. Li, Y.; Choi, P.S.; Casey, S.C.; Dill, D.L.; Felsher, D.W. Myc through mir-17-92 suppresses specific target genes to maintain survival, autonomous proliferation, and a neoplastic state. *Cancer Cell* **2014**, *26*, 262-272.
216. Fuziwara, C.S.; Kimura, E.T. Insights into regulation of the mir-17-92 cluster of mirnas in cancer. *Front Med (Lausanne)* **2015**, *2*, 64.
217. Murphy, B.L.; Obad, S.; Bihannic, L.; Ayrault, O.; Zindy, F.; Kauppinen, S.; Roussel, M.F. Silencing of the mir-17~92 cluster family inhibits medulloblastoma progression. *Cancer Res* **2013**, *73*, 7068-7078.
218. Huang, J.; Chen, Y.; Li, J.; Zhang, K.; Chen, J.; Chen, D.; Feng, B.; Song, H.; Feng, J.; Wang, R.*, et al.* Notch-1 confers chemoresistance in lung adenocarcinoma to taxanes through ap-1/microrna-451 mediated regulation of mdr-1. *Mol Ther Nucleic Acids* **2016**, *5*, e375.
219. Kumar, V.; Palermo, R.; Talora, C.; Campese, A.F.; Checquolo, S.; Bellavia, D.; Tottone, L.; Testa, G.; Miele, E.; Indraccolo, S.*, et al.* Notch and nf-kb signaling pathways regulate mir-223/fbxw7 axis in t-cell acute lymphoblastic leukemia. *Leukemia* **2014**, *28*, 2324-2335.
220. Gusscott, S.; Kuchenbauer, F.; Humphries, R.K.; Weng, A.P. Notch-mediated repression of mir-223 contributes to igf1r regulation in t-all. *Leuk Res* **2012**, *36*, 905-911.
221. Takebe, N.; Nguyen, D.; Yang, S.X. Targeting notch signaling pathway in cancer: Clinical development advances and challenges. *Pharmacol Ther* **2014**, *141*, 140-149.
222. Pear, W.S.; Aster, J.C.; Scott, M.L.; Hasserjian, R.P.; Soffer, B.; Sklar, J.; Baltimore, D. Exclusive development of t cell neoplasms in mice transplanted with bone marrow expressing activated notch alleles. *J Exp Med* **1996**, *183*, 2283-2291.
223. Smyth, G.K. Linear models and empirical bayes methods for assessing differential expression in microarray experiments. *Stat Appl Genet Mol Biol* **2004**, *3*, Article3.
224. BENJAMINI, Y.; HOCHBERG, Y. Controlling the false discovery rate - a practical and powerful approach to multiple testing. *Journal of the Royal Statistical Society Series B-Methodological* **1995**, *57*, 289-300.
225. Liberzon, A.; Birger, C.; Thorvaldsdóttir, H.; Ghandi, M.; Mesirov, J.P.; Tamayo, P. The molecular signatures database (msigdb) hallmark gene set collection. *Cell Syst* **2015**, *1*, 417-425.
226. López-Romero, P. Pre-processing and differential expression analysis of agilent microrna arrays using the agimicrorna bioconductor library. *BMC Genomics* **2011**, *12*, 64.

227. López-Romero, P.; González, M.A.; Callejas, S.; Dopazo, A.; Irizarry, R.A. Processing of agilent microrna array data. *BMC Res Notes* **2010**, *3*, 18.
228. Livak, K.J.; Schmittgen, T.D. Analysis of relative gene expression data using real-time quantitative pcr and the 2(-delta delta c(t)) method. *Methods* **2001**, *25*, 402-408.
229. Subramanian, A.; Tamayo, P.; Mootha, V.K.; Mukherjee, S.; Ebert, B.L.; Gillette, M.A.; Paulovich, A.; Pomeroy, S.L.; Golub, T.R.; Lander, E.S*., et al.* Gene set enrichment analysis: A knowledge-based approach for interpreting genome-wide expression profiles. *Proc Natl Acad Sci U S A* **2005**, *102*, 15545-15550.
230. Sicinska, E.; Aifantis, I.; Le Cam, L.; Swat, W.; Borowski, C.; Yu, Q.; Ferrando, A.A.; Levin, S.D.; Geng, Y.; von Boehmer, H*., et al.* Requirement for cyclin d3 in lymphocyte development and t cell leukemias. *Cancer Cell* **2003**, *4*, 451-461.
231. Jiang, X.; Hu, C.; Arnovitz, S.; Bugno, J.; Yu, M.; Zuo, Z.; Chen, P.; Huang, H.; Ulrich, B.; Gurbuxani, S*., et al.* Mir-22 has a potent anti-tumour role with therapeutic potential in acute myeloid leukaemia. *Nat Commun* **2016**, *7*, 11452.
232. Liu, L.; Ren, W.; Chen, K. Mir-34a promotes apoptosis and inhibits autophagy by targeting hmgb1 in acute myeloid leukemia cells. *Cell Physiol Biochem* **2017**, *41*, 1981-1992.
233. Koshizuka, K.; Hanazawa, T.; Kikkawa, N.; Arai, T.; Okato, A.; Kurozumi, A.; Kato, M.; Katada, K.; Okamoto, Y.; Seki, N. Regulation of itga3 by the anti-tumor mir-199 family inhibits cancer cell migration and invasion in head and neck cancer. *Cancer Sci* **2017**, *108*, 1681-1692.
234. Li, B.; He, L.; Zuo, D.; He, W.; Wang, Y.; Zhang, Y.; Liu, W.; Yuan, Y. Mutual regulation of mir-199a-5p and hif-1α modulates the warburg effect in hepatocellular carcinoma. *J Cancer* **2017**, *8*, 940-949.
235. Chen, J.; Shin, V.Y.; Siu, M.T.; Ho, J.C.; Cheuk, I.; Kwong, A. Mir-199a-5p confers tumor-suppressive role in triple-negative breast cancer. *BMC Cancer* **2016**, *16*, 887.
236. Tosello, V.; Ferrando, A.A. The notch signaling pathway: Role in the pathogenesis of t-cell acute lymphoblastic leukemia and implication for therapy. *Ther Adv Hematol* **2013**, *4*, 199-210.
237. Piccinin, E.; Peres, C.; Bellafante, E.; Ducheix, S.; Pinto, C.; Villani, G.; Moschetta, A. Hepatic pparγ coactivator 1β drives mitochondrial and anabolic signatures that contribute to hepatocellular carcinoma progression. *Hepatology* **2017**.
238. Fragoso, R.; Mao, T.; Wang, S.; Schaffert, S.; Gong, X.; Yue, S.; Luong, R.; Min, H.; Yashiro-Ohtani, Y.; Davis, M*., et al.* Modulating the strength and threshold of notch oncogenic signals by mir-181a-1/b-1. *PLoS Genet* **2012**, *8*, e1002855.
239. Wang, X.; Li, J.; Dong, K.; Lin, F.; Long, M.; Ouyang, Y.; Wei, J.; Chen, X.; Weng, Y.; He, T*., et al.* Tumor suppressor mir-34a targets pd-l1 and functions as a potential immunotherapeutic target in acute myeloid leukemia. *Cell Signal* **2015**, *27*, 443-452.
240. Yin, D.; Ogawa, S.; Kawamata, N.; Leiter, A.; Ham, M.; Li, D.; Doan, N.B.; Said, J.W.; Black, K.L.; Phillip Koeffler, H. Mir-34a functions as a tumor suppressor modulating egfr in glioblastoma multiforme. *Oncogene* **2013**, *32*, 1155-1163.
241. Welch, C.; Chen, Y.; Stallings, R.L. Microrna-34a functions as a potential tumor suppressor by inducing apoptosis in neuroblastoma cells. *Oncogene* **2007**, *26*, 5017-5022.
242. Baer, C.; Claus, R.; Frenzel, L.P.; Zucknick, M.; Park, Y.J.; Gu, L.; Weichenhan, D.; Fischer, M.; Pallasch, C.P.; Herpel, E*., et al.* Extensive promoter dna hypermethylation and hypomethylation is associated with aberrant microrna expression in chronic lymphocytic leukemia. *Cancer Res* **2012**, *72*, 3775-3785.

243. Bader, A.G. Mir-34 - a microrna replacement therapy is headed to the clinic. *Front Genet* **2012**, *3*, 120.
244. Song, S.J.; Ito, K.; Ala, U.; Kats, L.; Webster, K.; Sun, S.M.; Jongen-Lavrencic, M.; Manova-Todorova, K.; Teruya-Feldstein, J.; Avigan, D.E.*, et al.* The oncogenic microrna mir-22 targets the tet2 tumor suppressor to promote hematopoietic stem cell self-renewal and transformation. *Cell Stem Cell* **2013**, *13*, 87-101.
245. Shen, C.; Chen, M.T.; Zhang, X.H.; Yin, X.L.; Ning, H.M.; Su, R.; Lin, H.S.; Song, L.; Wang, F.; Ma, Y.N.*, et al.* The pu.1-modulated microrna-22 is a regulator of monocyte/macrophage differentiation and acute myeloid leukemia. *PLoS Genet* **2016**, *12*, e1006259.
246. Yang, M.; Jiang, N.; Cao, Q.W.; Sun, Q. Edd1 predicts prognosis and regulates gastric cancer growth in vitro and in vivo via mir-22. *Biol Chem* **2016**.
247. Yang, C.; Ning, S.; Li, Z.; Qin, X.; Xu, W. Mir-22 is down-regulated in esophageal squamous cell carcinoma and inhibits cell migration and invasion. *Cancer Cell Int* **2014**, *14*, 138.
248. Damavandi, Z.; Torkashvand, S.; Vasei, M.; Soltani, B.M.; Tavallaei, M.; Mowla, S.J. Aberrant expression of breast development-related micrornas, mir-22, mir-132, and mir-212, in breast tumor tissues. *J Breast Cancer* **2016**, *19*, 148-155.
249. Budd, W.T.; Seashols-Williams, S.J.; Clark, G.C.; Weaver, D.; Calvert, V.; Petricoin, E.; Dragoescu, E.A.; O'Hanlon, K.; Zehner, Z.E. Dual action of mir-125b as a tumor suppressor and oncomir-22 promotes prostate cancer tumorigenesis. *PLoS One* **2015**, *10*, e0142373.
250. Ghisi, M.; Corradin, A.; Basso, K.; Frasson, C.; Serafin, V.; Mukherjee, S.; Mussolin, L.; Ruggero, K.; Bonanno, L.; Guffanti, A.*, et al.* Modulation of microrna expression in human t-cell development: Targeting of notch3 by mir-150. *Blood* **2011**, *117*, 7053-7062.
251. Lin, J.; Handschin, C.; Spiegelman, B.M. Metabolic control through the pgc-1 family of transcription coactivators. *Cell Metab* **2005**, *1*, 361-370.
252. Maniati, E.; Bossard, M.; Cook, N.; Candido, J.B.; Emami-Shahri, N.; Nedospasov, S.A.; Balkwill, F.R.; Tuveson, D.A.; Hagemann, T. Crosstalk between the canonical nf-κb and notch signaling pathways inhibits pparγ expression and promotes pancreatic cancer progression in mice. *J Clin Invest* **2011**, *121*, 4685-4699.
253. Song, N.J.; Yun, U.J.; Yang, S.; Wu, C.; Seo, C.R.; Gwon, A.R.; Baik, S.H.; Choi, Y.; Choi, B.Y.; Bahn, G.*, et al.* Notch1 deficiency decreases hepatic lipid accumulation by induction of fatty acid oxidation. *Sci Rep* **2016**, *6*, 19377.

Supplementary

A)

Probe Name	Gene Name	FC	p-value	FDR
A_55_P2073694	Gm266	-17,74	1,85E-10	1,03E-05
A_52_P337259	Heyl	-18,41	5,37E-10	1,16E-05
A_55_P2137527	Fam183b	-21,29	6,26E-10	1,16E-05
A_51_P510418	Aldh1b1	-14,86	1,12E-09	1,56E-05
A_51_P474701	Fbp1	-50,94	1,98E-09	1,93E-05
A_55_P1980796	Il2ra	-50,03	2,08E-09	1,93E-05
A_55_P1954393	Susd4	-14,79	2,82E-09	2,25E-05
A_51_P212741	Scn2b	-9,57	5,86E-09	3,89E-05
A_55_P2002968	Coro2a	-8,61	6,27E-09	3,89E-05
A_52_P460734	Crhbp	-8,12	9,26E-09	5,17E-05
A_55_P2155856	Gm12253	-7,43	1,42E-08	7,19E-05
A_55_P2116111	D8Ertd82e	-9,11	1,99E-08	9,12E-05
A_55_P2169888	D8Ertd82e	-8,94	2,12E-08	9,12E-05
A_55_P2162688	U07554	-8,84	2,64E-08	1,05E-04
A_52_P322421	Mpzl2	-11,01	2,94E-08	1,06E-04
A_51_P367866	Egr1	-5,41	3,11E-08	1,06E-04
A_51_P202050	Dtx1	-41,42	3,46E-08	1,07E-04
A_51_P444137	Syce1	-11,46	3,95E-08	1,09E-04
A_55_P2037454	Etv5	-5,94	3,98E-08	1,09E-04
A_51_P305628	Atp8a2	-12,04	4,09E-08	1,09E-04
A_66_P128297	4930417O13Rik	-7,48	7,23E-08	1,76E-04
A_55_P2000783	Axin2	-7,90	7,26E-08	1,76E-04
A_55_P2150876	Als2cr12	-4,32	8,29E-08	1,93E-04
A_51_P516870	Itm2a	-5,64	9,15E-08	2,04E-04
A_55_P2010429	X04315	-6,94	1,06E-07	2,18E-04
A_52_P200125	M34969	-7,06	1,07E-07	2,18E-04
A_55_P2117082	M54990	-6,63	1,15E-07	2,18E-04
A_52_P345078	Wdr25	-10,56	1,18E-07	2,18E-04
A_55_P2124228	Uaca	-9,38	1,21E-07	2,18E-04
A_55_P2004162	BC051070	-5,14	1,26E-07	2,18E-04
A_51_P317031	Ccdc109b	-4,14	1,41E-07	2,18E-04
A_51_P113195	Upk1b	-7,91	1,48E-07	2,18E-04
A_55_P1998066	Tmem121	-8,63	1,52E-07	2,18E-04
A_55_P2118362	Tmem121	-8,45	1,55E-07	2,18E-04
A_55_P2022604	1200009I06Rik	-5,40	1,59E-07	2,18E-04
A_51_P445841	Depdc6	-4,55	1,61E-07	2,18E-04
A_55_P2117081	M54990	-6,24	1,66E-07	2,18E-04
A_52_P246277	LOC633417	-5,06	1,69E-07	2,18E-04
A_52_P659312	Spsb4	-9,32	1,72E-07	2,18E-04
A_55_P2155853	LOC100044609	-8,02	1,84E-07	2,26E-04
A_52_P502141	Hectd2	-6,00	1,87E-07	2,26E-04

A_55_P2138500	Gm6189	-6,83	1,92E-07	2,26E-04
A_55_P1957249	Pdgfrb	-4,89	1,95E-07	2,26E-04
A_51_P279437	Mfsd2a	-7,48	1,98E-07	2,26E-04
A_52_P398998	Gfra1	-6,23	2,26E-07	2,43E-04
A_55_P2012439	Tnfrsf19	-5,61	2,27E-07	2,43E-04
A_55_P2157195	LOC100047308	-4,46	2,65E-07	2,78E-04
A_55_P1989563	Cd163l1	-8,37	3,09E-07	3,14E-04
A_52_P382886	Gjb2	-4,31	3,22E-07	3,21E-04
A_51_P405912	Lmcd1	-5,21	3,38E-07	3,25E-04
A_51_P220162	Notch3	-7,55	3,49E-07	3,30E-04
A_55_P2162695	X03802	-8,12	3,56E-07	3,31E-04
A_52_P69558	Gm8221	-5,52	3,77E-07	3,41E-04
A_51_P348433	Rasal1	-5,97	3,79E-07	3,41E-04
A_55_P1956837	ENSMUST00000051210	-4,14	3,89E-07	3,41E-04
A_55_P2345631	Tcrg-V1	-7,88	4,01E-07	3,41E-04
A_51_P349691	Ano10	-6,23	4,04E-07	3,41E-04
A_55_P2123673	Trnp1	-8,41	4,21E-07	3,51E-04
A_30_P01028951	chr4:46583780-46614788_R	-6,09	4,52E-07	3,60E-04
A_55_P2122884	Ptcra	-10,99	4,84E-07	3,70E-04
A_52_P375312	Amica1	-4,29	5,54E-07	4,12E-04
A_55_P2046245	Hes1	-5,66	5,91E-07	4,33E-04
A_55_P2100884	Fjx1	-5,52	6,05E-07	4,33E-04
A_55_P1990373	Trnp1	-6,91	6,05E-07	4,33E-04
A_51_P137336	Cdh1	-4,34	6,13E-07	4,33E-04
A_51_P279232	Dennd2d	-7,19	6,98E-07	4,65E-04
A_52_P507578	Slamf6	-4,54	7,04E-07	4,65E-04
A_55_P2182467	Slamf6	-5,58	7,13E-07	4,65E-04
A_55_P2170737	Igf2bp2	-5,29	7,87E-07	4,88E-04
A_55_P2016962	A_55_P2016962	-4,07	7,97E-07	4,89E-04
A_66_P139088	AK080422	-4,95	8,37E-07	4,97E-04
A_55_P2054817	Rxfp1	-4,48	9,28E-07	5,34E-04
A_52_P387009	Egln3	-5,52	1,05E-06	5,71E-04
A_55_P2005552	Arhgef10l	-5,22	1,17E-06	6,18E-04
A_55_P2405106	Iqch	-5,03	1,25E-06	6,22E-04
A_51_P467110	Dpp4	-5,07	1,33E-06	6,30E-04
A_52_P278354	Bmp7	-5,01	1,36E-06	6,33E-04
A_55_P1956048	H2-T3	-7,39	1,45E-06	6,52E-04
A_55_P2111970	Ofcc1	-4,37	1,49E-06	6,64E-04
A_55_P2153122	Zap70	-4,26	1,52E-06	6,73E-04
A_51_P164296	Adamdec1	-4,64	1,59E-06	6,85E-04
A_51_P126067	Cd2	-5,15	1,59E-06	6,85E-04
A_55_P1984976	Wnt5b	-4,23	1,62E-06	6,91E-04
A_66_P121965	1110032F04Rik	-4,37	1,69E-06	7,04E-04
A_55_P2422826	Tcrg-V2	-5,60	1,85E-06	7,32E-04

A_55_P2069485	Ptpn13	-4,52	1,87E-06	7,36E-04
A_66_P112495	Scn4b	-5,37	1,89E-06	7,36E-04
A_55_P1960916	Egln3	-5,10	1,90E-06	7,36E-04
A_51_P414243	C85492	-4,06	1,96E-06	7,50E-04
A_55_P2076871	Lef1	-6,01	2,03E-06	7,59E-04
A_30_P01020519	chr9:96664617-96683617_R	-4,96	2,21E-06	7,98E-04
A_55_P2156229	Cd3e	-4,37	2,22E-06	7,98E-04
A_51_P315682	Igf2bp2	-4,76	2,25E-06	8,02E-04
A_30_P01032514	chr9:96664617-96683617_R	-5,91	2,50E-06	8,38E-04
A_55_P1959393	Hhat	-4,09	2,69E-06	8,74E-04
A_51_P264495	Pgam2	-4,66	2,79E-06	8,91E-04
A_55_P2258375	2700008G24Rik	-4,00	2,95E-06	9,05E-04
A_55_P1969861	Zap70	-4,02	3,26E-06	9,38E-04
A_51_P183051	Upb1	-8,77	3,53E-06	9,62E-04
A_55_P1981306	Hdgfrp3	-5,41	4,12E-06	1,06E-03
A_51_P167263	Cd5	-5,15	4,90E-06	1,18E-03
A_55_P1958215	Ccr4	-5,58	4,97E-06	1,19E-03
A_52_P220810	Trib2	-4,09	5,31E-06	1,21E-03
A_55_P2039359	Tnfsf11	-4,15	5,73E-06	1,24E-03
A_51_P420400	Lef1	-7,76	5,98E-06	1,26E-03
A_30_P01019479	chr14:26834450-26847000_F	-4,26	7,09E-06	1,38E-03
A_52_P208521	Khdc1a	-8,99	7,50E-06	1,42E-03
A_52_P257625	Esm1	-4,09	8,05E-06	1,47E-03
A_51_P402144	2300002M23Rik	-4,48	8,51E-06	1,53E-03
A_55_P2032659	Tox	-4,05	9,77E-06	1,58E-03
A_51_P377171	5830405N20Rik	-4,64	1,08E-05	1,63E-03
A_55_P2019312	Car12	-4,25	1,31E-05	1,79E-03
A_51_P104418	Dusp10	-4,29	1,33E-05	1,81E-03
A_52_P622850	Hes5	-6,31	1,51E-05	1,95E-03
A_55_P2010152	Sell	-4,31	2,70E-05	2,72E-03
A_66_P111011	Gata3	-4,11	2,86E-05	2,80E-03
A_55_P2044554	5830405N20Rik	-4,16	3,01E-05	2,87E-03
A_55_P2077901	Cd2	-4,61	4,07E-05	3,36E-03
A_55_P1989653	Slco4a1	-4,76	4,63E-05	3,53E-03
A_52_P319438	Ankrd37	-4,79	5,23E-05	3,81E-03

B)

Probe Name	Gene Name	FC	pvalue	FDR
A_55_P2045055	Clec10a	8,02	3,23E-08	1,06E-04
A_55_P2133195	Gm4951	5,18	1,26E-07	2,18E-04
A_55_P1990633	Iigp1	4,49	1,41E-07	2,18E-04
A_51_P460954	Ccl6	4,03	3,38E-07	3,25E-04
A_55_P2008740	Fcgr1	4,87	4,78E-07	3,70E-04

A_52_P338066	Ubd	5,57	3,12E-06	9,21E-04
A_51_P359570	Ifit3	4,75	2,95E-05	2,84E-03
A_55_P2122605	Cbr2	4,11	3,10E-05	2,90E-03
A_55_P2118441	Mx1	4,12	4,47E-05	3,51E-03
A_52_P30312	Ccr9	4,43	5,64E-05	3,96E-03
A_66_P137219	Elane	4,28	8,67E-05	5,01E-03
A_55_P2019719	Oas2	4,59	1,62E-04	7,13E-03
A_51_P464703	Ccl8	4,12	2,04E-04	8,09E-03
A_51_P483576	ENSMUST00000103743	4,15	2,53E-04	9,20E-03
A_55_P2057283	ENSMUST00000103749	4,42	2,57E-04	9,28E-03

Supplementary Table 1. Significantly differentially expressed genes with |FC|>4 following GSI treatment in NOTCH1-induced T-ALL *in vivo*. Gene expression profiling using SurePrint G3 Mouse GE 8x60K Agilent Microarray was performed in three biological replicates of the same HD-ΔPEST NOTCH1 T-cell tumors treated *in vivo* with vehicle only (DMSO) or with 5mg/kg of a potent GSI, Dibenzazepine (DBZ), for three times every 8 hours. A) Genes significantly down-regulated (FDR<0.01 and FC<-4). B) Genes significantly up-regulated (FDR<0.01 and FC>4).

A)

GENE SET	SIZE	NES	FDR
HALLMARK_MYC_TARGETS_V1	183	-2,56	0,00
HALLMARK_MYC_TARGETS_V2	57	-2,31	0,00
HALLMARK_E2F_TARGETS	185	-1,80	0,00
HALLMARK_NOTCH_SIGNALING	31	-1,79	0,00
HALLMARK_G2M_CHECKPOINT	183	-1,69	0,01
HALLMARK_DNA_REPAIR	136	-1,59	0,01
HALLMARK_WNT_BETA_CATENIN_SIGNALING	41	-1,57	0,01

B)

GENE SET	SIZE	NES	FDR
HALLMARK_EPITHELIAL_MESENCHYMAL_TRANSITION	190	2,73	0
HALLMARK_INTERFERON_GAMMA_RESPONSE	176	2,63	0
HALLMARK_INTERFERON_ALPHA_RESPONSE	83	2,53	0
HALLMARK_COAGULATION	131	2,31	0
HALLMARK_ANGIOGENESIS	35	2,31	0
HALLMARK_HEME_METABOLISM	178	2,22	0
HALLMARK_COMPLEMENT	183	2,13	0
HALLMARK_IL6_JAK_STAT3_SIGNALING	83	1,87	2,74E-04
HALLMARK_APOPTOSIS	153	1,87	2,44E-04
HALLMARK_MYOGENESIS	195	1,86	2,20E-04
HALLMARK_P53_PATHWAY	185	1,80	8,14E-04
HALLMARK_IL2_STAT5_SIGNALING	190	1,80	7,46E-04

HALLMARK_CHOLESTEROL_HOMEOSTASIS	72	1,79	6,89E-04
HALLMARK_INFLAMMATORY_RESPONSE	197	1,79	7,16E-04
HALLMARK_APICAL_JUNCTION	185	1,76	8,90E-04
HALLMARK_PROTEIN_SECRETION	96	1,62	5,00E-03
HALLMARK_ADIPOGENESIS	186	1,62	4,70E-03
HALLMARK_UV_RESPONSE_DN	137	1,62	4,65E-03
HALLMARK_KRAS_SIGNALING_UP	190	1,50	0,017
HALLMARK_ALLOGRAFT_REJECTION	185	1,47	0,021
HALLMARK_BILE_ACID_METABOLISM	109	1,46	0,022
HALLMARK_REACTIVE_OXIGEN_SPECIES_PATHWAY	45	1,44	0,027
HALLMARK_APICAL_SURFACE	43	1,41	0,032
HALLMARK_TNFA_SIGNALING_VIA_NFKB	195	1,39	0,039
HALLMARK_XENOBIOTIC_METABOLISM	185	1,37	0,042

Supplementary Table 2. Functional analysis using GSEA on the MSigDB hallmark collection of the MSigDB. A) Gene sets significantly down-regulated. B) Gene sets significantly up-regulated.

PROBE	miRNA	FC	p-value	FDR
A_54_P1431	mmu-miR-19a-3p	-1,74	2,00E-05	0,0018
A_54_P1266	mmu-miR-130b-3p	-1,67	3,00E-05	0,0018
A_54_P3922	mmu-miR-20b-5p	-2,01	4,00E-05	0,0018
A_54_P1305	mmu-miR-20a-5p	-1,90	5,00E-05	0,0018
A_54_P1267	mmu-miR-19b-3p	-2,09	5,00E-05	0,0018
A_54_P2476	mmu-miR-18a-5p	-1,60	8,00E-05	0,0023
A_54_P3502	mmu-miR-17-3p	-1,26	1,20E-04	0,0025
A_54_P2925	mmu-miR-467b-5p	-1,29	1,30E-04	0,0025
A_54_P2285	mmu-miR-126-3p	1,27	1,40E-04	0,0025
A_54_P2098	mmu-miR-709	1,42	1,60E-04	0,0025
A_54_P00004585	mmu-miR-17-5p	-1,39	1,70E-04	0,0025
A_54_P2405	mmu-miR-143-3p	1,29	1,70E-04	0,0025
A_54_P00002291	mmu-miR-128-3p	-1,84	1,80E-04	0,0025
A_54_P2678	mmu-miR-363-3p	-1,24	2,20E-04	0,0028
A_54_P00005485	mmu-miR-3096b-3p	-1,50	3,00E-04	0,0036
A_54_P2496	mmu-miR-92a-3p	-1,70	3,30E-04	0,0036
A_54_P2440	mmu-miR-301a-3p	-1,27	3,70E-04	0,0038
A_54_P2982	mmu-miR-181d-5p	-1,24	4,20E-04	0,0041
A_54_P00004988	mmu-miR-669f-3p	-1,34	0,0010	0,0093
A_54_P4402	mmu-miR-1224-5p	1,43	0,0011	0,0093
A_54_P1342	mmu-miR-103-3p	-1,23	0,0012	0,0096
A_54_P00002769	mmu-miR-466b-3p	-1,28	0,0014	0,0111

A_54_P1309	mmu-miR-22-3p	1,36	0,0015	0,0113
A_54_P3245	mmu-miR-467e-5p	-1,18	0,0017	0,0121
A_54_P3517	mmu-miR-181a-1-3p	-1,20	0,0017	0,0121
A_54_P2629	mmu-miR-223-3p	1,47	0,0019	0,0129
A_54_P00005754	mmu-miR-5622-3p	1,19	0,0021	0,0135
A_54_P2651	mmu-miR-181b-5p	-1,53	0,0024	0,0139
A_54_P00005116	mmu-miR-677-3p	-1,19	0,0024	0,0139
A_54_P2282	mmu-miR-125b-5p	1,32	0,0025	0,0139
A_54_P1012	mmu-miR-29b-3p	1,26	0,0025	0,0139
A_54_P00004689	mmu-miR-1839-3p	-1,15	0,0025	0,0139
A_54_P00005823	mmu-miR-378d	-1,17	0,0029	0,0155
A_54_P00005052	mmu-miR-466i-5p	2,30	0,0030	0,0155
A_54_P00005688	mmu-miR-378b	-1,13	0,0033	0,0166
A_54_P00005505	mmu-miR-467a-3p	-1,16	0,0039	0,0190
A_54_P2317	mmu-miR-146a-5p	1,23	0,0045	0,0213
A_54_P2682	mmu-miR-378a-3p	-1,12	0,0053	0,0239
A_54_P2488	mmu-miR-29a-3p	1,38	0,0054	0,0239
A_54_P2315	mmu-miR-145a-5p	1,13	0,0055	0,0239
A_54_P1010	mmu-miR-27b-3p	-1,17	0,0067	0,0282
A_54_P4409	mmu-miR-497-5p	1,15	0,0068	0,0282
A_54_P1264	mmu-miR-106b-5p	-1,27	0,0092	0,0375
A_54_P2573	mmu-miR-342-3p	1,27	0,0097	0,0385
A_54_P00005602	mmu-miR-5128	1,32	0,0109	0,0424
A_54_P3440	mmu-miR-20a-3p	-1,10	0,0116	0,0439
A_54_P2492	mmu-miR-29c-3p	1,20	0,0118	0,0439
A_54_P1484	mmu-miR-181c-5p	-1,10	0,0126	0,0460
A_54_P1433	mmu-miR-25-3p	-1,23	0,0130	0,0464
A_54_P00004590	mmu-miR-1895	1,12	0,0133	0,0464
A_54_P2336	mmu-miR-155-5p	1,09	0,0135	0,0464
A_54_P2381	mmu-miR-199a-3p	1,18	0,0153	0,0515
A_54_P2409	mmu-miR-30e-5p	-1,11	0,0158	0,0522
A_54_P3154	mmu-miR-574-5p	1,98	0,0161	0,0522
A_54_P1044	mmu-miR-130a-3p	1,16	0,0201	0,0638
A_54_P2594	mmu-miR-101b-3p	-1,11	0,0215	0,0670
A_54_P00005698	mmu-miR-5107-5p	1,09	0,0260	0,0797
A_54_P00004436	mmu-miR-1187	1,72	0,0266	0,0803
A_54_P00006059	mmu-miR-6366	1,23	0,0278	0,0818
A_54_P1327	mmu-miR-93-5p	-1,26	0,0281	0,0818
A_54_P2498	mmu-miR-34a-5p	1,13	0,0287	0,0823
A_54_P4384	mmu-miR-26a-5p	1,25	0,0293	0,0827
A_54_P1421	mmu-miR-107-3p	-1,12	0,0306	0,0845
A_54_P2377	mmu-miR-199a-5p	1,10	0,0309	0,0845
A_54_P1422	mmu-miR-10a-5p	1,07	0,0328	0,0883
A_54_P1301	mmu-miR-16-5p	-1,13	0,0333	0,0883

A_54_P2504	mmu-miR-322-5p	1,09	0,0342	0,0894
A_54_P1274	mmu-miR-148a-3p	1,09	0,0386	0,0993

Supplementary Table 3. MicroRNAs significantly regulated following NOTCH1 pathway inhibition *in vivo*. MicroRNA expression profiling using mouse miRNA 8x60K microarrays (release 19.0; Agilent) was performed in three biological replicates of the same HD-ΔPEST NOTCH1 T-cell tumors treated *in vivo* with vehicle only (DMSO) or with 5mg/kg of a potent GSI, Dibenzazepine (DBZ), for three times every 8 hours Bioinformatic analysis revealed 68 significantly differentially expressed microRNAs with FDR < 0.10.

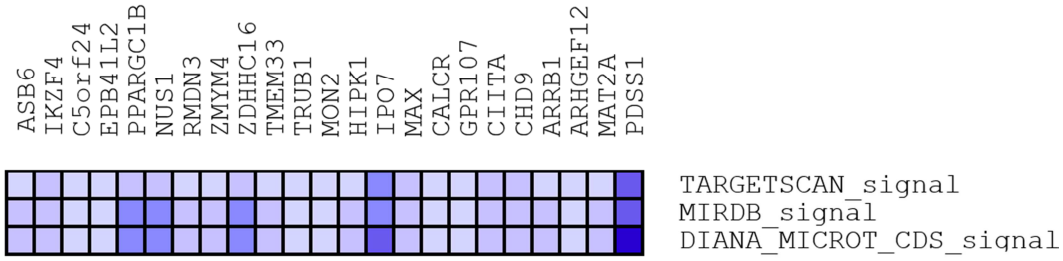

Supplementary Figure 1. Heat map of the 23 down-regulated genes that were consistently contributing to the negative enrichment of the three selected gene sets of miR-22 targets. GSEA was run on the dataset of human T-ALL cell lines treated with GSI (CompE) [102] against the C3 sub-collection of miR targets in the MSigDB v6.0, including additional gene sets with putative targets of miR-22 obtained from different microRNA target prediction softwares. Three negatively enriched gene sets of miR-22 targets, i.e. those obtained with the DIANA-microT-CDS software, TargetScan and miRDB, were selected for a leading edge analysis. The heat map reports the 23 genes that were consistently contributing to the negative enrichment of the three selected gene sets. Expression values are represented as colors, where the range of colors (light blue, dark blue) shows the range of expression values (low, lowest).